SPATIAL VARIABILITY OF PHYSICAL, HYDRAULIC AND HYDROLOGIC PROPERTIES OF A TROPICAL SOIL.

A Major Dissertation Submitted to the School of Research and Graduate Studies,

Kwame Nkrumah University of Science and Technology

In Partial Fulfillment of the Requirements for the Degree of

Master of Science

In

Soil Science

BY

HENRY OPPONG TUFFOUR

(BSc. Agriculture, KNUST, 2008)

JUNE, 2011

Stand unshod upon it.

For the ground is holy,

Being even as it came from the creator.

Keep it, guard it, care for it.

For it keeps men, guards men, cares for men.

Destroy it and man is destroyed.

Alan Paton, Cry the beloved country

DECLARATION

I, Henry Oppong Tuffour, hereby declare that the study entitled **"SPATIAL VARIABILITY OF PHYSICAL, HYDRAULIC AND HYDROLOGIC PROPERTIES OF A TROPICAL SOIL"** being presented here in the partial fulfillment for the award of the Degree of Master of Science (Soil Science), is a genuine documentation of my own work carried out by me under the guidance and supervision of Rev. Fr. (Prof.) Mensah Bonsu of Department of Crop and Soil Sciences, Faculty of Agriculture, College of Agriculture and Natural Resources, Kwame Nkrumah University of Science and Technology.

I, further assert that this thesis has not been submitted to any other Institute/University for the award of any degree or diploma or any other purpose, whatsoever and other people's works cited have been duly acknowledged.

.... 23/01/12

OPPONG, HENRY TUFFOUR **DATE**

(STUDENT)

.... 23/01/12

REV. FR. (PROF.) MENSAH BONSU **DATE**

(SUPERVISOR)

.... 24/01/2012

REV. DR. J. SARKODIE-ADDO **DATE**

(HEAD OF DEPARTMENT)

DEDICATION

This dissertation is dedicated to honour and express my appreciation to the most influential person in my education, Rev. Fr. (Prof.) Mensah Bonsu, whose immeasurable love, patience, attention, guidance and encouragement to persevere made this possible.

ACKNOWLEDGEMENTS

Except the Lord build the house, they labour in vain that build it. I will give thanks unto the Lord, the God of gods for he is good: for his mercy endures forever. Glory and honour be to my God in heaven and my Lord Jesus Christ for the infinite mercy, grace and the power through the Holy Spirit who has established the work of my hands.

It is my distinct pleasure to express my deep sense of gratitude and indebtedness to my learned supervisor, Rev. Fr. (Prof.) Mensah Bonsu for many things, but especially for accepting to take charge of my studies, determining my project and efficient review of all submitted manuscripts. He has been instrumental in fuelling my interest, sharpening my critical faculties, providing immense intellectual support, encouragement and zeal in developing my attitude towards this very new research field. I am sincerely grateful to him for his mentorship. It was my privilege to have been guided by this brilliant scientist.

In addition, I appreciate and thank Dr. Alfred Duker, Mr. John Ayeh, and Maxwell, all of the Department of Geomatic Engineering and Mr. Thomas Adjei-Gyapong of the Department of Crop and Soil Sciences, Faculty of Agriculture. Their expertise, guidance, and academic support helped me to understand this research deeply.

I am grateful also to Mr. Acquah, Mr. Nortey, Mr. Brako, Bright, Bintu, Yahaya, Godfred, Alberta and Aziz for extending their kind support and sharing their valuable time for the completion of this project. I am also grateful to all the members of my class for providing thoughtful insights and camaraderie in fulfilling my mission.

My deep appreciation to Fr. Seth, Pastors Amoako, Kwabi, Ntoso and Opoku for their encouragement and steady fast prayers. In addition, I appreciate and thank Petra, Mr. Ntiamoah, Twumasi, Dennis, Yaw, Alfah, Fiifi, Gema, Sampson, Bruno, Frank, Atta, Boat, Fred, Sly, Alphonse, Kobby, Parker, Primus, Ayowa and Mike for their support and encouragement. To the many friends who boosted my morale and helped me to move on, I am grateful. My deep thanks are also due to great number of people who provided help with other fundamental phases of this work.

My sincere appreciation to my parents, who stood by me throughout this challenging ordeal, was a regular source of inspiration and determination, and without them this dream could not have been achieved. This thesis has also been possible with the love and support of my sisters Maame Gyamfuah, Maame Amma, Maame Serwaah, Adwubi and Adjapomah and my brothers, Livingstone, Jimmy, Mark, Michael, Ahmed, Nasir, Osei-Bonsu, Oware, Affum, and Eric. Their confidence, strength and sacrifice have helped me focus on my work and maintain an inner harmony to complete this thesis. My heartfelt thanks to all other members of my family for their love, concern, encouragement, and prayers.

Henry Oppong Tuffour

ABSTRACT

Soil varies naturally due to product of the factors of formation and variations due to management. Describing spatial distribution patterns of soil properties within a field or watershed is thus, important for site-specific soil and plant management and environmental modeling. The objective of this study was to determine spatial distribution patterns of soil texture and structure, organic carbon, pH, saturated hydraulic conductivity and infiltration characteristics of soil in an uprooted oil palm field in the Plantation Crops Research Station of the Department of Crop and Soil Sciences, KNUST. Classical statistical and geostatistical procedures were used in describing the amount and form of variability and spatial distribution pattern of soil physical and chemical properties in the field. Scaling (based on the similar media and linear variability theories) and fractal geometry analyses were also performed to describe the variability and distribution of soil hydraulic and hydrologic properties. GraphPad Prism SPSS 16.0 and GS+ version 9.0 softwares were used for geostatistical and classical statistical analysis of data, respectively.

The descriptive statistics revealed that soil properties exhibited weak to higher variations at the surface and sub-surface layers across the field with aggregate stability being the most reliable property and K_s, the most variable property in the field. The results also suggested that scaling can successfully be used for describing variability of soil hydraulic and hydrologic properties of different soil map units and horizons. The results from fractal geometry analysis point out that soil hydraulic and hydrologic properties show fractal behaviour. The spatial distribution model and spatial dependence level showed remarkable variations in field. Distribution patterns of soil properties studied showed variations across the field for both depths. The significance of semivariogram modeling for the subsequent interpolation was, thus proven.

TABLE OF CONTENTS

Page

Declaration....ii
Dedication....iii
Acknowledgements....iv
Abstract....vi
Chapters....viii

List of Tables....xi
List of Figures....xii
List of Appendices....xiv

CHAPTERS

CHAPTER ONE

1.0 INTRODUCTION......1
1.1 Problem statement......2
1.2 Justification......3
1.3 Objectives......4
1.3.1 General objective......4
1.3.2 Specific objectives......4
1.4 Expected output......4

CHAPTER TWO

2.0 LITERATURE REVIEW......5
2.1 Background......5
2.2 Spatial variability of soil physical properties......7
2.2.1 Soil moisture content......7
2.2.2 Other soil physical properties......10
2.3 Spatial variability of soil hydraulic and hydrologic properties......11
2.3.1 Saturated hydraulic conductivity......12
2.3.2 Infiltration characteristics......12
2.4 Spatial variability of crop yield......14
2.5 Addressing spatial variability......16
2.5.1 Scaling......16
2.5.2 Fractal Geometry analysis......18
2.5.3 Statistical and geostatistical techniques......22
2.7 Precision farming......25

CHAPTER THREE

3.0 MATERIALS AND METHODS......28
3.1 Site location and characteristics......28
3.2 Land preparation......28
3.3 Soil sampling and laboratory analyses......28
3.4 Assessment of hydro-physical properties......30
3.4.1 Particle size analysis......30

3.4.2 Bulk density..........31
3.4.3 Total porosity..........32
3.4.4 Aeration Porosity..........32
3.4.5 Aggregate stability..........32
3.4.6 Moisture content..........33
3.4.7 Saturated hydraulic conductivity..........34
3.4.8 Field infiltration..........34
3.5 Statistical and Spatial analyses..........35
3.5.1 Descriptive statistics..........36
3.6.2 Scaling and Fractal Geometry analyses..........37
3.6.2.1 Scaling of Saturated hydraulic conductivity..........37
3.6.2.2 Scaling of Cumulative infiltration amount..........38
3.6.2.2 Fractal Geometry analysis..........42
3.6.3 Geostatistical analyses..........45
3.6.3.1 Spatial structure analyses..........46
3.6.3.1.1 Semivariogram..........46
3.6.3.1.2 Autocorrelation analysis..........49
3.6.3.2 Kriging and Cross-validation..........50

CHAPTER FOUR

4.0 RESULTS AND DISCUSSION..........52
4.1 Descriptive statistics..........52
4.1.1 Soil physical properties..........52
4.1.1.1 Variation in particle size fraction..........58
4.1.1.2 Variation in bulk density, porosity, aeration and aggregate stability..........59
4.1.1.3 Variation in moisture content..........62
4.1.2 Soil Hydraulic and Hydrologic properties..........63
4.1.2.1 Saturated hydraulic conductivity..........66
4.1.2.2 Infiltration parameters..........67
4.2 Scaling and Fractal Geometry analyses..........71
4.2.1 Scaling results..........71
4.2.1.1 Cumulative infiltration amount..........72

4.2.1.2 Saturated hydraulic conductivity....74
4.2.1.3 Fractal Geometry analysis....76
4.3 Geostatistical analyses....80
4.3.1 Spatial structure and attributes....80
4.3.1.1 Particle size fractions....89
4.3.1.2 Bulk density, porosity, aeration and aggregate stability....91
4.3.1.3 Moisture content....92
4.3.2 Kriging and Cross-validation....93
4.3.2.1 Soil texture....101
4.3.2.2 Bulk density, porosity, aeration and aggregate stability....102
4.3.2.3 Moisture content....104

CHAPTER FIVE

5.0 CONCLUSION AND RECOMMENDATIONS....106
5.1 Conclusion....106
5.2 Recommendations....107

REFERENCES....108
APPENDICES....134

LIST OF TABLES

Table	Title	Page
Table 3.1:	Relationship between Fractal Dimension and Hurst's Coefficient	44
Table 3.2:	Relationship between Fractal Dimension and Nature of soil	45
Table 4.1:	Descriptive statistics of soil physical properties	53
Table 4.2:	Descriptive statistics of soil hydraulic and hydrologic properties	64
Table 4.3:	Scaling parameters for K_s and I	72
Table 4.4:	Fractal indices of hydraulic and hydrologic properties	77
Table 4.5:	Semivariogram models and parameters for soil physical properties	83
Table 4.6:	Cross-validation parameters for soil physical properties	95

LIST OF FIGURES

HISTOGRAMS

Table	Title	Page
Figure 1a:	Sand content in both layers of sampling	54
Figure 1b:	Clay content in both layers of sampling	54
Figure 1c:	Silt content in both layers of sampling	55
Figure 1d:	Bulk density in both layers of sampling	55
Figure 1e:	Total porosity in both layers of sampling	56
Figure 1f:	Aeration porosity in both layers of sampling	56
Figure 1g:	Aggregate stability of both layers of sampling	57
Figure 1h:	Volumetric moisture content in both layers of sampling	57
Figure 2a:	Saturated hydraulic conductivity of both layers	64
Figure 2b:	Infiltration parameters	65

LINE GRAPHS

Figure 3a: Variations of cumulative infiltration amount....68

Figure 3b: Variations of sorptivity....68

Figure 3c: Variations of infiltration rates....69

SCALING

Figure 4a: Cumulative infiltration amount....73

Figure 4b: Fractal diagrams of K_s and $ln\ K^*$ of the surface layer....74

Figure 4c: Fractal diagrams of K_s and $ln\ K^*$ of the sub-surface layer....75

FRACTAL GEOMETRY

Figure 5a: Log-log variogram plots of K_s of both layers....77

Figure 5b: Log-log variogram plots of infiltration parameters....78

SEMIVARIOGRAMS AND AUTOCORRELOGRAM

Figure 6a: Sand content in the top layer....84

Figure 6b: Clay content in the top layer....84

Figure 6c: Silt content in the top layer....84

Figure 6d: Sand content in the sub-surface layer....85

Figure 6e: Clay content in the top sub-surface layer....85
Figure 6f: Silt content in the top sub-surface layer....85
Figure 6g: Bulk density in the top layer....86
Figure 6h: Total porosity in the top layer....86
Figure 6i: Aeration porosity in the top layer....86
Figure 6j: Bulk density in the sub-surface layer....87
Figure 6k: Total porosity in the sub-surface layer....87
Figure 6m: Aeration porosity in the sub-surface layer....87
Figure 6n: Aggregate stability of the top layer....88
Figure 6p: Volumetric moisture content in the top layer....88
Figure 6q: Aggregate stability of the sub-surface layer....88
Figure 6r: Volumetric moisture content in the sub-surface layer....89

KRIGED MAPS AND CROSS-VALIDATION GRAPHS

Figure 7a: Sand content in the top layer....96
Figure 7b: Clay content in the top layer....96
Figure 7c: Silt content in the top layer....96
Figure 7d: Sand content in the sub-surface layer....97
Figure 7e: Clay content in the top sub-surface layer....97
Figure 7f: Silt content in the top sub-surface layer....97
Figure 7g: Bulk density in the top layer....98
Figure 7h: Total porosity in the top layer....98
Figure 7i: Aeration porosity in the top layer....98
Figure 7j: Bulk density in the sub-surface layer....99
Figure 7k: Total porosity in the sub-surface layer....99
Figure 7m: Aeration porosity in the sub-surface layer....99
Figure 7n: Volumetric moisture content in the top layer....100
Figure 7p: Aggregate stability of the top layer....100
Figure 7q: Volumetric moisture content in the sub-surface layer....100
Figure 7r: Aggregate stability of the sub-surface layer....101

APPENDICES

Page

Appendix A: T-test results of soil physical properties..........134

A-1 Sand content..........134

A-2 Clay content..........134

A-3 Silt content..........135

A-4 Bulk density..........135

A-5 Total porosity..........136

A-6 Aeration-porosity..........136

A-7 Volumetric moisture content..........137

A-8 Aggregate stability..........137

Appendix B: T-test results of saturated hydraulic conductivity..........138

CHAPTER ONE

1.0 INTRODUCTION

The soil is an anisotropic medium having both vertical and horizontal variability, and consequently, can be seen to exhibit marked spatial variation operating over the micro- and macro-scales, most especially in tropical soils. This is an indication that the factors influencing spatial variability differ with scale. Since the nature of soil structure is highly specific, variation in soil structure under field conditions is the cause of the anisotropic property.

One of the fundamental features of soils, causing the variations in soil structure under field conditions is horizonation (or stratification), which represents systematic spatial variation in the vertical direction as a result of soil development. In a soil profile, the different horizons may be of varying thickness causing differences in their properties and processes. Horizontal variation can also be very large and systematic, relating to slope position, vegetation cover, management history, and parent material. Arid soils are often characterized by a finer scale, systematic variation in the horizontal direction related to the *"islands of fertility"* phenomenon, wherein soil organic matter and nutrient concentrations are higher beneath shrubs and trees than in interspaces (Schlesinger *et al.*, 1996).

These islands of fertility are thought to be caused by a combination of wind-blown topsoil and other debris blown from interspaces and trapped by the shrubs or trees (often on the leeward side), uptake of nutrients from surrounding soils and recycling them via litter fall to soils beneath the shrubs and trees, and excreta from animals taking shelter beneath these trees and shrubs.

Tropical soils are, thus, inherently variable over time and space, indicating that they are not composed of homogeneous units as indicated on maps, or considered as a closed body, but always have some degree of variability presenting significant problems for both sampling and characterisation. This heterogeneity in soils is due to the fact that:

- They are a product of the interaction of several factors and processes of formation that operate with different intensities and at different scales. These interactions, therefore, transmit complexity to the soil and produce a dynamic and heterogeneous system.
- The various systems of soil preparation substantially increase the heterogeneity of its attributes: when the soil is cropped, it has additional sources of heterogeneity, caused exclusively by the anthropic effects of agriculture.

Heterogeneity, therefore, can be considered as an innate quality of soils that typifies their anisotropy. In a natural landscape, it represents a wide variety of soil attributes, both spatial and volumetric, because of the interaction of the processes that rule soil formation (Júnior *et al.*, 2005). Spatial variability of soil properties, as a result, is a serious problem in the management of tropical soils and has been one of the major objectives in investigations related to agricultural and environmental sciences.

1.1 Problem statement

Considering the major categories of production systems, there is no clear distinction between intensive industrial agriculture and extensive small-scale agriculture. Whatever the type of agriculture, the most important thing is to develop rational use of inputs such as tillage, irrigation, fertilization and other agrochemicals to help protect the environment and biodiversity, while at the same time trying to intensify production. Normally farmers do not consider spatial variability while applying these management strategies (inputs) to the soil.

The common practice is for them to apply the inputs uniformly to their fields. Additionally, yields of crops from the farmers' fields are also influenced by spatial variability emanating from soil heterogeneity.

As a consequence, researchers have traditionally attempted to remove spatial variability by blocking and/or statistical averaging procedures. The consequence has often been a failure to understand processes acting in the soil (interdependency over space). On the contrary, geostatistics provides a body of statistical techniques designed to detecting and modeling the patterns of spatial dependence of attributes in space, rather than evaluating linear spatial average values.

1.2 Justification

These observations concerning the management of spatial variability point to variability as a key soil attribute that should be studied for the physical, hydraulic and chemical attributes of soil under different management regimes. Thus, it is important to properly characterize the spatial patterns in soils for a number of reasons. Therefore, an appropriate understanding of spatial variation of soil properties and the relationships between them is needed to scale up measured soil properties and to model soil processes since knowledge of spatial variation of soil properties is important in precision farming and environmental modeling: analyses and modeling of field-scale solute transport processes, crop quality and yield and groundwater chemistry.

1.3 Objectives

1.3.1 General Objective

The main objective of the study was to assess and analyse the variability of soil on an uprooted oil palm field spatially. To reach this objective, the following specific objectives were evaluated:

1.3.2 Specific objectives

The specific objectives, therefore, were to:

- Evaluate the structure of spatial variability in hydraulic and hydrologic processes using scaling techniques and fractal geometry analysis.
- Analyse the extent of spatial variability in selected soil physical properties using semivariograms, Kriging and autocorrelation analyses.

1.4 Expected output

The study would, for that reason, serve as a reference point to researchers, farmers and policy makers trying to make sustainable agricultural production a priority in their activities by producing overall analyses on how spatial variability can be incorporated into the management of spatially variable tropical soils.

CHAPTER TWO

2.0 LITERATURE REVIEW

2.1 Background

Knowledge about the variability of soil properties is probably as old as the soil classification system (Vieira *et al.*, 1981). Spatial properties of field soils vary in a complex manner, especially, in arid and semi-arid areas, where this variability affects plant quality and crop production (Berndtsson and Bahri, 1996). Jafarzadeh *et al.* (2010) evaluated some physical and chemical properties and their spatial variability and frequency distribution within and between landforms and reported that the spatial distribution of soil properties at the field and watershed scale (region scale) affects yield potential, hydrologic responses, and transport of herbicides to surface and/or groundwater. They went further to suggest that strong spatial dependence could be due to the effects of intrinsic factors such as parent material, relief and soil types. Also, soil properties variations result from variation in depositional environments and/or differences in pedogenic or hydrologic processes for different landform positions, and so it can be affected by flood irrigation, fertilizer addition, and high water table level or agricultural practices. These effects may cause data departure from normal distribution and cause skewness (positive or negative) for soil mapping unit.

Soil variability is often considered to be composed of *"functional"* (explained) variations in addition to *"random fluctuations or noise"*. Nonetheless, the distinction between these two components is scale dependent because increasing the scale of observation almost always reveals structure in the noise (Burrough, 1983). In agreement with this description, the *"nature of variability"* is considered as a qualitative term describing the kind of variability in contrast to quantitative terms such as variance or correlation length which describes the *"amount of variability"*. Specifically, the nature of variability may be represented as deterministic and/or stochastic (Philip, 1980; Rao and Wagenet, 1985), but the total variability of a given parameter is a composite of the deterministic and stochastic components. An important special case is when homogeneity or no variability is assumed (Seyfried and Wilcox, 1995). In the case of deterministic variability, various soil properties vary spatially and possibly, temporally in a known way (Philip, 1980). Spatial variation may be "known" or deterministic from:

- Theoretically derived relationships
- Empirically observed and described relationships
- Mappable trends

Deterministic descriptions of variability result in exact parameter values for specific field locations. Stochastic variability is essentially random. In the most common form, this randomness is assumed to be independent of position or stationary. Stochastic descriptions of variability result in estimates of the probability of a certain parameter value occurring at a given field location. In simplest cases, areas may be represented by *"effective"* mean values, but more generally a probability distribution function would be required (Seyfried and Wilcox 1995). In reality, spatial variability is rarely entirely deterministic or stochastic. Within any deterministic trend or distribution of parameter values, there is invariably some degree of uncertainty or a stochastic component. Similarly stochastic variation may be non-stationary, containing systematic trends or be composed of nested deterministic variability. As the name implies, scale (or scale of interest) refers to the size of the area under consideration which is simply the effect of altering the size of the study area (Seyfried and Wilcox 1995).

Technologies, such as crop yield monitoring systems (Eliason *et al.*, 1995) and site-specific fertilizer applicators (Persson and Bangsgaard, 1999), remote sensing from satellites, aircrafts and tractors and sophisticated crop and soil sensors (Viscarra Rossel and Mcbratney, 1997) have, in consequence, been developed to help farmers better manage their fields utilizing spatially varying prescription intensities based on localized plant growth requirements or deficiencies (Mulla and Schepers, 1997; Stafford, 1997).

2.2 Spatial variability of soil physical properties

Spatial variability of soil physical properties within or among agricultural fields is inherent in nature due to geologic and pedologic soil forming factors, but some of the variability may be induced by tillage and other management practices (Iqbal *et al.*, 2005). They further and documented that these factors interact with each other across spatial and temporal scales and are further modified locally by erosion and deposition processes.

2.2.1 Soil moisture content

Soil moisture occurs as a balance between the competing demands of the atmosphere, vegetation, and gravitational drainage (Williams *et al.*, 2009). The soil water content is a variable of great importance in various hydrological processes including land-atmosphere interactions (evaporation and precipitation), flooding, erosion, solute transport and others (Georgakakos, 1996), which, in turn, are relevant in many different fields as hydrology, meteorology, agriculture, civil engineering and so on.

Soil moisture content and its form of availability are crucial for the growth and development of plants. It influences the dissolution, absorption and transportation of plant nutrients, soil biological activity, soil temperature variation and oxidation and reduction state of soil matrix (Adhikari *et al.*, 2009). Hydrologists have, thus, recognized the critical role of soil moisture and tried to develop models that extend the point-scale or local-scale physics of soil hydrology to the larger domains of mesoscale meteorological and global circulation models (GCMs) (Mohanty *et al.*, 2002).

On top, surface soil moisture exhibits an important variability in terms of spatial and temporal domains, which may result in critical uncertainties for agricultural water management (Hu *et al.*, 2008). Spatial distribution and movement of water in the soil vary both vertically and laterally due to evapotranspiration (ET), irrigation and precipitation, influence by topography, soil depth, texture, and structure, depth of water table, SOM content, temperature and other climatic parameters and vegetation (Oldak *et al.*, 2002; Adhikari *et al.*, 2009). Soil moisture content can vary in deterministic or stochastic ways or in a combination of the two (Seyfried and Wilcox, 1995; Western *et al.*, 1999), therefore, it can be expressed in the form of a map or mathematical relationship with spatial data such as topography or land use type (Qiu *et al.*, 2001).

This spatial variability in soil system depends on the volume and distribution of water in soil because it may decrease with the increase in soil moisture content (Adhikari *et al.*, 2009), and it is a necessary and preliminary part for parametric soil and land survey (McKenzie and Austin, 1993), spatial prediction of soil moisture (Lark *et al.*, 1999), soil and land evaluation for sustainable use (Fu *et al.*, 2000), specific farm planning and management (Odeh *et al.*, 1994; Lark *et al.*, 1999), hydrological modeling and watershed management (Jordan, 1994; Western and Grayson, 1998) and climate models (Robock *et al.*, 1998).

The spatial and temporal distribution of soil moisture control numerous catchment processes including runoff generation, groundwater recharge, ET, soil respiration, and biological productivity (Williams *et al*., 2009). Shallow surface soil moisture is a key status variable in hydrologic processes on the land surface, which tends to be variable in both time and space (Hu *et al*., 2008). Top layer soil moisture variability can be controlled by a large number of factors, such as vegetation (Reynolds, 1970), soil properties (Hawley *et al*., 1983) and topography (Western and Blöschl, 1999). Therefore, relationships between soil moisture and environmental factors need to be studied in a variety of places and over a large range of scales (Qiu *et al*., 2001). It may be limited to estimate the catchment mean soil moisture using a small number of sampling sites (Owe *et al*., 1982).

Land use, an alternative attribute that is easily obtained, also plays an important role in controlling spatial patterns of soil moisture by influencing the infiltration, runoff and ET, particularly during the growth season (Fu and Chen, 2000; Fu *et al*., 2000). The difference in transpiration of vegetation resulting from land use can eliminate the effects of topography, particularly, aspect (Ng and Miller, 1980). Thus, knowledge of the land use can improve the extent of the prediction power of environmental indices. It is, therefore, not clear-cut to make out the different dominating processes or factors influencing soil moisture distributions along different study areas since the dominating factors may also be different under different soil moisture conditions (Famiglietti *et al*., 1998; Leij *et al*., 2004). For this reason, knowledge of the characteristics of soil moisture variability is essential for calibration and validation of satellite based soil moisture products (Entekhabi *et al*., 1999; De Lannoy *et al*., 2006), understanding and predicting many hydrologic processes (Western *et al*., 2004), land surface processes that vary based on topography, soil texture and vegetation at different spatial and temporal scales (Teuling and Troch, 2005).

2.2.2 Other soil physical properties

Variation in soil texture and structure are very common phenomena which directly influence the yield potential of any site. Textural variability may contribute to the variation in nutrient storage and availability, water retention, availability, transport, binding and stability of soil aggregates and the like, hence, may influence yield potential of any site (Adhikari *et al.*, 2009). Warrick and Gardner (1983) found a significant impact of this variability on soil performances and therefore on crop yield. Similarly, Tanji (1996) has shown that among the different soil physico-chemical properties measured, variability in soil texture component is a primary soil factor influencing crop yield. This may be influenced by nature and properties of parent material, type of land management practices and other processes like erosion and sedimentation. Additionally, soil properties of the plough layer may show less variability than the lower horizons through mixing by tillage operations (Adhikari *et al.*, 2009).

Crave and Gascuel-Odoux (1997) found that variation in soil moisture content was directly related to the soil textural variability. These findings clearly show that soil texture is a property of primary concern. Hence, there is a great need to investigate the spatial variability of this important soil property through more precise quantification techniques to refine and support different agricultural and land use management practices (Adhikari *et al.*, 2009).

The structure in a cropped land may be different from soils of rangeland or pastures. Compacted soils have degraded structure while pulverized soils may show good structure. Soil structure governs the biological activity, physical penetration, growth and anchorage of roots, air and water movement, porosity and so on (Adhikari *et al.*, 2009). Likewise, pore structure of soil aggregates affects the storage of water and its availability for plants. These characteristics are largely influenced by management systems and soil compaction (Horn, 2004; Lipiec *et al.*, 2006).

2.3 Spatial variability of soil hydraulic and hydrologic properties

The hydraulic conductivity of a soil is a measurement of its ability to transmit water; moisture constants related to the water retention curve show the ability of the soil to store water (Klute and Dirksen, 1986) and it is one of the most important soil physical properties for determining infiltration rate, irrigation frequency, drainage practices and other hydrological processes. Hydraulic conductivity is not an exclusive property of the soil alone, since it depends on the properties of the soil and of the fluid together (Gülser and Candemir, 2008) and may change as water permeates and flows in a soil due to various chemical, physical and biological processes.

Some soil physical characteristics, which affect hydraulic conductivity, are the total porosity, the distribution of pore sizes, and the pore geometry of the soil (Hillel, 1982). Many extrinsic factors (such as traffic, vegetation, or land use) and intrinsic factors (such as soil types, pore size distribution) are responsible for the variation of soil physical and hydraulic properties from field to field in a watershed (Gupta *et al.*, 2006). Field observations show that the hydraulic properties of soils vary significantly with spatial location even within a given soil type (Warrick and Nielsen, 1980). This variability in hydraulic conductivity as well as water retention characteristics of the soil have been reported to have an enormous control on the vertical and lateral water transmission properties (Mohanty *et al.*, 2002). Gupta *et al.* (2006) studied hydraulic conductivity at different soil depths under tillage and no-tillage conditions and concluded that spatial variability is higher on the surface than the subsurface.

2.3.1 Saturated hydraulic conductivity (K_s)

Among the hydraulic properties of the soil, saturated hydraulic conductivity (K_s) is one of the most important properties that affect the water and chemical movement within or through the soil (Kumar *et al.*, 1994). The saturated hydraulic conductivity (K_s) has been recognized as a highly spatially correlated variable than other soil physical and hydraulic characteristics and the modeling process requires estimation of representative values of this parameter for every field or sub-basin in a watershed (Gupta *et al.*, 2006). Studies indicate that preferential flow paths and spatial variability in the K_s of the soil significantly influence the chemical transport from agricultural fields to shallow groundwater (Kanwar *et al.*, 1991).

Rahman *et al.* (1996) examined the spatial variability of soil properties across the landscape and concluded that the geostatistical techniques provide a better description of the nature of variability in soil properties than conventional statistical techniques such as variance and regression analysis. Most studies have highlighted the spatial variability of K_s only in one direction, either along the slope or across the slope, but very little attention has been given to the variations in K_s along ~~and across~~ the slope (Gupta *et al.*, 2006).

2.3.2 Infiltration characteristics

Soil hydrology is a component of the environment that could play a strong role in shaping tropical forest structure and composition (Jirka *et al.*, 2007). Infiltration, the term applied to the process of water entry into the soil, generally by downward flow through all or part of the soil surface is known to represent the main hydrological process. The rate of this process, relative to the rate of water supply, determines how much water will enter the root zone, and how much, if any, will run off (Hillel, 1998). Water infiltration is a driving force influencing crop growth, soil erosion, and chemical leaching processes. Knowledge of the relative precision and accuracy of infiltration models is needed for best characterization of the infiltration parameters (Clausnitzer *et al*., 1998).

Agricultural operations like tillage have influenced greatly the local surface runoff, infiltration and surface storage by altering soil hydrologic properties and soil surface roughness (Mwendera and Feyen, 1993). Tillage generally increases infiltration by increasing soil porosity and breaking up crusts. In addition, the ditch and the drain networks influence the water transfer from the fields to the catchment outlet (Hughes and Sami, 1992).

A single infiltration rate or a lumped average is often used to define the infiltration capacity of a watershed without considering the location of areas of high and low infiltration capacity (the variability) (Morin and Kosovsky, 1995). Lumping of distributed parameters can lead to distortions in the results of distributed process based models (Lane *et al.,* 1995). Measurement of the variability of vegetation and soil properties is relatively easy; quantifying the effects of that variability on the infiltration process and subsequent impacts on runoff generation is difficult. This is due in part to difficulty in measuring the infiltration process. Due to this variation in space, soil sampling or measurements at a finite number of places often give incomplete pictures (Heuvlink and Webster, 2001). Spatial variability of infiltration is first attributed to the inherent heterogeneity of the soil infiltration characteristics, and second to the method of measurement itself (Aboulabbes, 1984; Jury, 1985; Merzougi, 1982). Famiglietti *et al.* (1998) demonstrated the effects of soil heterogeneity on flux rates using a distributed catchment-scale water balance model and found that soil properties are equally or even more important for controlling upward (evapotranspiration) and downward (infiltration) fluxes than topography, vegetation, or precipitation, with the relative importance depending on the antecedent moisture content and the wetting or drying sequence of the soil.

2.4 Spatial variability of crop yield

Variations in crop yield are common in agricultural fields and these variations could be due to ground-, climate- and input-related factors and their interactions or crop genetics and biotic (such as insect pests and other pathogens) and abiotic components (such as soil factors) (Yang *et al.*, 1998; Adhikari *et al.*, 2009). Soil properties like available water, texture, bulk density, clay content, organic carbon, pH, subsoil acidity and soil thickness have been found to affect crop yield. Other factors like variation in soil fertility and hydraulic properties, slope position and orientation of the land are also found to affect crop yield (Adhikari *et al.*, 2009). Drainage probably causes more variability in the yield of certain crops than any other factors, hence, erosion and sedimentation can influence yield significantly (Adhikari *et al.*, 2009).

Crop yield is the cumulative effect of all such variations, therefore, considering crop as the sensor of its own environment, the crop yield data could be used to understand the field variations and manage it in a site-specific manner (Legg and Stafford, 1998). However, some of the yield influencing factors such as input and climate vary significantly from season to season. Consequently, crop yield in a field could be quite different from year to year even if the crop is same, hence, the yield of one season is not a reliable indicator of the field variations and accumulation of yield data from a number of seasons and crops in the same field can provide an excellent means of gaining a precise understanding of the field and yield variations (Plant, 2001).

Schepers *et al.* (2004) observed not only significant within-field spatial variability, but also significant temporal variability in grain yield and accredited the temporal variability in grain yields to be likely due to the marked differences in total growing season precipitation among years, with the driest (2000) and wettest (1999) seasons receiving 62 % and 124 % of average precipitation, respectively. Machado *et al.* (2002) observed changes in spatial yield patterns from year to year and concluded that they were expectedly due to the interaction of soil factors influencing crop yield with climate variability. Spatial and temporal variability of crop factors within a field, thus, can have a significant influence on agricultural production (Zhang *et al.*, 2002) by reducing yield and quality of produce (Raine *et al.*, 2005).

According to Moore *et al.* (1993) and Gessler *et al.* (2000), soil factors that influence crop yield include landscape factors controlling water distribution (viz., elevation and slope), physical properties affecting water-holding capacity (viz., texture and bulk density), and chemical properties affecting fertility (i.e., pH, EC, and OM). Khakural *et al.* (1998) reported on lower yields of corn and soybean at eroded slopes. Topography is regarded as one of the most important factors affecting yields (Changere and Lal, 1997) and as a source of easily obtained information that is useful for soil and field characterization (Odeh *et al.*, 1994; de Bruin and Stein, 1998).

2.5 Addressing spatial variability

2.5.1 Scaling

According to Bonsu and Laryea (1989), one way to deal with the problem of variability is by using scaling approach. Scaling factors have, thus, been described as simple conversion factors that relate the characteristics of one system to the corresponding characteristics of another (Tillotson and Nielsen, 1984; Bonsu and Laryea, 1989). The definition of scaling factors comes from the work of Miller and Miller (1956). They introduced the similar media concept (microscopic geometric similitude or Miller similitude) which is based upon assumptions concerning the microscopic geometric structure of porous media ("capillary flow" of fluids in porous media). Similar media differ only in the scale of their internal microscopic geometries and have therefore equal porosities.

The fundamental concept underlying the algorithm is that two media M_1 and M_2 are similar when the variables that describe the physical phenomena that occur within them, differ by a linear factor λ, called microscopic characteristic length, which relates their physical characteristics (Reichardt *et al.*, 2003). Similitude then results from the use of this length scale as a factor to render transport coefficients and potentials for water in porous media in a scaled form (Sposito and Jury, 1990). The best way to visualize this concept is to consider M_2 as an amplified (or reduced) photograph of M_1 by a factor λ. For these media, the particle diameter of one is related to the other by: $D_2 = \lambda D_1$. The surface of this particle by: $S_2 = \lambda^2 S_1$, and its volume by $V_2 = \lambda^3 V_1$. Because the particle and void geometry is magnified without reorientation or shape change, the characteristic length scale λ can characterize the relative magnification of a particular region relative to the reference region. Under these conditions, if the flow of water through M_1 is known, it would be possible to estimate the flow through M_2, based only on λ (Reichardt *et al.*, 2003).

For such a medium, the hydraulic and retention properties of any region i can be calculated from those of the reference region (where $\lambda = 1$) (Jury *et al*., 1984). In principle, the similar media concept allows results, either experimental or computed, of soil water behaviour in one soil to be used to describe the behaviour in another by employing reduced variables defined in terms of appropriate microscopic characteristic lengths. Using artificial porous media (glass beads), Klute and Wilkinson (1958) and Wilkinson and Klute (1959) obtained results on water retention and hydraulic conductivity that validated the similar media concept.

The single objective of scaling, therefore, is to coalesce a set of functional relationships into a single curve using scaling factors that describe the set as a whole. The scaling approach has, thus, been extensively used to characterize soil hydraulic spatial variability, and to develop a standard methodology to assess the variability of soil hydraulic functions and their parameters. The purpose of scaling, for that reason, simplifies the description of statistical variation of soil hydraulic properties. By this simplification, the pattern of spatial variability is described by a set of scale factors α_i relating the soil hydraulic properties at each location i to a representative mean (Hopmans 1987). Thus, the philosophy behind the application of scaling methods to water in field soils has been either to simplify the task of making replicate measurements on a field or to help calibrate a field-wide transport model formulated from scaling relationships (Warrick and Nielsen, 1980).

Methods to determine scale factors were described by Warrick *et al*. (1977) and Russo and Bresler (1980). These methods are based on regression analysis and can also be described as functional normalization methods (Tillotson and Nielsen, 1984). Peck *et al*. (1977), Lascano and Van Bavel (1982), and Ahuja *et al*. (1984) have shown how the distribution function of scale factors can be used to assess the effects of variable soil hydraulic properties on soil water flow. The procedure consists of using scaling factors to relate the hydraulic properties at a given location to the mean properties at an arbitrary reference point. This physically based scaling concept provides for the simultaneous scaling of the soil water retention (Kosugi and Hopmans, 1998) and unsaturated hydraulic conductivity functions (Tuli *et al.*, 2001), leading to scaled mean soil hydraulic soil functions for each structural unit, to serve as effective soil hydraulic functions (Mohanty *et al.*, 1997).

2.5.2 Fractal Geometry analyses

A fractal is a shape made of parts similar to the whole in some way (Addison, 1997), i.e. they are shapes in which parts of the shape resemble the whole shape in some way (Strecker, 2004). Thus, the basic premise upon which fractal concepts are based is the notion of self-similarity. The term self-similarity (or statistical self-similarity) implies that regular (or statistically regular) patterns appear in nature at all scales of observation. For example, a coastline exhibits statistical self-similarity since irregularities (bays, estuaries, wave scallops) can be found at any scale of observation. This definition has been warily and roughly formulated, in that it does not pin down the term fractal in such a way that some objects that look like fractals are excluded from the definition (Mandelbrot, 1982).

In place of a more specific definition, two qualities are frequently associated with fractals: *invariance under displacement* and *invariance under scaling*. For an object to be invariant under displacement, different regions of the object must look similar to each other. For an object to be invariant under scaling, magnifications of parts of the object at different levels of scaling must look similar to the whole object. It is clear from this description that, on some levels of scaling, particle paths are self-similar (Mandelbrot, 1982). A function is statistically self-similar if the statistical properties of the function scale with the length of time for which the function is observed (Addison, 1997).

The concept of fractals (Mandelbrot, 1982; Feder, 1988) and fractal scaling offers another viewpoint on quantifying the spatial variability of soil properties. A fundamental property of fractals that is of practical importance in its application to transport in porous media is that quantities such as mass, length, area, and volume (and other quantities such as density that are derived from these basic quantities) do not have intrinsic values. Fractal dimensions of the solid matrix (i.e., soil particle size distribution and soil texture) and the void phase (i.e., soil pore size distribution and soil pore surface) can characterize the fractal nature of soils (Tyler and Wheatcraft, 1992; Fazeli *et al.*, 2010).

Among objects classified as fractals, the fractal dimension of the object is usually (but not always) a non-integer dimension greater than its topological dimension (which is related to the shape of an object and remains the same for the object irrespective of deformations involving such motions as stretching, shrinking, bending, but without tearing and without identifying any distinct points) (Baker, 1997; Strecker, 2004). Empirically, the fractal dimension can be visualized as a degree of the crinkliness or degree of convolution of an object (Addison 1997). Many types of fractal dimension exist, including the similarity dimension, the divider dimension, the Hausdorff dimension, the box counting dimension, the correlation dimension, the information dimension, the point wise dimension, the Lyapunov dimension, and others (Strecker, 2004).

As the names suggest, different dimension measures emphasize different aspects of the fractal object and may yield different results. What all of these dimension measures have in common is that they probe the fractal object to discover how much of it there is. The amount of space the object occupies is closely tied to the way that the object expresses its invariance under scaling (Addison 1997). Among the numerous measures of fractal dimension, the most basic are the similarity dimension, the box counting dimension, and the Hausdorff dimension. Of all of these measures of dimension, the Hausdorff dimension is perhaps the most authoritative, since Mandelbrot (1982) defined a fractal as an object whose Hausdorff dimension exceeds its topological dimension. For the topologic objects, or Euclidean forms, the dimension is an integer (0 for a point, 1 for a line, 2 for a surface and 3 for a volume). The fractal dimension is, thus, a measure of the degree of irregularity of the object under consideration. It is related to the "speed" by which the estimate of the measure of an object increases as the measurement scale decreases (Reichardt *et al.*, 2003).

According to Mandelbrot (1989), the fractal geometry can be defined as the study of geometric shapes that may seem chaotic, but are in fact perfectly orderly. Fractal geometry, in contrast to the Euclidean geometry, admits fractional dimensions (Reichardt *et al.*, 2003). Fractal geometry has, thus, become an important source of scaling laws in soil hydrology. Fractal geometry focuses on geometric objects in which total length, area, or volume depends on the scale. Such objects exhibit similar geometric shapes when observations are made at different scales (Tarquis *et al.*, 2007). Fractal geometry was initially formulated and termed fractals by Mandelbrot (1982) who suggested that fractals rather than regular geometric shapes like segments, arcs, circles, spheres, etc., are more appropriate to approximate irregular natural shapes that have hierarchies of ever-finer detail and was expanded upon by Feder (1988). Fractals and the concepts of self-similar scaling have been applied to a wide range of natural processes (Feder, 1988) and in recent years, a great deal of attention has been placed on fractal scaling in porous media and heterogeneous soils.

This observation marked the beginning of the application of fractal geometry, which has become very popular during the last 20 years because of its promise to relate features of natural objects observed at different scales (Gimenez *et al.*, 1997). Fractals, have thus been defined as spatial and temporal model systems that exhibit scaling symmetry, i.e. they are constructed by repeatedly copying a pattern or "generator" on a starting object known as the "initiator" (Mandelbrot, 1982). They are characterized by a power law relation between the number and size of objects, whose exponent *D* is called the "fractal dimension". For soils, Rieu and Sposito (1991a), and Tyler and Wheatcraft (1992) showed that D values should be less than 3. However, these boundary conditions depend on soil texture, as values exceeding 3 have been obtained with the number-based model used for scaling particle size distribution (Tyler and Wheatcraft, 1989; 1992; Millán *et al.*, 2003).

Fractal scaling has been used as a fragmentation model to describe particle size distribution and soil behaviour (Tyler and Wheatcraft, 1989; 1992; Rieu and Sposito, 1991a; 1991b; Anderson *et al.*, 1998) and has been proposed as a model for soil aggregate size distribution (Perfect and Kay, 1991). Fractal geometry offers a powerful descriptive tool for soil scientists, because it provides a quantitative framework for integrating soil biological, chemical and physical phenomena over different spatial and temporal scales. In agronomic research it is used to study the dynamic processes that occur in soils (water, solute, heat and gas movements), soil structure, plant architecture and development, drainage of watersheds, etc. Fractal models that simulate soil structure (Figure 9) are also used to better understand soil behaviour. The fractal characteristic of several soil attributes has led to the use of these new technologies in substitution to several empirical procedures. (Reichardt *et al.*, 2003). Moreover, Perfect and Kay (1991) compared the performance of *D* as a statistical descriptor of fragmentation to that of the other indices. They showed that *D* was more sensitive to cropping treatments.

Fractal geometry characterizes and parameterizes scaling relationships across a range of scales. In theory, the wider the range of scales, the more reliable are the scaling parameters such as fractal dimensions or multifractal structure function. Depending on the application, the change in variability with scale may also be of interest for the cases in which changes in scale are not large. Fractal models are not meant for this type of analysis, and other tools of multiscale analysis have to be used. Ideally, they should allow one to parameterize the joint effect of small changes in location and scale on variability (Tarquis *et al.*, 2007).

2.5.3 Statistical and geostatistical techniques

Soil physicists (Rogowski, 1972, Biggar and Nielsen, 1976) have studied the variability of soil properties in conventional statistical terms (i.e. probability density function with associated moments, analysis of variance and coefficient of variation). These classical statistical procedures which assume that variation is randomly distributed within sampling units do not consider the correlation between measurements taken at different locations. Actually, soil properties are continuous variables whose values at any location can be expected to vary according to direction and distance of separation from neighbouring samples (Burgess and Webster, 1980). The coefficient of variation (CV) has commonly been used to describe the variability of these properties; however, it is only an indicator of the extent of and not the distribution of the variability over an area. Emphasis has been placed on the fact that the variations of a soil property are not completely disordered over the field and this spatial structure must be taken into account in the treatment of the data (Al-Kayssi, 2002).

Investigators have, thus, shown increasing interest in analyzing measured soil parameters for their interdependency over space, i.e., to study the dependency of a measured parameter on location in the field. In order to describe the spatial distribution of the variability, researchers began to use geostatistical methods. Geostatistical methods have been successfully used to determine the spatial variability of soil properties and sampling requirements. Therefore, geostatistical techniques can be used to analyse the spatial correlation structure of soil physical and hydraulic properties, such as % sand, % silt, and % clay, bulk density, effective porosity, organic matter content and saturated hydraulic conductivity (Nielson *et al.*, 1973; Gupta, 1993; Diiwu *et al.*, 1998).

Although soil properties show continuous changes on earth, the sample mean values for measured soil properties are commonly used to represent soil populations. There is no way to measure a property at every location within a study area. But, many soil properties produce great variations among sample values measured at several points. Therefore, classical statistical methods may not be used safely for characterizing variations in soil properties. It is assumed that samples are independent from each other and the mean value is the best representative of population mean in classical statistics (Turgut *et al.*, 2008). However, it is well known that samples taken close together may produce more related values than those far apart. That means that sample pairs produce values as a function of distance between them (Öztaş, 1995).

The fundamental aspect of the geostatistical methods is based on the idea that at some scale, the properties in the soil are in some way positively related to each other (autocorrelation) and geostatistical techniques can be applied to estimate the values of soil properties at unsampled locations. Geo-spatial statistics are, therefore based on the theory of regionalized variable (a variable distributed in space or time which exhibits a specific structure) (Webster and Oliver, 2007). Webster and Oliver (2001) recommended the application of geostatistical methods for the description and interpretation of the spatial variability of soil physical and hydraulic properties. The most important way to gather knowledge in this aspect is to prepare soil maps through spatial interpolation of point-based measurements of soil properties (Santra *et al.*, 2008).

Geostatistics often consists of variography and Kriging. Variography uses semivariograms to characterize and model the spatial variance of the data while Kriging uses the modelled variance to estimate values between samples (Journel and Huijbregts, 1978). Among the different methods of spatial interpolation of soil properties, inverse distance weighing and ordinary Kriging are most common (Weisz *et al.*, 1995). Various geostatistical interpolation techniques capitalize on the spatial correlation between observations to predict attribute values at unsampled locations using information related to one or several attributes (Adhikari *et al.*, 2009). The presence of a spatial structure where observations close to each other are more alike than those that are far apart (spatial autocorrelation) is, thus, a prerequisite to the application of geostatistics (Goovaerts, 1999).

Advantage of geostatistics is the use of quantitative measures of spatial correlation, commonly expressed by variograms (Diodato and Ceccarelli, 2005). According to Uyan and Cay (2010), a major advantage of geostatistics (especially, Kriging) is that it is more flexible than other methods used for interpolation and spatial averaging such as inverse distance weighing and deterministic splines, which are used in interpolation and contouring, or Thiessen polygons (Proximal mapping). Another advantage of geostatistics is that it provides the means to evaluate the magnitude of the estimation error. The mean square error is a useful rational measure of the reliability of the estimate. It depends only on the variogram and the location of the measurements (Kitanidis, 1996). It provides advanced tools to quantify the spatial features of soil parameters and to perform spatial interpolation (Liu *et al*., 2006), as a result geostatistical methods are used to make available suitable tools for analyzing spatial data and their use in SSLM is growing rapidly (Lark *et al*., 1999; Cassel *et al*., 2000).

2.6 Precision Farming (PF) or Site Specific Land Management (SSLM)

Relationships among crop yields, the level of input applied, and soil characteristics determine spatial variability within a field. These relationships also determine yield response variability, where yield response variability is defined as the differences in magnitudes of yield response among management zones (English *et al*., 1999; Roberts *et al*., 2000). Considering this inherent variability, management decisions should be specific to time and place, rather than rigidly scheduled and uniform (Mandal and Ghosh, 2000).

Since the evolution of commercialization in agriculture, as can be seen through the increased farm holdings or larger parcels, intensive crop cultivation, mechanization and automation in agriculture, individual and manual treatment of each parts of land in a large scale became more and more difficult or rather impossible. Then again, the cost involved increased so high that the farm income keeps on always lagging behind (Adhikari *et al*., 2009). With the enlargement of fields and intensive farming practices, it has become more difficult to take account of their local field variability manually without a revolutionary development in technologies (Stafford, 2000).

For that reason, the farmers started treating their whole field as a single management unit for uniform inputs application and management (such as fertilizers, herbicides, insecticides, fungicides and irrigation) and local variability did not get much attention (conventional agriculture), but since long, it has been recognized that crops and soils are not uniform within a given field (Cassman and Plant, 1992; Mandal and Ghosh, 2000). This uniform application of farm inputs caused reduced input use efficiency as inputs were applied in some parts of the field, which, eventually, ended up with the waste of inputs accompanied with economic losses as well as, more importantly, unfavourable environmental impacts (Mulla and Schepers, 1997). The farmers have always responded to such variability to take actions, but such actions are inappropriate and less frequent (Mandal and Ghosh, 2000).

This has led to the design of a new crop and land management idea, precision farming (PF) or site specific land management (SSLM) which campaigns for the judicious utilization of input resources to the field to alleviate the ill-effects of over and under usage of inputs and could be economically and environmentally friendly (Mandal and Ghosh, 2000; Adhikari *et al.*, 2009). Precision agriculture is, for that reason, the management of variability of yield in different points of a farm to increase the benefit and decrease the environmental damages (Shamsi and Mazloumzadeh, 2009). Fundamentally, PF acknowledges the conditions for agricultural production as determined by soil, weather and prior management across space and over time (Heimlich, 1998). PF is, therefore, a management philosophy or approach to the farm and is not a definable prescriptive system (Dawson, 1997). It identifies the critical factors where yield is limited by controllable factors, and determines intrinsic spatial variability and it is essentially more precise farm management made possible by modern technology. The variations occurring in crop or soil properties within a field are noted, mapped and then management actions are taken as a consequence of continued assessment of the spatial variability within that field (Mandal and Ghosh, 2000). Several works have provided very precise information for site-specific recommendations. However, most of the spatial variability studies about fertility are referred to soil analysis and they have been carried out in various temperate countries, e.g. UK (Blackmore *et al*., 1998), Belgium (Geypens *et al*., 1999) or in Iowa, USA (Cambardella and Karlen, 1999).

Since it is a system approach to manage crop and land selectively, according to their needs, in most cases, PF requires special tools and resources to recognize the inherent spatial variability associated with soil characteristics, crop growth and to prescribe the most appropriate management strategy on a site specific basis which farmers in developing countries cannot afford (Mandal and Ghosh, 2000; Roberts *et al*., 2000), but offers a potential step change in productive efficiency (Dawson, 1997). Hence, Precision farming technologies promise the ability to apply farm chemicals only where needed and in the appropriate amount, thus reducing the potential for pollution (Blumhorst *et al*., 1990). Thus, precision farming technology (PF) is designed to provide data and information to assist farmers when making site-specific management decisions in order to increase profit margins and ensure environmental quality.

CHAPTER THREE

3.0 MATERIALS AND METHODS

3.1 Site location and characteristics

The study was conducted at the Plantations Research station of the Department of Crop and Soil Sciences of the Faculty of Agriculture, KNUST, Kumasi. The site chosen for the measurements was located in an uprooted oil palm (*Elaies guineensis*) field, where spatial variability was predictable because of probable biological activity and the presence of dead root channels and burrows of soil animals. The area is within the semi-deciduous forest zone subjected to two growing seasons (a major and a minor season) with a bimodal rainfall pattern. The major season starts in May and is interrupted by a dry period in August. The minor season starts from September to October. Annual rainfall is about 1375 mm. Annual temperature ranges from 25°C to 35°C. The soil is well drained with a lot of gravel and belongs to the Kumasi series described as Plinthi Ferric Acrisol (FAO/UNESCO, 1990) or Typic Plinthustult (Soil Survey Staff, 1998).

3.2 Land preparation

Modified-No-tillage system was employed in the land preparation process, since the vegetation was overgrown and tall in order to maintain the soil in its natural and undisturbed state. The weeds were first slashed with a cutlass. The trash was not burnt, but was left over the soil surface. The weeds were allowed to regrow and they were then sprayed with, "Sunphosate" (Glyphosate), a non-selective herbicide.

3.3 Soil sampling and Laboratory analyses

A total field of 75 m x 40 m was gridded with a 10 m x 5 m interval in the north-south and east-west directions. The sampling grid size was chosen because a rule of thumb to be observed in the interpretation of semivariograms $\gamma(h)$ is that estimation of $\gamma(h)$ *is* considered reliable for lags not exceeding 20% of the total transect length (Nielsen *et al.*, 1997). Sample points were systematically located at the nodes of a rectangular shaped object superimposed on the field. Grid locations were established and maintained using a Global Positioning System (GPS) device. Systematic grid sampling, which is necessary where there is little prior knowledge of within-field variability and permits application of simple techniques to map attributes within fields, was employed. The method also, allows the inclusion of data in geographic information systems, analysis of relationships between multiple attribute layers and interpolation or generalization of sample data to finer or coarser grids or map units, as a basis for management decisions. Because the soil is an anisotropic medium, its horizontal and vertical variability is indisputable and cannot be overlooked, hence, horizonation, which is a fundamental feature of soils, was considered and soil samples were taken from the 0-20 cm and 20-40 cm depths from 80 intersection points.

The samples were used for the analyses of particle size, moisture content, bulk density, porosity, aeration and aggregate stability. Core samplers with cylindrical cores of 8.1 cm diameter and 20 cm length were used for undisturbed soil sample collection, while disturbed soil samples were collected in black sampling (polythene) bags with a spade. Sampling for studies on saturated hydraulic conductivity was taken from 0-10 cm and 10-20 cm depths.

Some of the disturbed samples were:

- Oven-dried at 105°C for 24 hours to a constant mass and analyzed in the Soil Science Laboratory for moisture content, or

- Air-dried and analyzed in the Soil Science Laboratory and used for particle size and aggregate stability determination.

Undisturbed samples were collected in cores and used for bulk density and saturated hydraulic conductivity determination.

3.4 Assessment of Hydro-physical Properties

3.4.1 Particle size analyses

The hydrometer method (Klute, 1986) was used in the determination of the particle size. This method was used because it allows for the non-destructive sampling of suspensions undergoing settling and also, provides for multiple measurements on the same suspension so that detailed particle-size distribution can be obtained with minimum effort. Fifty one grams (51 g) of air-dried soil from each plot were weighed into milk-shake cup bottles. Ten millilitres (10 ml) of 5 % Calgon (Sodium hexametaphosphate) alongside with 100 ml of distilled water were added to the soil. The Calgon served as a dispersing agent for the soil particles.

The mixture was shaken with a mechanical shaker for twenty (20) minutes and the content was poured into a 1000 ml measuring cylinder, the milk-shake bottle cap was rinsed with distilled water and added to the content to reach the 1000 ml mark. The cylinder with the content was shaken to distribute the particles equally throughout the suspension and first hydrometer and temperature readings were taken after 40 seconds. The suspension was left to stand for three (3) hours to allow the soil particles to settle. Hydrometer and temperature readings were taken after three hours and the percent fractions of each soil component was calculated as follows:

$$\% \boldsymbol{Sand} = \mathbf{100} - [\boldsymbol{H_1} + \mathbf{0.2}(\boldsymbol{T_1} - \mathbf{20}) - \mathbf{2}] \times \mathbf{2} \qquad (1)$$

$$\% Clay = H_2 + [0.2(T_2 - 20) - 2] \times 2 \quad (2)$$

$$\% Silt = 100 - (\% Sand + \% Clay) \quad (3)$$

Where, H_1 is the first hydrometer reading after 40 seconds; H_2 is the second hydrometer reading after three hours, T_1 is the first temperature reading after 40 seconds and T_2 is the second temperature reading after three hours. The textural class was determined using the textural triangle.

3.4.2 Bulk density (ρ_b)

The dry bulk density was determined from soil cores collected at the field with core sampler (Klute, 1986). The cylindrical metal sampler (core sampler) with a diameter of 8.1 cm and a height of 20 cm was driven into the soil vertically with the aid of wooden plank and a mallet to fill the sampler. In order to prevent compression of the soil, another cylinder of equal diameter was placed directly on top of the sampling cylinder. The sampler and its contents were then removed carefully to maintain the natural structure and packing of the soil. Soils that extended beyond the sampler were trimmed with a sharp knife and the volume of the soil was taken to be the same as the volume of the cylinder. The cylinders were covered and sent to the laboratory and oven dried at 105°C for 24 hours to a constant mass. The oven dried soils were weighed and the dried bulk densities were calculated by dividing the oven dried mass (M_s) by the total volume of the soil (V_t). Thus, the dry bulk density was calculated from the formula:

$$\rho_b = \left(\frac{M_s}{V_t}\right) \quad (4)$$

3.4.3 Total porosity (f)

Total porosity was calculated by the formula:

$$f = 1 - \left(\frac{\rho_b}{\rho_s}\right) \quad (5)$$

Where, f is total porosity, ρ_b is bulk density and ρ_s is particle density (assumed to be 2.65 g/cm^3 for all soils).

3.4.4 Aeration porosity (ξ_a)

Soil aeration porosity was calculated from the formula:

$$\xi_a = f - \theta_v \quad (6)$$

Where, ξ_a is aeration porosity, f is the total porosity and θ_v is volumetric water content.

3.4.5 Aggregate stability (ASt)

The modified wet sieving method (Kemper and Rosenau, 1986) was employed in the determination of the stability of soil aggregates for each spot and depth. Soil samples from each spot and depth were collected with a spade into aluminum containers and air dried in the laboratory. The aggregates sizes between 2 mm to 4 mm were prepared. Twenty grams (20 g) of the aggregates were weighed unto a 0.25 mm sieve. The aggregates were wetted with an atomizer spray. The sieve was immersed in water contained in a basin and gently rotated 50 times. It was ensured that the aggregates on the sieve were totally covered with water. The wet sieved aggregates were emptied into Pyrex beaker and oven dried at 105°C for 24 hours to a constant mass (M). Another 20 g sample was weighed and oven dried at 105°C for 24 hours to a constant mass (m). After oven drying, the wet sieved aggregates were divided by the sub sample to give the aggregate stability, which was expressed as a percentage, aggregate stability was calculated as follows:

$$ASt = \left(\frac{M}{m} \times 100\right) \quad (7)$$

3.4.6 Moisture content

Soil water content was determined on volume basis. Moist soil samples were taken from the field two days after a heavy rainfall when the soil was assumed to be at or near field capacity, defined as the amount of water held in the soil after the excess gravitational water has drained away and after the rate of downward movement of water has materially ceased which is attained in the field after 48-72 hours of saturation (Veihmeyer and Hendrickson, 1931; USDA-NRCS, 2008). Soil samples were collected with the core sampler and sent to the laboratory where they were weighed to find their initial masses. They were then oven-dried at a temperature of 105°C to a constant mass M_s. The loss of water upon drying constituted the mass of water M_w contained in the sample. Moisture content was determined on volume basis from the relation:

$$\theta_v = \theta_g \times \left(\frac{\rho_b}{\rho_w}\right) \quad (8)$$

Where, θ_g is the gravimetric water is content, ρ_b is the dry bulk density and ρ_w is the density of water (assumed to be 1.0 g/cm^3).

$$\theta_g = \left(\frac{M_w}{M_s}\right) \quad (9)$$

Where, M_t is total mass of moist soil is M_s is the mass of the solid components of the soil and M_w is the mass of water contained in the soil.

$$M_w = M_t - M_s \quad (10)$$

3.4.7 Saturated hydraulic conductivity (K_s)

The saturated hydraulic conductivity (K_s) measurements were made on the cores in the laboratory using the falling head permeameter method similar to that described by Bonsu and Laryea (1989). In the measurement, core samples were obtained for each spot from the 0-10 cm and 10-20 cm depths. The cores were soaked for 24 hours in water until they were saturated. A large empty can with perforated bottom was filled with fine gravel. The core was placed on the gravel supported by a plastic sieve. The whole system was placed over a sink in the laboratory and water was gently added to give hydraulic head in the extended cylinder. The fall of the hydraulic head H_t at the soil surface was measured as a function of time t using a water manometer with a meter scale. Saturated hydraulic conductivity was calculated by the standard falling head equation as:

$$K_{s=}\left(\frac{aL}{At}\right).ln\left(\frac{H_o}{H_t}\right); \qquad (11)$$

Where, a is the surface area of the cylinder, A is the surface area of the soil, H_o is the initial hydraulic head and L is the length of the soil sample. By rewriting equation (1), a regression of $ln\left(\frac{H_o}{H_t}\right)$ on t with slope $b = K_s\left(\frac{A}{La}\right)$ was obtained. Since $a = A$ in this particular case, K_s was simply calculated as:

$$K_s = bL \qquad (12)$$

3.4.8 Field infiltration

A study on the vertical infiltration was conducted in the field using the single ring infiltrometer (Klute, 1986). Before the infiltration measurements were made, soil samples were taken to determine the moisture content of the soil at each spot. A cylinder infiltrometer of 10 cm diameter was driven into the soil to depth of 10 cm with the aid of a wooden plank and a mallet. The soil surface was mulched with plant debris (dry grass and leaves) to prevent the disturbance of soil surface (dispersion and clogging of soil pores) and false measure of infiltration amount when the soil surface in the infiltrometer was instantaneously ponded with water. A constant water head of 5 cm from the soil surface was maintained in the cylinder with water from a 1000 ml (1 litre) glass measuring cylinder. The volume of water that was used to maintain a constant head of 5 cm in the infiltrometer in a chosen time was used as a representation of the amount that entered the soil at the stipulated time. The vertical infiltration was measured from the cylinder for a period of 60 minutes for each spot. The initial infiltration was measured at 30 seconds interval for the first five minutes when infiltration was very fast after which the interval was increased to 60, 180 and 300 seconds respectively as infiltration slowed down over time towards the steady state.

The cumulative infiltration amounts (I) were plotted as a function of time for each spot on a linear scale. The slopes of the cumulative infiltration amounts taken at different time scales represented the infiltration rates (i). The infiltration rates were plotted against time and the steady state infiltrability (K_o) was obtained at the point where the infiltration rate curve became almost parallel to the time axis. Plots of Cumulative infiltration amount (I) as function of the square root of time ($t^{1/2}$) for the first five minutes were performed and sorptivity (S) was obtained from the slope of each plot.

3.5 Statistical and Spatial Analyses

Data analyses were performed in two stages. First the descriptive statistics including mean, skewness and kurtosis, and second, geostatistical analysis were used to describe soil property spatial dependency.

3.5.1 Descriptive statistics

Measured variables in the data set were analyzed using classical statistical methods to obtain the minimum, maximum, mean, standard deviation (SD) and coefficient of variation (CV %) for each soil property. Characterization of CV% values as reported by Wilding (1985) was employed, where CV values from 0 to 15 % were classed as little or low variability, from 16 to 35 % were moderate variability and greater than 35 % were high variability. Paired samples t-test was used to compare the means of a variable between the top and sub layers.

To settle on whether or not data followed the normal frequency distribution, the symmetry and peakedness of the data distribution were determined using coefficients of skewness and kurtosis. A distribution that is symmetrical and Gaussian (normal) has skewness and kurtosis values of zero. Since small variations can arise, producing a chance fluctuation of skewness and kurtosis measures from zero, each soil property was validated to determine the type of distribution from which the samples were taken. Therefore, the D'Agostino-Pearson "Omnibus K2" normality test (D'Agostino, 1986), which calculates how far each of the skewness and kurtosis values differs from the value expected with a Gaussian distribution, and computes a single P value from the sum of these discrepancies at 5 % level of significance ($\alpha = 0.05$) was used. GraphPad Prism version 5.0 and SPSS version 16 were used in all these statistical analyses.

3.5.2 Scaling and Fractal Geometry analyses

3.5.2.1 Scaling of Saturated hydraulic conductivity (K_s)

Peck *et al.* (1977) defined a scaling parameter a_i as the ratio of the microscopic characteristic length λ_i of a soil at a location i and the characteristic length λ_m of a reference soil, or:

$$a_i = \left(\frac{\lambda_i}{\lambda_m}\right) \tag{14}$$

where, i = 1,….,i denote locations.

Considering the scaling factors in the similar media concept (Miller and Miller, 1956), the spatial variability of K_s has been described in Warrick *et al.* (1977), Simmons *et al.* (1979) and Bonsu and Laryea (1989). As a result of the scaling theory one can relate the hydraulic conductivity function at given water contents at a given location to a scaled mean saturated hydraulic conductivity such that for the hydraulic conductivity:

$$K_i = a_i^2 K^* \tag{15}$$

Where, K_i is the saturated hydraulic conductivity of a certain profile depth at location i, K^* is the scaled mean saturated hydraulic conductivity for the given depths and a_i is the scaling factor for location i. By setting the mean of a_i values to 1, equation (15) can be redefined to obtain K^* from a sample size of n measurements of K_i (Warrick *et al.*, 1977; Bonsu and Laryea, 1989) as:

$$K^* = \left[\frac{1}{n}\sum_{i=1}^{n}\sqrt{(K_i)}\right]^2 \tag{16}$$

Since the fractal diagram is a graphical method used to provide visual information about the distribution of a property (Hald, 1952) and one of the easiest methods to determine whether or not a set of observations is normally distributed, fractal diagrams of $ln\ K^*$

values were consequently constructed for both layers. Where, $ln\, K^*$ is the lognormal transformation of K^*.

3.5.2.2 Scaling of Cumulative infiltration amount

The scaling method was based on the linear variability theory in soil physics (Vogel *et al.*, 1991), which has its roots in the similar media concept (Miller and Miller, 1956). According to Vogel *et al.* (1991), a soil is described as linearly non-homogeneous if its hydraulic properties obey the following rules:

- The space and time variability of its hydraulic properties can be expressed in terms of a linear transformation:

$$\boldsymbol{K(T,i,h) = \alpha_K(T,i)K^*(h^*)}$$

$$\boldsymbol{\theta(T,i,h) = \theta_i(T,i) + \alpha_\theta(T,i)[\theta^*(h^*) - \theta_i^*]} \quad \textbf{(17)}$$

Where,

$h = \alpha_h(T,i)h^*$

T = an index of time and allows for temporal changes in the hydraulic functions.

$i = (x, y, z)$ is a position vector with z positive upward.

$K(h)$ and $\theta(h)$ = soil hydraulic characteristics at point i ,i.e., the hydraulic conductivity-pressure head and soil moisture-pressure head relations.

$K(h^*)$ and $\theta(h^*)$ = space and time invariant reference soil hydraulic characteristics.

α_K , θ_h and α_h = scaling factors associated with soil hydraulic conductivity, moisture content and pressure head, respectively.

θ_i = residual moisture content.

- The overall spot-to-spot variability can be decomposed into two independent components: a local (within profile) and a global (between profiles) component:

$$\alpha_K(T,I,i) = \gamma_K(T,I,i)\beta_K(i)$$

$$\alpha_\theta(T,I,i) = \gamma_\theta(T,I,i)\beta_\theta(i) \quad (18)$$

$$\alpha_h(T,I,i) = \gamma_h(T,I,i)\beta_h(i)$$

Where,

I = Index which describes global variability (profile identifier).

i = Index which accounts for local variability and describes position within the local (profile) coordinate.

γ and β = global and local components of the respective scaling factors α.

Soil profile is defined in terms of one-, two- and three-dimensional soil region and the difference between them is determined by the global component of variability. With a set of soil profiles with hydraulic characteristics that vary according to the outlined linear variability concept, it is possible to define a reference soil profile as a profile for which

$$\gamma_K = \gamma_\theta = \gamma_h = 1 \quad (19)$$

The soil hydraulic properties of this reference profile can then be fully characterised by the pair of functions, $K^{\#}(i,h^{\#})$ and $\theta^{\#}(i,h^{\#})$ obtained by combining equations (17), (18) and (19).

$$K^{\#}(i,h^{\#}) = \beta_K(i)K^{*}(h^{*})$$

$$\theta^{\#}(i,h^{\#}) = \theta_i^{\#}\beta_\theta(i)\theta^{*}(h^{*}) - \theta_i^{*} \quad (20)$$

Where,

$$h^{\#} = \beta_h(i)(h^{*})$$

Water movement in any soil profile as well as in the reference profile can be described by Richard's equation.

$$\frac{\partial\theta}{\partial t} = div[K\,(grad\,h + grad\,z) \quad (21)$$

Assuming that certain initial and boundary conditions are satisfied and that the solution for the reference profile is available, the dynamic variables for the other profiles can be determined from:

$$v(T,t,I,i) = \gamma_K(T,I)v^{\#}(t^{\#},i^{\#})$$

$$\theta(T,t,I,i) = \theta_i(T,I,i) + \gamma_\theta(T,I)[\theta^{\#}(t^{\#},i^{\#}) - \theta_i^{\#}(i^{\#})] \tag{22}$$

$$h(T,t,I,i) = \gamma_h(T,I) + h^{\#}(t^{\#},i^{\#})$$

Where,

$$t^{\#} = \frac{\gamma_K(T,I)}{\gamma_\theta(T,I)\gamma_h(T,I)}t; \qquad i^{\#} = \frac{I}{\gamma_h(T,I)}i \tag{23}$$

Since these relationships can be used to compute pressure head, Darcian flux, v and moisture content at any point of any soil profile at time t from the distribution of respective reference variables at time $t^{\#}$, they can also be regarded as a linear model to describe variability of the dynamic characteristics of a soil water system. The described concept, as a consequence, corresponds to the similar media theory for homogeneous soils (Miller and Miller, 1956), but uses three instead of one scaling factor and applies to non-homogeneous soil profiles as well. In order to avoid dependency between soil profile geometry (depth of soil profile, thickness of soil layers etc.) and soil hydraulic properties through the presence of γ_h in the position vector transformation in equation (23), the following additional constraint is necessary:

$$\gamma_h(T,I) = 1 \tag{24}$$

As a result, the variability of the scaling factor α_h is restricted to its local component $\beta_h(i)$ only and $i^{\#} = i$. The two parameters γ_K and γ_θ denote a relative measure of cross-sectional available for water flow and permeability, respectively, and together contribute greatly to soil water flow. Based on the described concept, the mutual relationship between infiltration scaling factors was determined from:

$$\gamma_v = \frac{\gamma_I}{\gamma_t} \tag{25}$$

Given a set of field-determined infiltration curves that characterize the infiltration process for a set of soil profiles, the parameters of the reference infiltration curve I^* (t^*) and the respective sets of scaling factors γ_v, γ_I, and γ_t can be determined from each measured infiltration curve approximated by Philip's (1957) equation:

$$I(t) = St^{1/2} + K_o t \tag{26}$$

Where,

I = cumulative infiltration (m),

K_o = parameter known as transmissivity factor (m/s),

S = sorptivity (m/s$^{1/2}$), and

t = elapsed time since the start of infiltration (s).

The infiltration scaling factors γ_I, and γ_t were then derived from:

$$\gamma_I = \left(\frac{S}{S^*}\right)^2 \Big/ \left(\frac{K_o}{K_o^*}\right) \tag{27}$$

$$\gamma_t = \left(\frac{S}{S^*}\right)^2 \Big/ \left(\frac{K_o}{K_o^*}\right)^2 \tag{28}$$

$$\gamma_v = \left(\frac{K_o}{K_o^*}\right) \tag{29}$$

Where, S^* and K_o^* are the arithmetic means of the individual S and K_o values for each of the measured infiltration curves. γ_I is the scaling factor for cumulative infiltration amount (I), γ_t is the scaling factor for cumulative time (t) and γ_v is the scaling factor for infiltration rate. The scaling factors were normalized by dividing the scaling factors γ_v and γ_I by their respective mean values, and the scaling factor γ_t was recalculated from equation (25).

Consequently, scaling factors γ_v and γ_I have arithmetic means of 1. The normalization of the scaling factors, thus, required new values for S^* and K_o^*. The expressions in (19, 20 and 21) were used to find the parameters for the new reference curve:

$$S_{new}^* = \left(\overline{\gamma_I}\ \frac{K_{o\ new}^*}{K_o^*}\right)^{1/2} S^* \qquad (30);$$

$$K_{o\ new}^* = \overline{\gamma_v}\, K_o^* \qquad (31)$$

Where, $\overline{\gamma_v}$ and $\overline{\gamma_I}$ are the arithmetic means of the various scaling factors before the normalization process. The parameters for the reference cumulative infiltration amount were then determined as follows: The coordinates γ_I and γ_t of each measured data point was divided by the respective scaling factors.

3.5.2.3 Fractal Geometry analysis

The variogram method was used for estimating the fractal dimension (*D*) and this assessment was based on the assumption that the selected soil property has statistical properties similar to those of fractional Brownian surfaces. The self-similar properties of fractional Brownian motion (fBm) (a biased random walk in which the walker favours certain directions at each step) were expressed by a power law variogram in the spatial domain:

$$\gamma(h) = \frac{1}{2N(h)}\sum_{i=1}^{N(h)}[Z(x_i) - Z(x_i + h)]^2 = ch^a \qquad (32)$$

Where,

$\gamma(h)$ = semi-variance at lag h

h = distance (lag)

x = position in one dimensional space

c = constant of proportionality

a = slope

For a fractional Brownian motion (fBm) model, a belongs to the interval $0 < a < 2$ and is related to the Hurst exponent, H and subsequently to D by the following relationship given by Huang and Bradford (1992):

$$a = 2H \tag{33}$$

$$D = E_d + 1 - H \tag{34}$$

Where,

E_d = Euclidean dimension: the number of co-ordinates required to identify the object (Voss, 1985; Addison, 1997).

H = Hurst coefficient with a range of $0 < H < 1$.

Under certain limiting assumptions (Sugihara and May 1990), the relationship between H and D is:

$$H = 2 - D \tag{35}$$

Since the Hurst exponent measures the scaling properties of fractional Brownian motion (fBm), the assumption is that the Hurst exponent closely relates to the fractal dimension, which also measures scaling properties. As H increases, the fBm has more persistence and the plot of the function becomes smoother and D decreases accordingly. Contrariwise, as H decreases, the fBm is more anti-persistent and the plot of the function becomes rougher and D increases (Addison, 1997). This relationship between the fractal dimension and the Hurst exponent aligns perfectly with the notion of fractal dimension as a measure of the unevenness of an object.

Table 3.1: Relationship between Fractal Dimension and Hurst Coefficient

H	D	Nature of process
> 0.5	< 1.5	Persistent
$= 0.5$	$= 1.5$	Brownian random
< 0.5	> 1.5	Anti-persistent

Source: Sugihara and May (1990).

Taking logarithms on both sides of equation (32) and by plotting it on the arithmetic graph, the semivariogram approximates a straight line. The fractal dimensions (*D*) for both hydraulic and hydrologic data were, thus, calculated as a function of slope of the log-log variogram plot (fitted line) (Burrough, 1981, 1986):

$$D = 2 - \frac{m}{2} \qquad (36)$$

Where,

D = the fractal (or Hausdorff- Besicovitch statistic) dimension that is a fractional number between 1 and 2 (Feder, 1988; Tyler and Wheatcraft, 1989). At *D* = 0 the distribution is independent of observation size, therefore, the range of variability of *D* is strictly limited to $0 < D < 3$ (Tyler and Wheatcraft, 1989; Castriganó, and Stelluti, 1999).

m = Slope of the log-log variogram.

Table 3.2: Relationship between Fractal Dimension and Nature of soil

Fractal Dimension	Nature of soil
$D = 0$	All particles are of equal diameter
$D = 3$	Number of particles greater than a given radius R_i doubles with each corresponding decrease (by half) the double mass
$0 < D < 3$	Greater proportion of particles larger than $D = 3$ (sand)
$D > 3$	Greater proportion of particles smaller than $D = 3$ (silt)

Source: Tyler and Wheatcraft (1989).

Because D is based on the analysis of semivariance, it is sensitive to the same analysis parameters that affect semivariance analysis. The fractal depiction of spatial behaviour of soil hydraulic and hydrologic properties in the field, and description of their isotropic feature and possible impact on fractal dimension were, thus, performed thus, performed with GS+ 9.0 software. Scaling and Fractal analyses were, thus performed for soil hydraulic and hydrologic characteristics in the study area.

3.5.3 Geostatistical analyses:

To perform geostatistical analyses, a number of points in the measuring grid, at least 50 - 100 is required (Burrough and McDonnell, 1998). In the study, this was fulfilled in the case of the whole field (80 grid points) and semivariogram, auto-correlation and Kriging analyses were used to examine the spatial correlation structure of bulk density, total porosity, aeration porosity, moisture content, aggregate stability, percent composition of sand, silt and clay of soil at the field scale. Owing to an often neglected fact that normality of distribution is not a pre-requisite of geostatistical processing (Kroulík *et al.*, 2006); the original data set was processed without any transformation. Prediction performance was also evaluated by cross-validation. Geostatistical analyses for each soil property were conducted using GS+ 9.0 software.

3.5.3.1 Spatial structure analyses

Investigators have shown increasing interest in analyzing measured soil parameters for their interdependency over space, (to study the dependency of a measured parameter on location in the field). Semivariograms and autocorrelograms were used to study the spatial relationships of soil properties at each sampling depth.

3.5.3.1.1 Semivariogram $[\gamma(h)]$

The semivariogram is a fundamental tool in geostatistics. The empirical semivariogram $[\gamma(h)]$ is defined as half the average quadratic difference between two observations of a variable separated by a distance vector h (Journel and Huijbregts, 1978; Warrick *et al.*, 1986; Goovaerts, 1998). It was determined for each variable to ascertain the degree of spatial variability between neighbouring observations, and the appropriate model function was fitted to the semivariogram. The structure of spatial variance between observations was, thus, derived from the sample semivariogram calculated from the formula:

$$\gamma(h) = \frac{1}{2N(h)} \sum_{i=1}^{N(h)} [Z(x_i) - Z(x_i + h)]^2 \qquad (30)$$

Where, $\gamma(h)$ is the estimated semivariance for lag h (the distance between observations), $Z(x_i)$ is the value of the random variable Z at $x = x_i$, $Z(x_i + h)$ is the value of Z at a distance h from x_i and $N(h)$ is the number of pairs of points that are a distance h apart. The spatial structure of a semivariogram $[\gamma(h) = C_o + C_1]$ can be described by three basic parameters:

- Nugget effect (C_o), which is the variance when the lag distance is zero (or a scale finer than the sampling interval) which could be due to sampling errors, micro-scale variability, and/or measurement errors.
- Structural variance (C_1), which is the portion of the total variance resulting from spatial patterns (functional or explained variation).
- Sill or total variance ($C_o + C_1$), which is the maximum variance, σ^2 (asymptote of the semivariogram model).
- Range, which is the lag distance at which the semivariogram reaches the sill, also referred to as the correlation range since it is the range at which autocorrelation becomes zero. The range marks the limit of spatial dependence, such that places further apart than the range are spatially independent.

Various semivariogram model functions have been made available in the literature to represent the structure of a set of data (Isaaks and Srivastava 1989). The commonly used semivariogram models were fitted for each soil property. These were the spherical, exponential, linear and Gaussian models (Journel and Huijbregts, 1978; Warrick *et al.*, 1986; Deutch and Journel, 1992). All pairs of points separated by distance h ($lag\ h$) were used to calculate the experimental semivariogram. Semivariograms were calculated for both isotropical and anisotropical orientations. The anisotropic calculations were performed in four directions (0°, 45°, 90° and 135°) with a tolerance of 22.5° to determine whether semivariogram functions depended on sampling orientation and direction (i.e., they were anisotropic) or not (i.e., they were isotropic). The best fit model was chosen based upon minimum residual sum of squares (RSS) for each soil property at each soil depth. Expressions for different semivariogram models used in this study are as follows:

- Gaussian model, representing a Smooth transition, defined by:

$$\gamma(h) = C_o + C_1\left[1 - exp - \left(\frac{h^2}{a^2}\right)\right]; \; h \geq 0; \qquad (31)$$

- Spherical model, representing a clear transition, indicating that one pattern (either random or functional) dominates, defined by:

$$\begin{aligned}\gamma(h) &= C_o + C_1\left[1.5\left(\frac{h}{a}\right) - 0.5\left(\frac{h}{a}\right)^3\right]; \; h \leq a \\ &= C_o + C_1; \qquad h \geq a\end{aligned} \qquad (32)$$

- Exponential model, representing a Gradual transition, defined by:

$$\gamma(h) = C_o + C_1\left[1 - exp - \left(\frac{h}{a}\right)\right]; \; h \geq 0 \qquad (33)$$

- Linear model, defined by:

$$\gamma(h) = \left[\frac{C_{o+h}(C_{o-}C_1)}{a}\right]; \; 0 < h < a \qquad (34)$$

$$= C_o + C_1$$

Where, h is the offset, a is the range and C is the sill. In all these semivariogram models, nugget, sill and range were expressed by C_o, $(C_o + C_1)$ and a respectively. In the case of exponential and Gaussian models, a represents the theoretical range. From the semivariogram the structural variance was determined, which is the spatially structured proportion of the sample variance that is not random noise or measurement error (also referred to as the degree of spatial dependence, *SD*). The spatial dependence was defined using the nugget to sill ratio (Cambardella *et al.*, 1994; Cambardella and Karlen, 1999).

$$SD = \left(\frac{C_o}{C_1 + C_o}\right) \times 100 \qquad (35)$$

If the ratio was ≤ 25 %, the variable was considered to be strongly spatially dependent, or strongly distributed; if the ratio was between 25 % and 75 %, the soil variable was considered to be moderately spatially dependent; if the ratio was greater than 75 %, the soil variable was considered weakly spatially dependent; if the ratio was 100 %, or the slope of the semivariogram was close to zero, the soil variable was considered non-spatially correlated (pure nugget or no spatial dependency). The value of *SD* was, thus, used to evaluate the spatial dependence or independence of soil properties.

3.5.3.1.2 Autocorrelation analyses

Autocorrelation is the process of self-comparison for a random function that expresses the linear correlation between the members of a spatial series and other members of the same series separated by fixed intervals of space. Spatial dependency is thus, characterised by the autocorrelation function. Autocorrelation has, as a result, been used to express spatial changes in field-measured soil properties and the degree of dependencies among neighbouring observations. The sample autocorrelation function (r_h) was estimated as given by Warrick and Nielsen (1980):

$$r_h = \left(\frac{C_h}{\sigma_E^2}\right) \quad (36)$$

$$C_h = \left(\frac{1}{n-h-1}\right)\sum_{i=1}^{n-h}(x_i - \sigma_E)\,(x_{i+h} - \sigma_E) \quad (37)$$

Where, h is the index for separation of h intervals (lag h), C_h is the auto-covariance, σ_E is the standard deviation, and $x_1, x_2, x_3 \ldots x_n$ are values of the measured soil physical properties at different locations. A plot of the autocorrelation function against the lag number h is called an autocorrelogram. The autocorrelogram has a maximum value of 1 at $h = 0$, decreases as lag increases, ranges from +1 to -1 and is dimensionless. The rate of decay of the autocorrelogram depends on the degree of dependency of the variable upon its neighbouring values. Thus, for strongly dependent variables, the autocorrelogram will decay slowly, whereas for weakly dependency, the decay will be rapid. The range over which samples of the variable exhibit spatial structure is distance from $h = 0$ to the lag at which r_h no longer decreases. An autocorrelogram is, thus, a useful tool in determining the correlation between successive observations (Haan 1977) and the average distance over which observations are correlated (Gupta *et al.*, 2006).

3.5.3.2 Kriging and Cross-validation

Kriging is an interpolation (estimation of values from points that are not actually sampled) technique based on best linear unbiased estimate (Deutch and Journel, 1992; Geostat workshop, 1995). Semivariograms were applied to calculate the best linear unbiased estimate at locations where no measurements were available. This feature offered a measure of the estimation precision and reliability of the spatial variable distribution (Theodossiou and Latinopoulos, 2006). The random variable Z at a particular point x_i was estimated by interpolating values of Z around those points that were within the range of correlation. Thus, a linear estimator $Z^*(x_o)$ as defined by (Journel and Huijbregts, 1978):

$$Z^*(x_o) = \sum_{i=1}^{n} \lambda_i Z(x_i) \quad (38)$$

with;

$$\sum_{i=1}^{n(x_o)} \lambda_i = 1 \quad (39)$$

Where, n is the number of locations where measurements were made, $Z(x_i)$ are measurements selected in the x_o neighborhood for performing the estimation of $Z^*(x_o)$, $Z^*(x_o)$ is the Kriging estimate at location x_o, and λ_i are the weights associated with the distance between x_o and x_i. The following two conditions were required for computation of λ_i:

- Nonbiased condition: $E[Z^*(x_o) - Z(x_o)] = 0$ **(40)**

- Condition of minimum estimation variance given in expected value notation as to minimize $E[Z^*(x_o) - Z(x_o)]^2$ **(41)**

Accuracy of the soil maps was evaluated through cross-validation approach (Davis, 1987). Cross Validation allowed the comparison of estimated and actual values using the information available in the sample data set. The sample values were temporarily discarded from the sample data set; the value was then estimated using the remaining samples and the estimates were compared to the actual values. Clark (1986) recounted the history of validation and its usefulness in geostatistics and pointed out that this type of comparison was used to compare methods of estimation (David, 1976; Journel and Huijbregts, 1978) and to justify the use of Kriging as an estimation method (Parker *et al.*, 1979) and went further to establish that, the use of cross-validation for selecting a semivariogram model may be acceptable, but may not be sensitive enough to be very useful.

The evaluation indices used in this study were the regression coefficient, standard error (SE), correlation coefficient, Y-intercept and SE of prediction.

- The regression coefficient represents a measure of goodness-of-fit for the least-squares model describing the linear regression equation. A perfect 1:1 would, therefore have a regression coefficient of 1.00 and the best-fit line (the solid line in the graph) would coincide with the dotted 45° line on the graph.
- The standard error (SE) refers to the standard error of the regression coefficient.
- The r^2 value (square of the correlation coefficient) represents the portion of variation explained by the best-fit line.

CHAPTER FOUR

4.0 RESULTS AND DISCUSSION

4.1 Descriptive statistics

The measurements obtained from the experiment are presented in the following Tables and Figures. The results indicate substantial within-field variability in soil properties that would be overlooked when treated on the bases of averages in a whole field approach to management. Paired sample t-tests ($P < 0.05$) with two-tailed P value (shown in the Appendices A - C), also showed significant differences between the means of measured soil properties at both sampling depths. Therefore the observed differences could not have arisen by chance. The analysis also showed that pairing was effectively significant.

4.1.1 Soil Physical properties

Spot-to-spot variations in soil physical properties as observed for the measured descriptive statistical values are presented in Table 4.1. The results showed significant differences between mean values at both sampling depths across the field. This variation could be ascribed to a combination of factors including experimental error, temporal and spatial variations. As reported by Federer (1982), the distinctions between different horizons are often arbitrary and therefore would vary with investigator and field conditions such as moisture. Figs.1 (a-h) also display histograms with normal curves built on all the data available for the particular soil properties.

Table 4.1: Summary of descriptive statistics of measured soil physical properties

Soil property	Depth (cm)	Descriptive statistic							
		Min.	Max.	Mean	SD	‡CV (%)	Skew.	Kurt.	†K2
Sand (%)	0-20	60.80	86.80	78.31	5.98	7.64^{c}	-0.57	0.073	4.41^{ns}
	20-40	40.80	84.80	74.16	8.14	10.98^{c}	-1.35	3.11	27.93***
Clay (%)	0-20	8.00	36.00	14.50	5.65	38.98^{a}	1.60	2.76	31.46***
	20-40	10.00	44.00	21.06	7.43	35.28^{a}	1.01	0.89	13.88***
Silt (%)	0-20	3.20	17.20	7.24	3.37	46.50^{a}	0.81	0.17	8.28*
	20-40	1.20	17.20	4.75	2.76	58.11^{a}	1.37	4.03	31.15***
ρ_b (g cm^{-3})	0-20	1.204	1.517	1.409	0.064	4.51^{c}	-0.45	0.045	2.88^{ns}
	20-40	1.326	1.575	1.476	0.048	3.26^{c}	-0.59	0.89	6.98*
f (%)	0-20	42.75	54.57	46.82	2.40	5.12^{c}	0.45	0.048	2.88^{ns}
	20-40	40.57	49.96	44.31	1.82	4.10^{c}	0.59	0.90	7.08*
ξ_a (%)	0-20	20.40	53.25	35.62	4.30	12.08^{c}	0.40	3.98	15.05***
	20-40	23.65	40.10	31.62	3.07	9.70^{c}	0.15	0.61	1.74^{ns}
θ_v (%)	0-20	6.64	17.52	11.33	2.24	19.81^{b}	0.18	-0.064	0.49^{ns}
	20-40	7.78	17.44	12.68	2.33	18.33^{b}	-0.01	-0.45	0.80^{ns}
ASt (%)	0-20	19.86	19.98	19.93	0.032	0.16^{c}	0.00	-0.49	1.01^{ns}
	20-40	19.71	19.93	19.83	0.061	0.13^{c}	0.00	-0.68	2.91^{ns}

*ρ_b (g cm^{-3}) = Bulk density; f (%) = Total porosity; ξ_a (%) = Aeration; θ_v (%) = Volumetric water content; ASt (%) = Aggregate stability; Min. = Minimum value; Max. = Maximum value; SD = Standard deviation; Kurt. = Kurtosis; Skew. = Skewness; ‡CV (%) = Coefficient of variation (a, b, c = Very high, moderate and weak variations, respectively); †K2 = D'Agostino and Pearson "Omnibus" Normality Test value (***, **, *, ns = Highly significant, moderately significant, significant and not significant, respectively).*

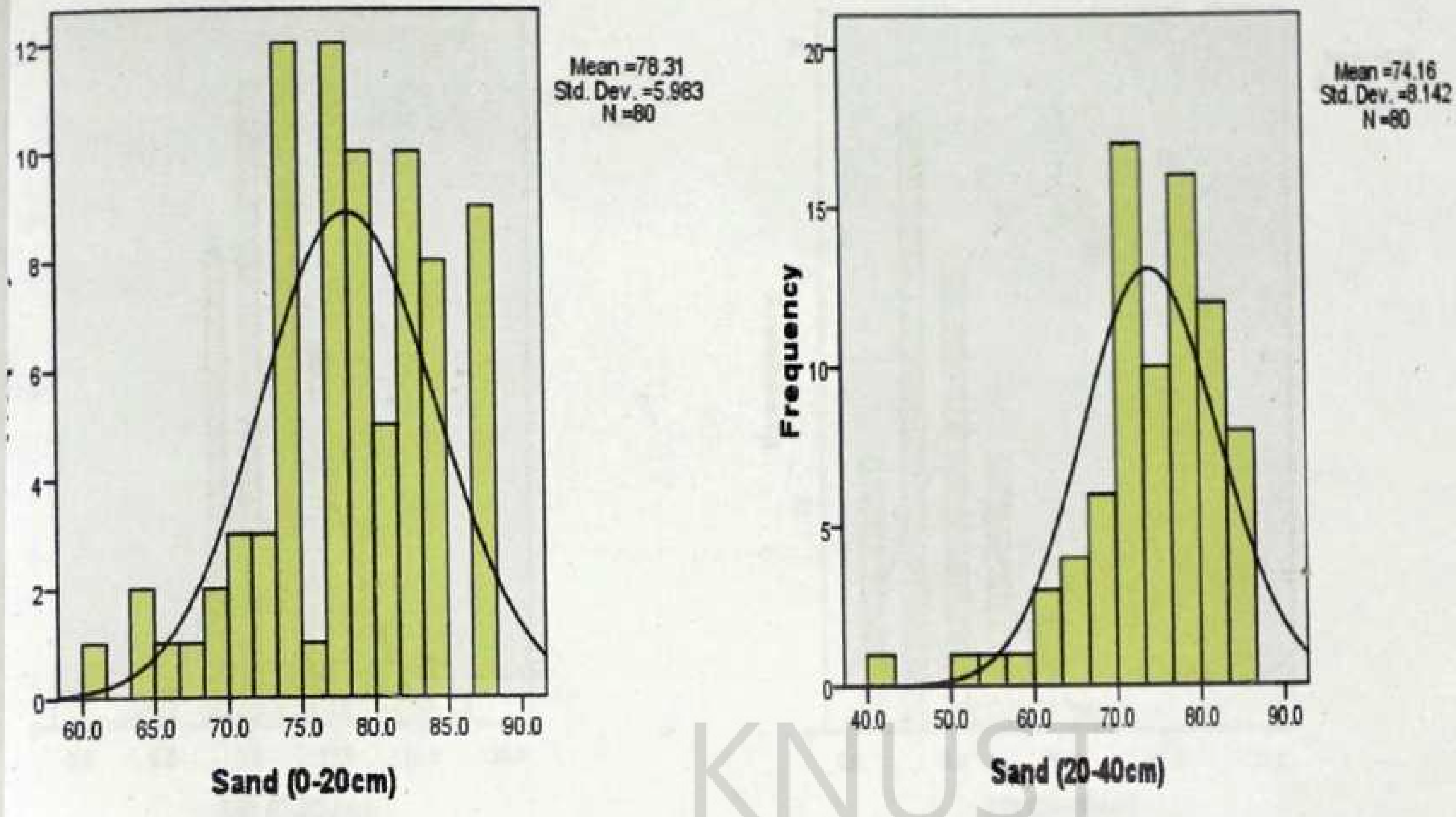

Fig.1a: Histograms of sand content in both layers of sampling.

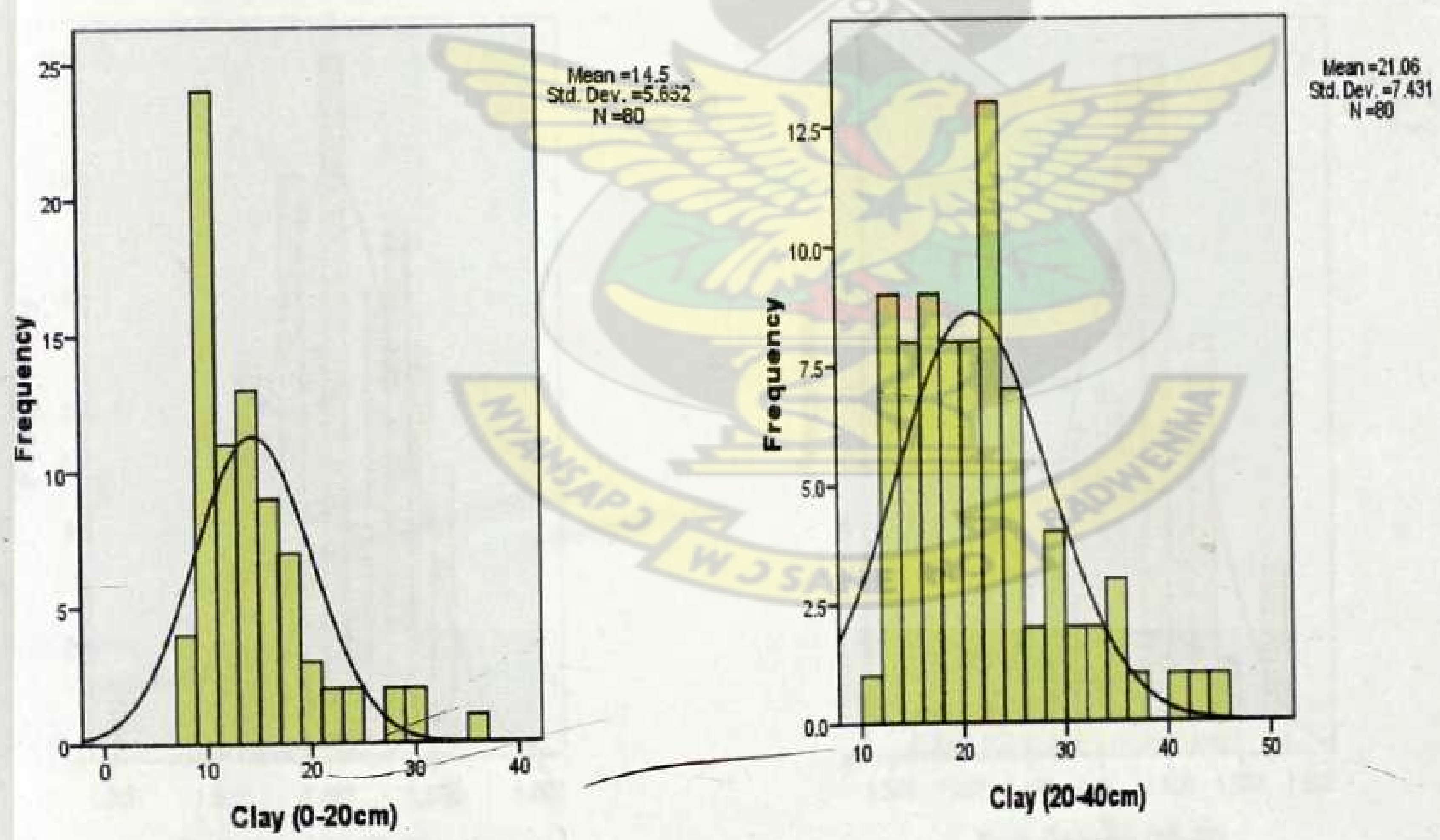

Fig.1b: Histograms of clay content in both layers of sampling.

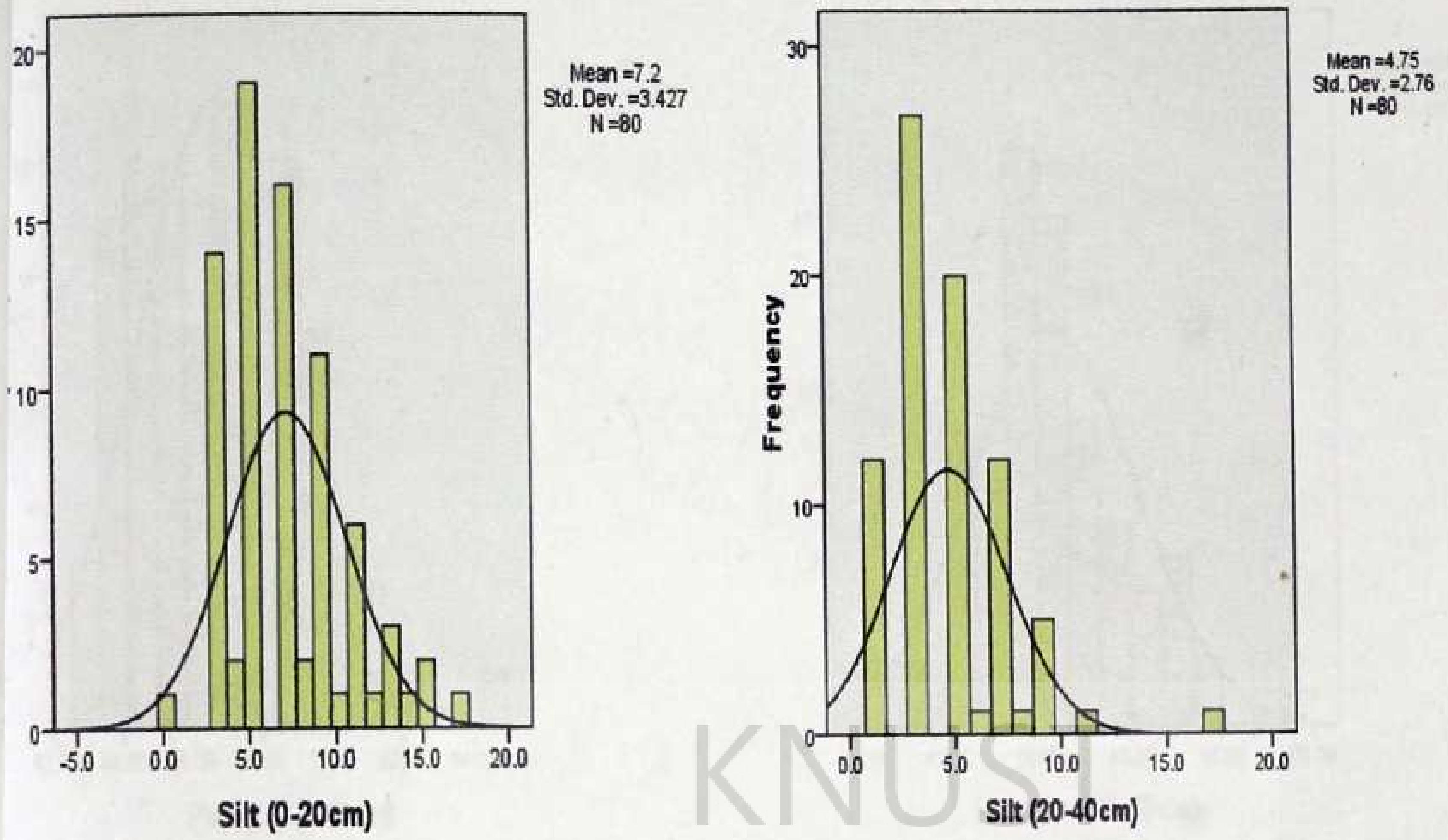

Fig.1c: Histograms of silt content in both layers of sampling.

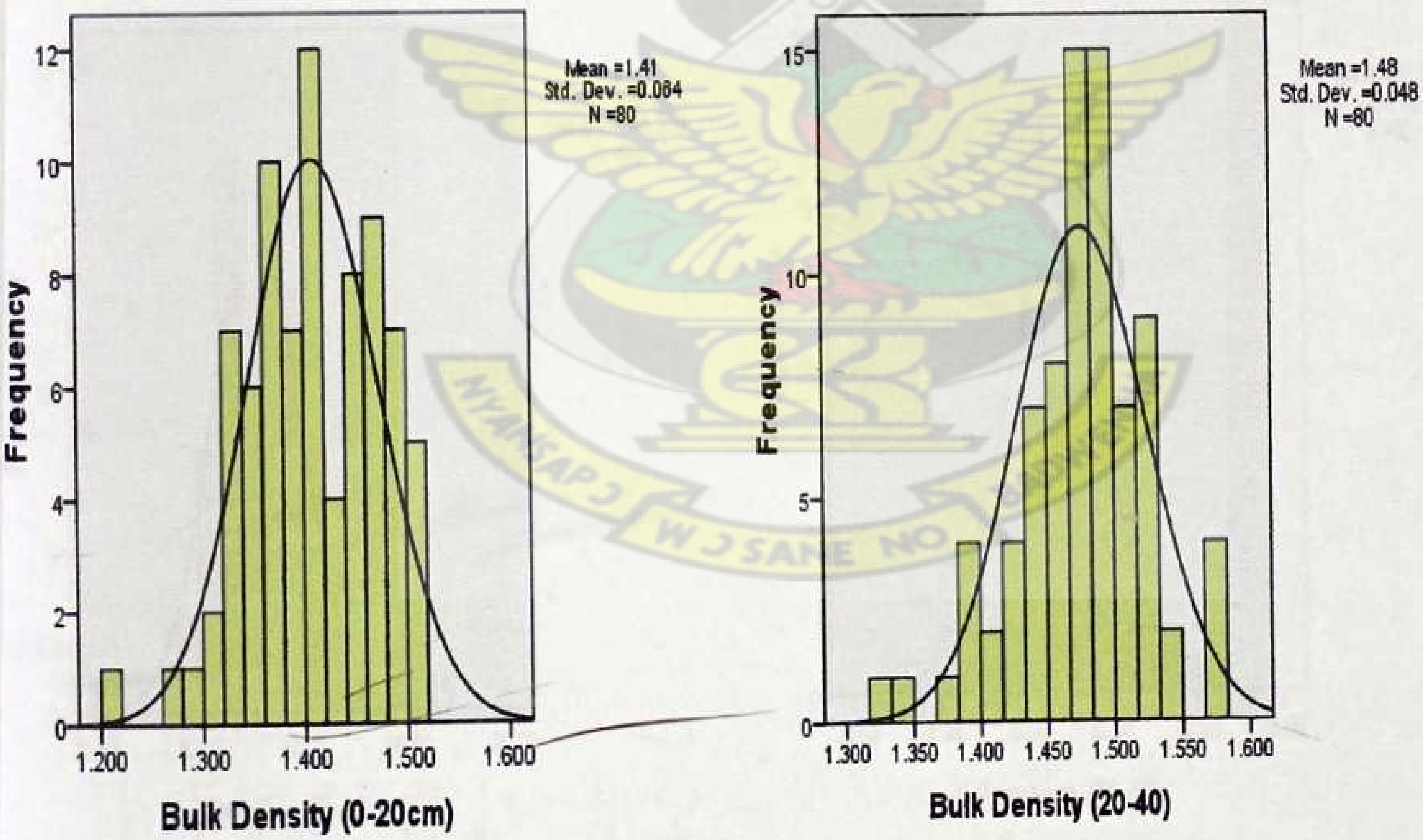

Fig.1d: Histograms of bulk density in both layers of sampling.

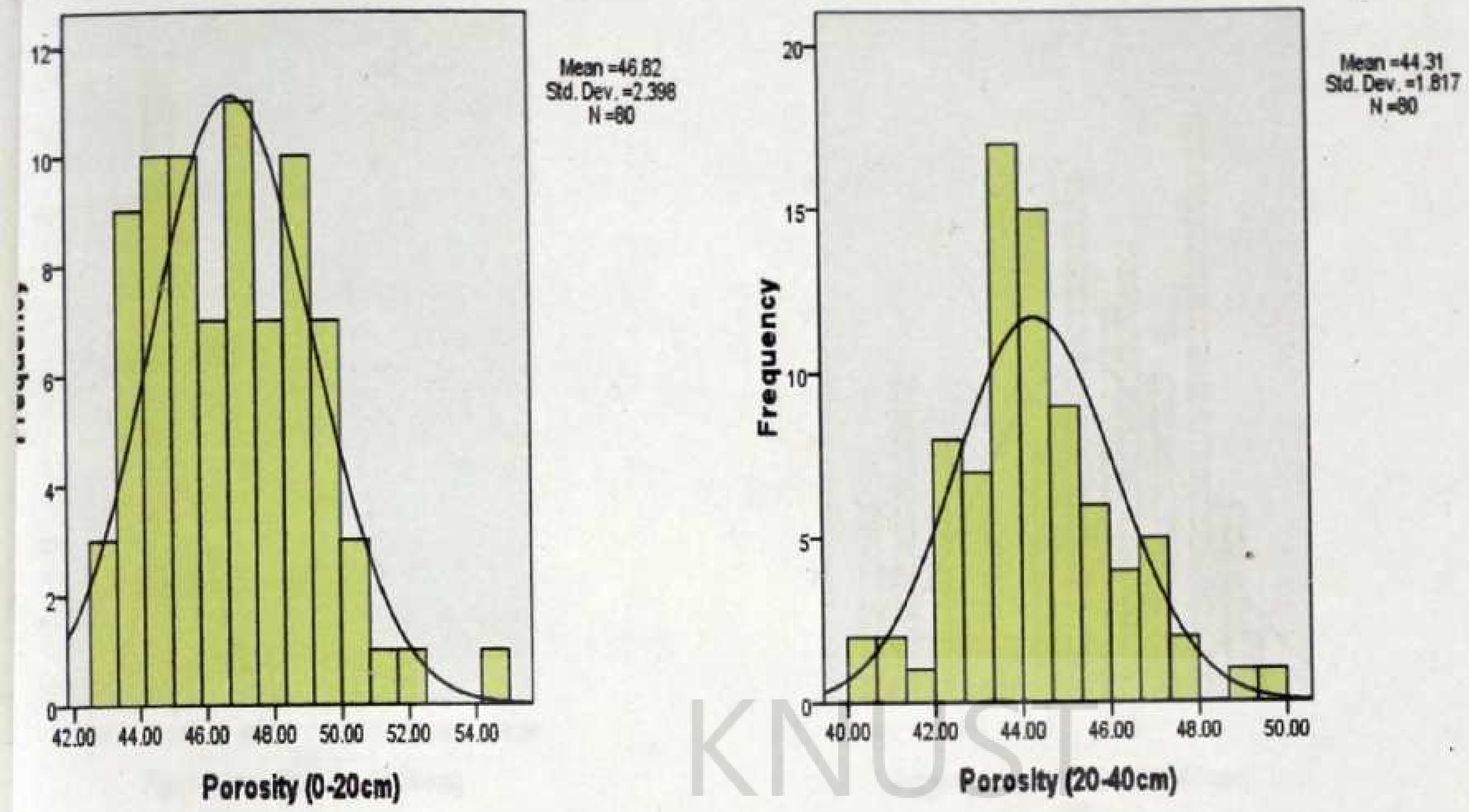

Fig.1e: Histograms of total porosity in both layers of sampling.

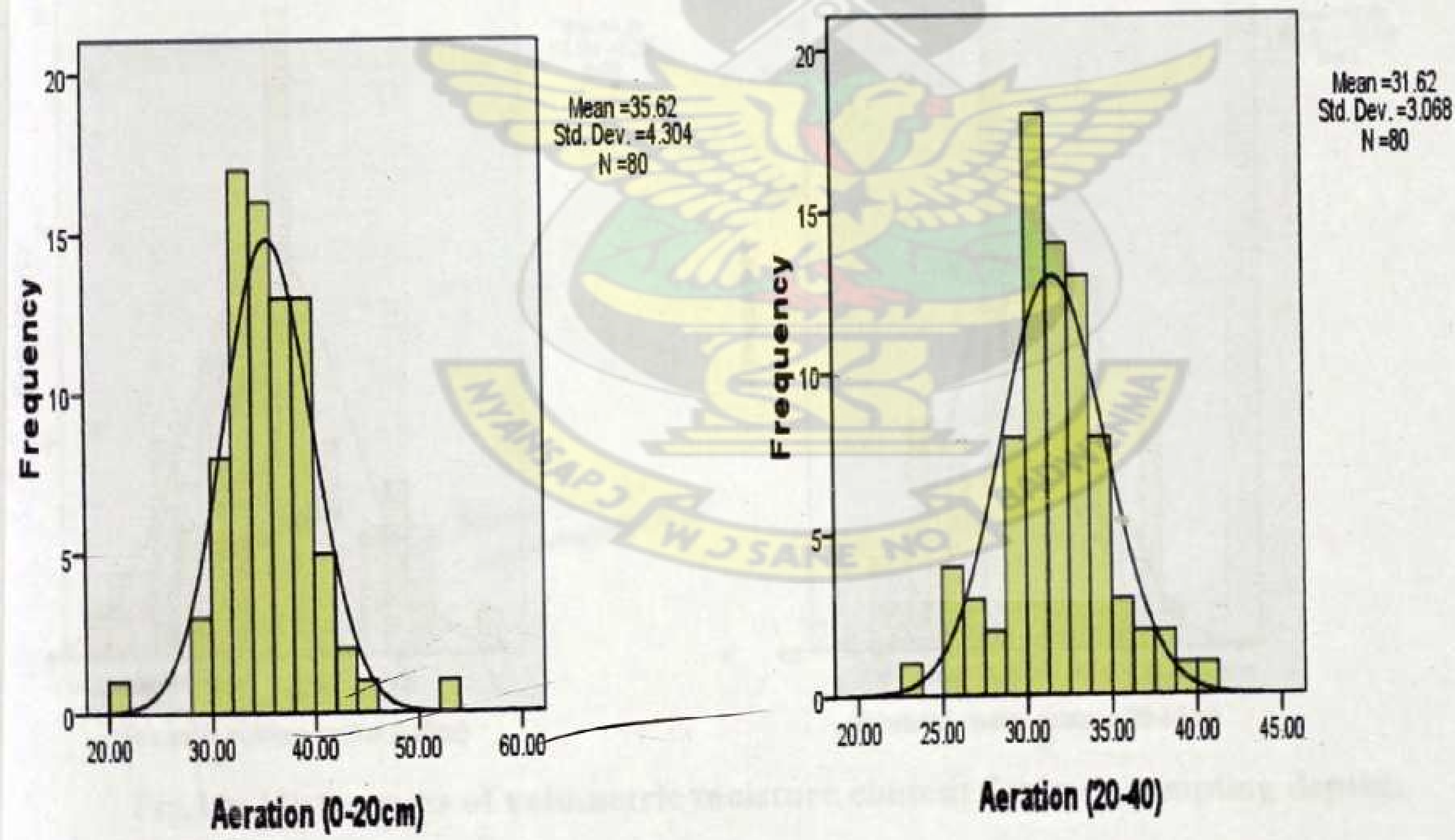

Fig.1f: Histograms of aeration-porosity in both layers of sampling.

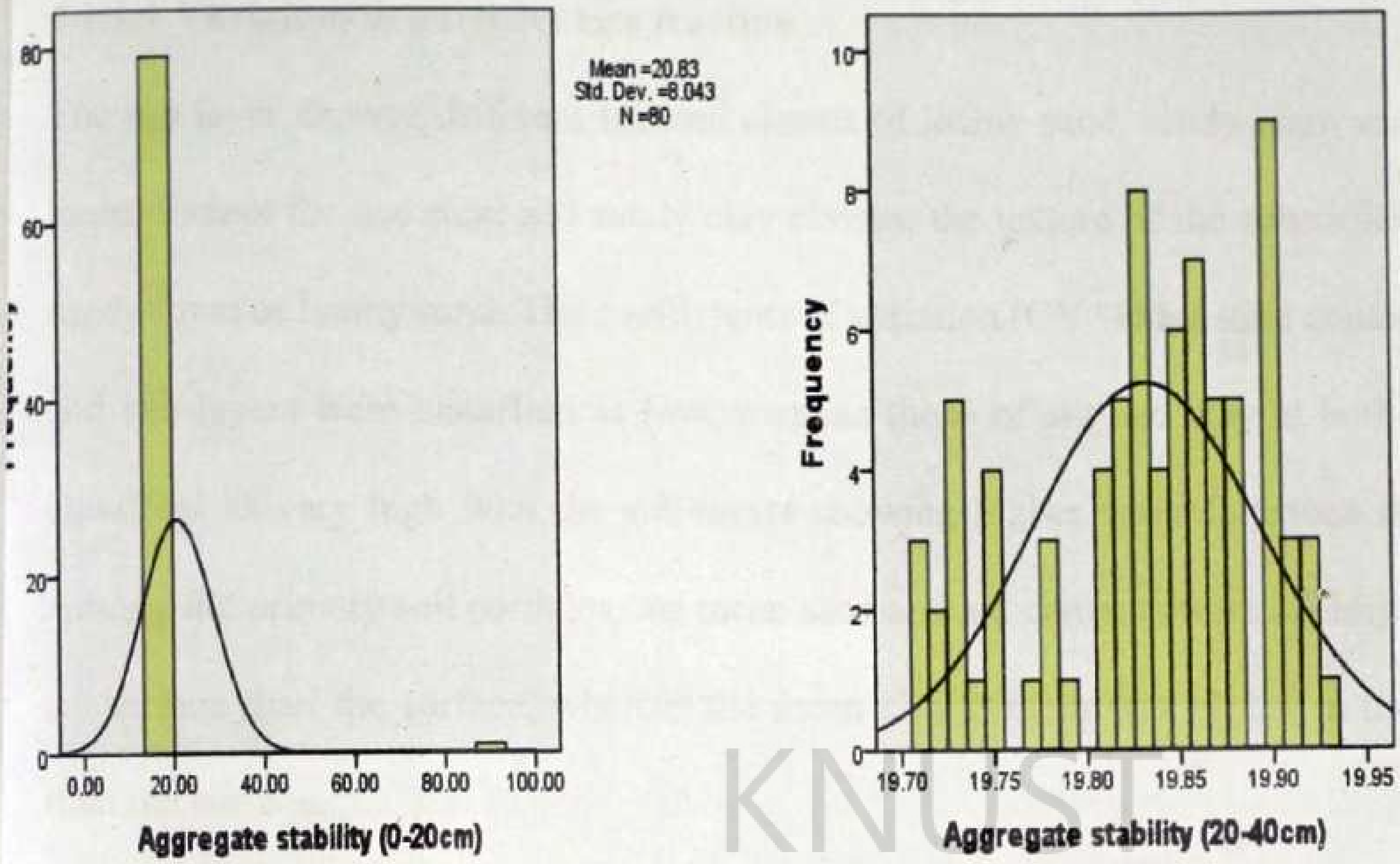

Fig.1g: Histograms of aggregate stability for both sampling depths.

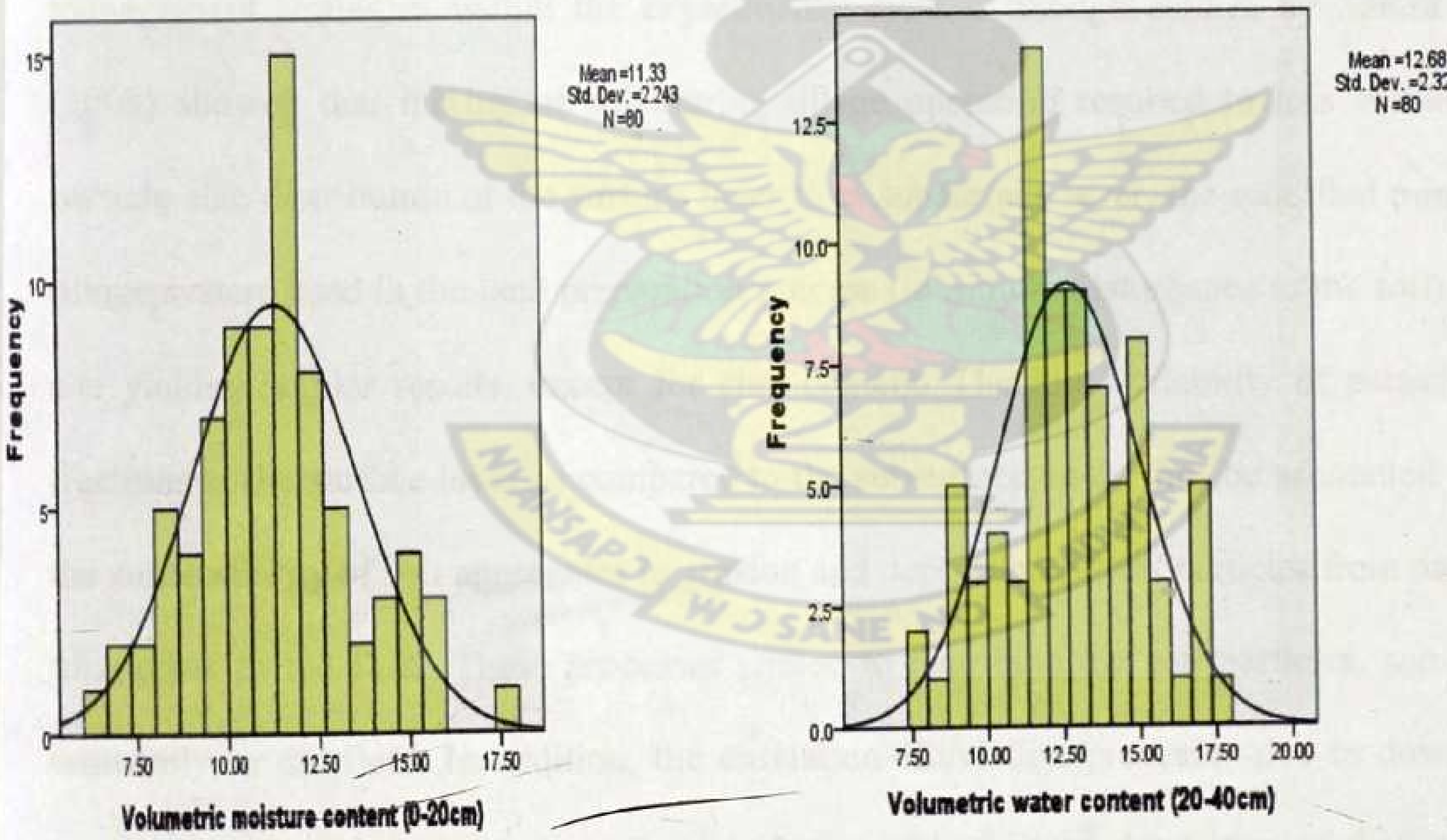

Fig.1h: Histograms of volumetric moisture content for both sampling depths.

4.1.1.1 Variation in particles size fraction

The top layer showed different textural classes of loamy sand, sandy loam and sandy clay loam. Except for one sand and sandy clay classes, the texture of the subsurface was either sandy loam or loamy sand. The coefficients of variation (CV %) for sand content at the top- and sub-layers were classified as low, whereas those of silt and clay at both layers were classified as very high with the sub-layers showing higher variability than the top-layer. Among the primary soil particles, the mean sand and silt contents were slightly lower in the subsurface than the surface, whereas the mean clay content was higher in the subsurface than the surface.

The high CV values for silt and clay may be due to the history of the land use and soil management strategies within the experimental field. Although studies by Santra *et al.* (2008) showed that mixing of soil during tillage operation resulted in less variation of particle size distribution at the surface layer than subsurface layer, the modified minimum tillage system used in the land preparation process (minimum disturbance to the soil) in the site yielded similar results, except for clay content. The low variability of particle size fractions at the surface layer as compared to the subsurface could thus be accounted for by the susceptibility of soil aggregates to erosion and deposition of soil particles from one spot to another in the field. These processes tended to distribute the soil particles, somehow, uniformly in the field. In addition, the eluviation–illuviation processes due to downward movement of water through the soil might have resulted in the deposition of the fine-size particles (clay particles) at the greater depth and differences in the influence of parent materials (resistance or susceptibility to weathering) at both surfaces.

The clay fraction gave positive and the highest kurtosis (2.76) in the surface layer, whereas in the subsurface, it was observed for silt (4.03). This explains why clay and silt in these depths are more slender (leptokurtic) than a normal distribution as shown in Figs. 1b and c. The kurtosis value for sand in the top layer (0.073), though positive (tall and slender distribution), showed a mesokurtic (normal) distribution, not only because it was closer to zero, but also established from the value of the K2 test (4.41). This indicates that the variation of sand content in this layer as demonstrated by the coefficients of variability could be due to chance (sampling error, spatial and temporal variations). On the other hand, all the kurtosis values for the lower depth were too tall or slender than a normal distribution.

The distribution also showed positive skewness (symmetric tail extends towards more positive values) for clay and silt contents in both layers, but negative skewness (symmetric tail extends towards more negative values) for sand content in both surfaces. The coefficient of skewness of sand in the top-layer (-0.57), extends towards the left showing, a shift from normal distribution but the K2 test reveals it is normally distributed across the field. This variation of the coefficient of skewness from normality could, therefore be attributed to chance.

4.1.1.2 Variation in Bulk density, Porosity, Aeration and Aggregate stability

Average bulk density for surface (0–20 cm) and subsurface (20–40 cm) layers were 1.409 ~~g/cm^3~~ and 1.476 g/cm^3, respectively. Soil bulk density variability was lower in the top-layer (CV = 4.51 %) than the sub-layer (CV = 3.26 %), but both layers were categorized as weak in terms of heterogeneity. The surface showed higher mean value of total porosity (46.82 %) than the subsurface (44.31 %) with accompanying variation coefficients of 5.12 % and 4.10 %, respectively. Thus, the surface porosity was higher and highly variable in comparison with the subsurface. The mean measure for soil aeration porosity in the surface layer (35.62 %) was higher and showed a higher variability (CV = 12.08 %) when compared with the subsurface values (31.62 % and CV = 9.70 %). Aggregate stability ranged from 19.86 % to 19.98 % with a mean value of 19.93 % and CV of 0.16 % for the top layer and 19.71 % to 19.93 % with a mean value of 19.83 % and CV of 0.31 % for the sub-layer, depicting a higher variation in the sub-layer than the top-layer.

The kurtosis values for aggregate stability at top and lower depths (-0.49 and -0.68), though exhibited a platykurtic (flat) distribution, had measures for the coefficient of skewness at both depths being zero, signifying a normal distribution of aggregate stability across the study area. Except for one outlier which presented a tall peaked distribution, the aggregate stability of the surface layer displayed an almost uniform and flat distribution across the field, and this could be appreciated from the CV (0.16 %) at this depth being the weakest for the entire data set. These values obtained from the K2 test (1.01 and 2.91) further proved the normal distribution of this property within both layers of study.

For other parameters, such as bulk density (Kurt. = 0.045) and porosity (Kurt. = 0.048) in the surface layer (leptokurtic), the kurtosis values fell close to 0, both being positive; this signified that the distribution of these properties as indicated in Figs. 1 (b and c) in the top layer was similar or close to a normal. In addition, the coefficients of skewness (-0.45 and -0.59 ~~for bulk~~ density and porosity respectively), indicated a distribution towards the more negative values, but the outcome of K2 test (2.88) which is the same for both parameters specified a normal distribution. Hence, the reason for the nearly normal distribution of these properties as displayed by the normal curve on the histograms (Figs. 1d and 1e).

On the other hand, a higher positive value (3.98) was recorded for aeration at the surface, which made it more slender than a normal distribution as shown in Fig.1d. Skewness coefficient (0.40) disclosing a distribution towards more positive values together with K2 test (15.05), confirmed the deviation of the distribution from a normal one as shown by the normal curve in Fig.1d. Somehow higher positive values were recorded in the sub-surface for these properties, with aeration porosity recording the least (0.61) and porosity, the highest (0.90). The normal curve on Fig.1d showed that, the distribution of aeration porosity was nearly normal (mesokurtic). Furthermore, the coefficient of skewness (0.15) tended to extend towards the right but, K2 test value (1.74) showed that the distribution was normal.

The low stability of aggregates at both layers could be accredited to previous tillage practices (ploughing) causing disturbance and/or destruction to the surface and subsurface structure of the soil, organic matter and clay contents. This is because mechanical forces operating on the field surface during tillage can cause significant soil compaction, hence increasing bulk density which causes the destruction of soil aggregates (Aksakal and Öztaş, 2010). Furthermore, the higher stability of aggregates at the surface as compared to the subsurface could be attributed to the accumulation of organic residues (high content of OC) at the soil surface hence modifying the matrix with the formation of granular aggregates.

The results also indicated a low variability in aggregate stability for both surfaces indicating an almost homogeneous aggregate stability across the field at both depths, though the surface showed a lower variability in comparison with the subsurface. This could be related to the susceptibility of the soil aggregates to erosion and depositional events occurring at the soil surface, causing an almost evenly distribution of the soil aggregates in the field. The differences in SOC and soil moisture content within both depths along the field may also explain the unequal distribution of aggregate stability within the field. Thus, the amounts of SOC and soil moisture of the experimental field are related to the extent to which aggregates are stable. From the results, it can be realized that stability of aggregates is positively correlated with SOC content.

4.1.1.3 Variability of moisture content

The soil moisture values (volumetric water content) measured at the different sampling locations and depths were used to represent the spatial variation of moisture content in the field. The average soil moisture in the surface layer was 11.33 % and 12.68 % in the subsurface layer by volume. However, the spot to spot measurement values ranged from 6.64 % to 17.52 % and 7.78 % to 17.44 %, respectively. Although the average soil moisture value was slightly lower in the surface layer than the subsurface layer, results from paired samples t-test (Appendix A-7) revealed significant differences between them. K2 test (0.49) revealed that soil moisture was distributed normally across the field at both depths, being positively skewed with a negative kurtosis close to zero.

The coefficient of variation was higher on the surface (19.81 %) than the subsurface (18.33%), both being moderately heterogeneous. The soil moisture variability reflects to some extent the variability of soil porosity, and hence, soil particle distribution (clay content), bulk density, organic matter content, vegetation, meteorological factors (evapotranspiration) and topography (elevation, slope, profile curvature etc.). Likewise, the variation of different particle sizes might explain the variability of soil moisture content.

The spatial variability of the water content (initial water content) may have an important impact on rainfall-runoff processes, in particular under high rainfall conditions. This variation of soil water content between layers across the field may be due to variation in soil textural and structural properties as well as changes in micro-topography (Mapfumo *et al.*, 2006). Similarly, the controls on the spatial distribution of soil moisture may include static (topography and soil properties) and dynamic (precipitation and antecedent soil moisture) variables (Reynolds, 1970). The superposition of static and dynamic controls can lead to different soil moisture patterns for a given catchment during wetting, draining, and drying periods (Western *et al.*, 2004).

The reasons for these variations in the selected soil physical properties include:

- Variation in the composition of parent material within the range of centimetres and differential deposition of litter depending on wind conditions (Orndorff and Lang, 1981; Peterson and Campbell, 1993).
- The differential types of soil development as a result of litter from different tree species (Lodhi and Johnson, 1989), plants growing at different times and different parts of the field.
- The modified soil physical environment for each crop and the burrowing activity of soil animals (Lavelle and Spain, 2001).

These variations may result in the spatial variation in available water for plants which could be identified as one of the major reasons for the variability in crop productivity.

4.1.2 Soil Hydraulic and Hydrologic properties

A summary of the experimental data on the hydraulic and hydrologic properties and processes obtained from the study are presented in Table 4.2. Coefficients of normality (skewness, kurtosis and K2 test values) showed K_s distribution in the area deviates from a Gaussian one, whereas all the hydrologic properties followed a Gaussian distribution as displayed by the trend of the normal curves on the histograms in Figures 2a and b.

Table 4.2: Descriptive statistics of measured soil hydraulic and hydrologic properties

Soil property	Depth (cm)	Descriptive statistic							
		Min.	**Max.**	**Mean**	**SD**	**‡CV (%)**	**Skew.**	**Kurt.**	**†K2**
K_s (mm s^{-1})	0-10	5.09E-6	4.76E-4	1.26E-4	1.25E-4	99.12^a	1.25	2.37	16.89***
	10-20	4.21E-6	2.36E-4	4.81E-5	4.32E-5	89.71^a	0.50	6.59	55.59***
I (mm)	0-10	680.00	5920.00	2695.00	1261.00	46.80^a	0.38	-0.56	3.57^{ns}
S (mm $s^{-1/2}$)	0-10	13.28	72.75	36.27	14.41	39.74^a	0.30	-0.55	2.84^{ns}
i (mm s^{-1})	0-10	0.19	1.64	0.75	0.35	46.81^a	0.37	-0.59	3.69^{ns}
K_o (mm s^{-1})	0-10	2.71E-4	1.06E-3	5.74E-4	1.78E-4	31.03^b	0.41	-0.57	3.99^{ns}

K_s (mm s^{-1}) = Saturated hydraulic conductivity; I (mm) = Infiltration amount; S (mm $s^{-1/2}$) = Sorptivity; i (mms^{-1}) = infiltration rate, Min. = Minimum value; Max. = Maximum value; SD = Standard deviation; Kurt. = Kurtosis; Skew. = Skewness; ‡CV (%) = Coefficient of variation (a, b = very high and moderate variations, respectively); †K2 =D'Agostino and Pearson "Omnibus" Normality Test value.

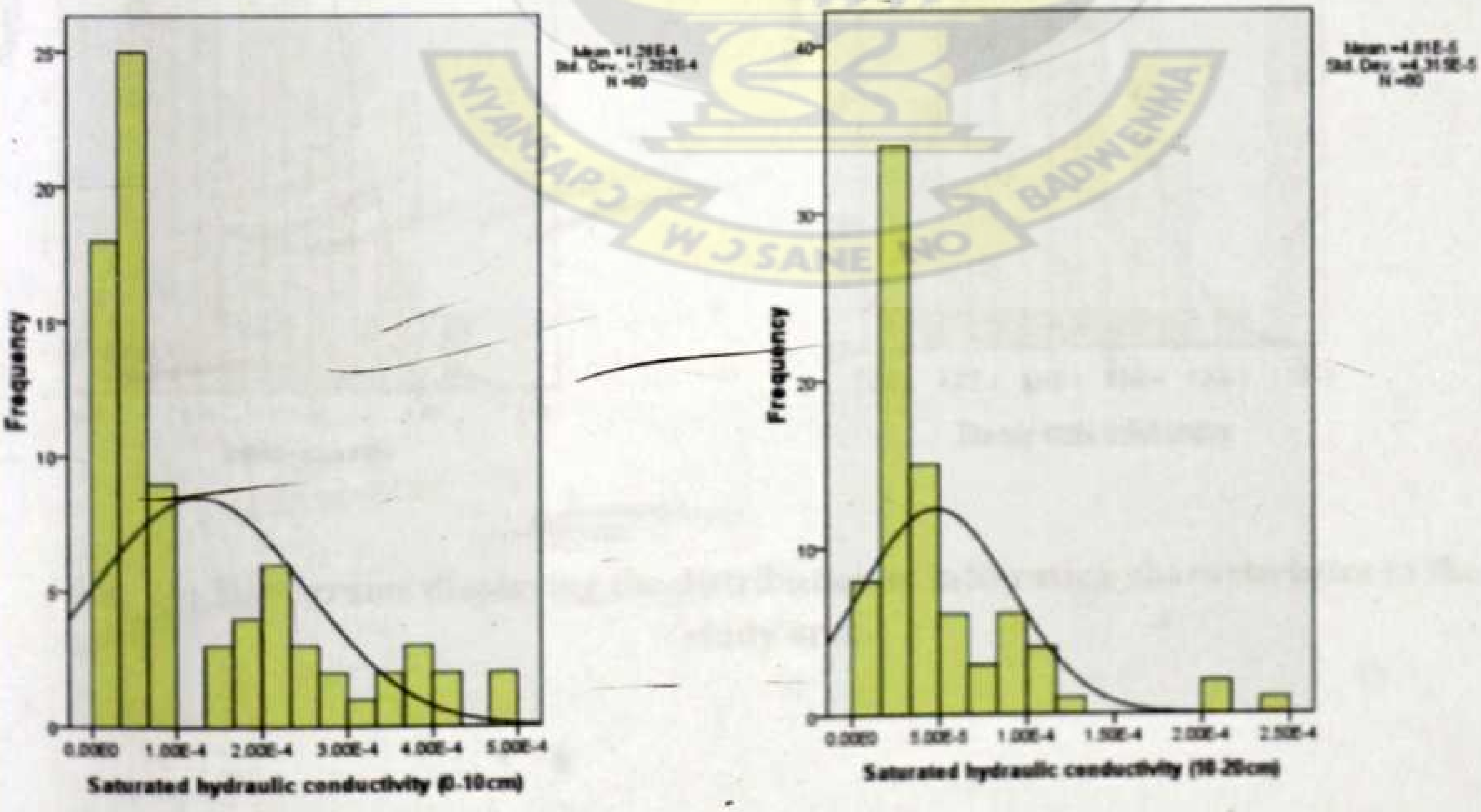

Fig. 2a: Histograms displaying the distribution of saturated hydraulic conductivity in both layers.

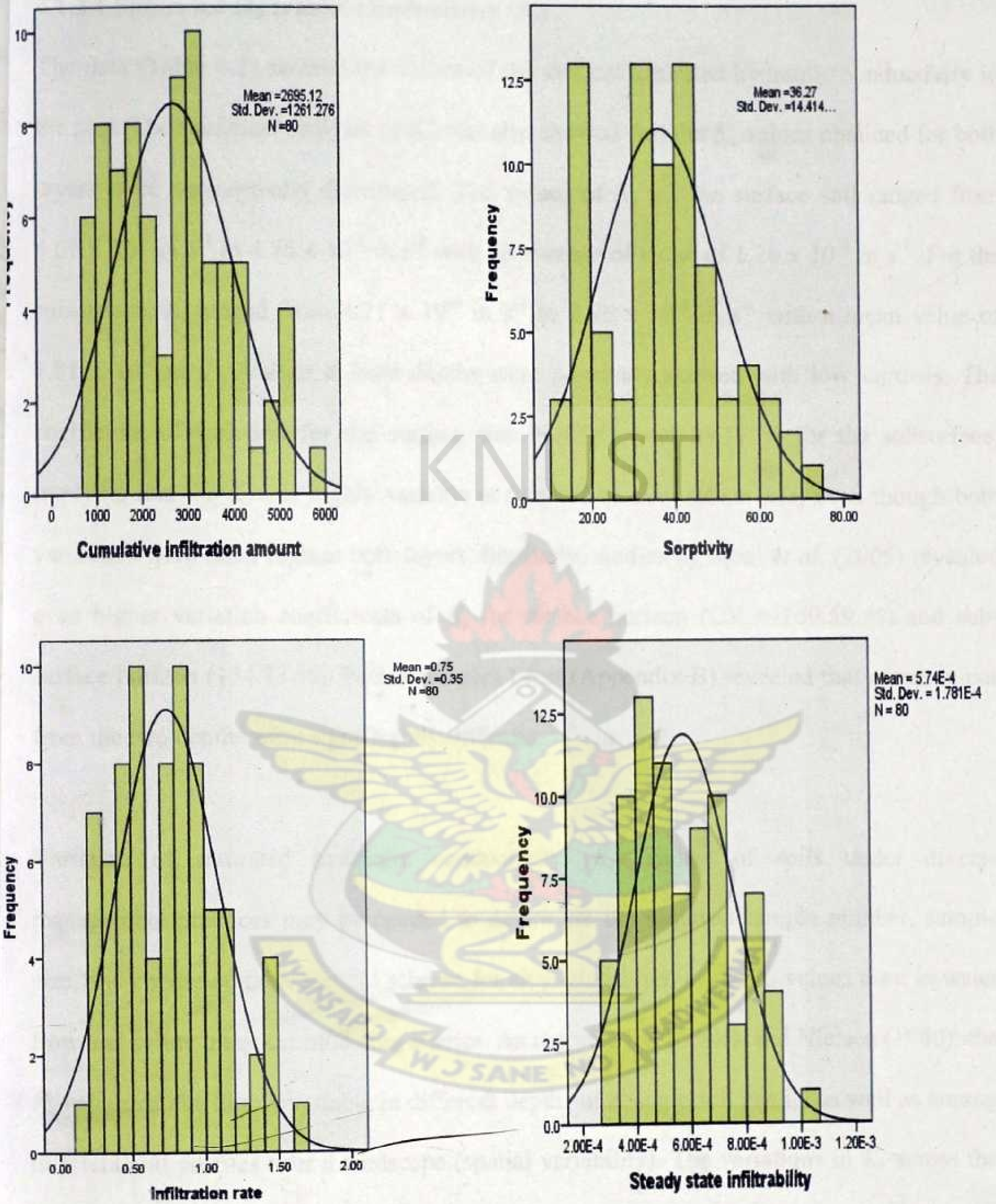

Fig. 2b: Histograms displaying the distribution of infiltration characteristics in the study area.

4.1.2.1 Saturated Hydraulic Conductivity (K_s)

The data (Table 4.2) showed the values of the vertical saturated hydraulic conductivity in the plot. The statistical analysis of K2 test also showed that the K_s values obtained for both layers were not normally distributed. The values of K_s for the surface soil ranged from 5.09×10^{-6} m s^{-1} to 4.76×10^{-4} m s^{-1} with an average of value of 1.26×10^{-4} m s^{-1}. For the subsurface, K_s ranged from 4.21×10^{-6} m s^{-1} to 2.36×10^{-4} m s^{-1} with a mean value of 4.81×10^{-5} m s^{-1}. Values at both depths were positively skewed with low kurtosis. The coefficient of variation for the surface was 99.12 %, and 89.17 % for the subsurface, implying that the K_s was highly variable at the surface than subsurface, even though both variations were rated high at both layers. Similarly, studies by Iqbal *et al.* (2005) revealed even higher variation coefficients of K_s for surface horizon (CV = 160.59 %) and sub-surface horizon (154.73 %). Paired samples t-test (Appendix B) revealed that mean values from the two depths were significantly different.

Variation of saturated hydraulic conductivity (K_s) values of soils under diverse management practices may be needed to determine the required sample number, sample size, and choose suitable sample scheme for characterization of the K_s values used in water flow and solute transport modeling studies. As reported by Warrick and Nielsen (1980), the K_s values can be highly variable in different depths of a single soil profile as well as among different soil profiles over a landscape (spatial variability). The variations in K_s across the field and along the different depths are as a result of the variability in porosity (pore size distribution), which is also affected by the variations in aggregate stability, organic matter and bulk density (soil structure) and particle size distribution (texture).

The K_s values varied significantly at both depths since the structure of pores in soil also varied and were affected by different rates of biological, physical, and chemical processes. This variability could also be attributed to the use of small-sized undisturbed soil cores in the determination of K_s in the laboratory (Mallants *et al.*, 1997) or the presence or absence of open-ended macropores (Mohanty *et al.*, 1994). The lower K_s value at the subsurface layer could be accredited to the higher bulk density at the layer. Although Mason *et al.* (1957) concluded that bulk density was a poor indicator of soil permeability, Bouma and Hole (1971) reported that low K_s values agreed well with high bulk density.

The higher mean K_s value with larger CV at the surface layer could be attributed to the modified-no-tillage system which was employed in the land preparation process. This is confirmed by Cameira *et al.* (2003), who indicated that minimum tillage has the tendency of producing higher K_s than conventional tillage, associated with larger coefficients of variation. However, the effect of tillage on the spatial structure of saturated hydraulic conductivity is not clear from literature. Logsdon and Jaynes (1996) reported that the increase in the variability induced by tillage makes it difficult to determine the spatial structure of saturated hydraulic conductivity. On the contrary, Diiwu *et al.* (1998) indicated that tillage can reduce the variability in saturated hydraulic conductivity compared to no tillage, resulting in an increase in its spatial autocorrelation.

4.1.2.2 Infiltration parameters

Figures 3a, 3b and 3c show the magnitude of spatial variation as well as spatial pattern of infiltration parameters (cumulative infiltration amount, sorptivity and infiltration rate, in that order) within the field. Very high variations (CV > 35%) were recorded for the measured infiltration parameters (Table 4.2).

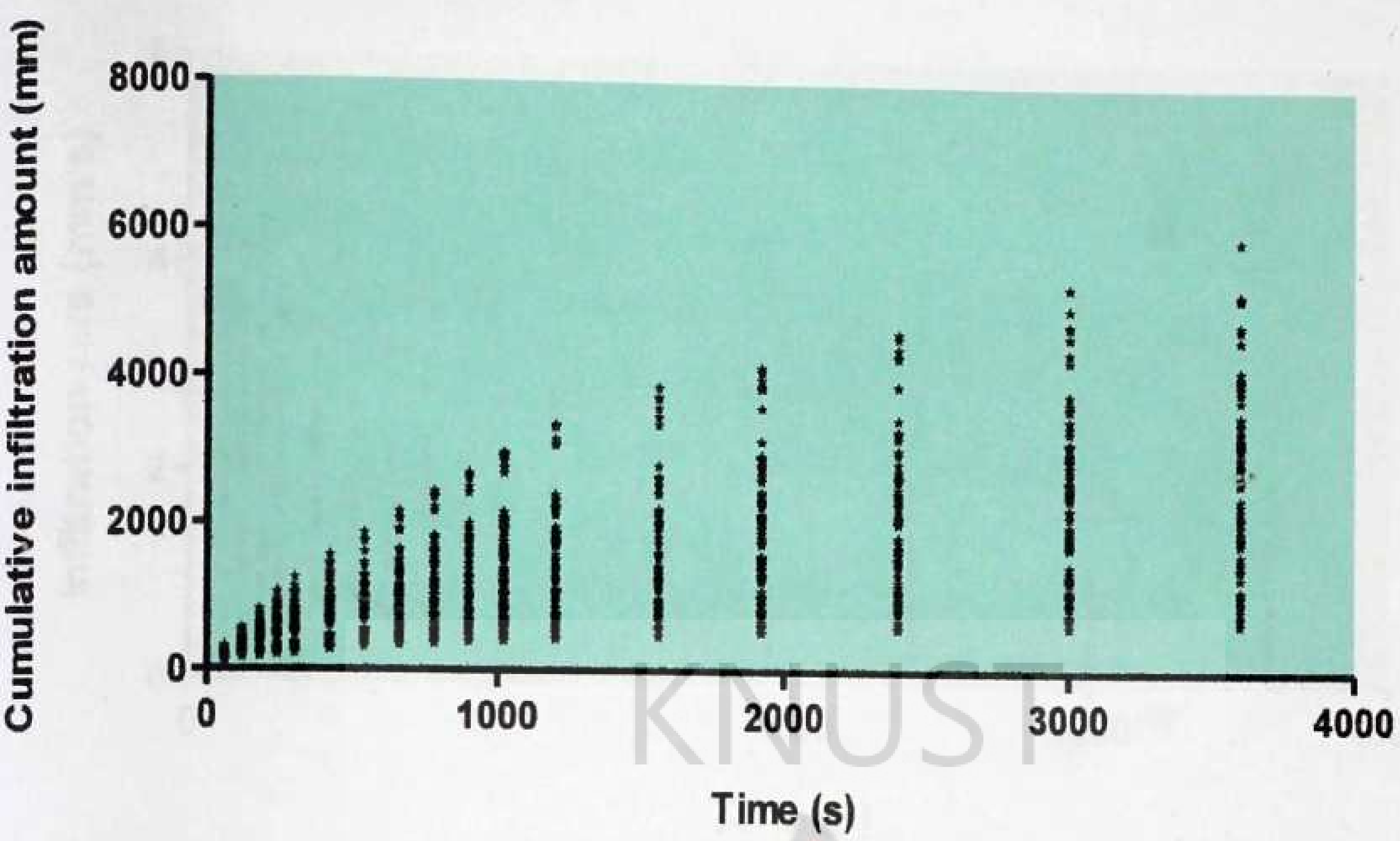

Fig. 3a: Graphical representation of the variations of cumulative infiltration amounts with time in the field.

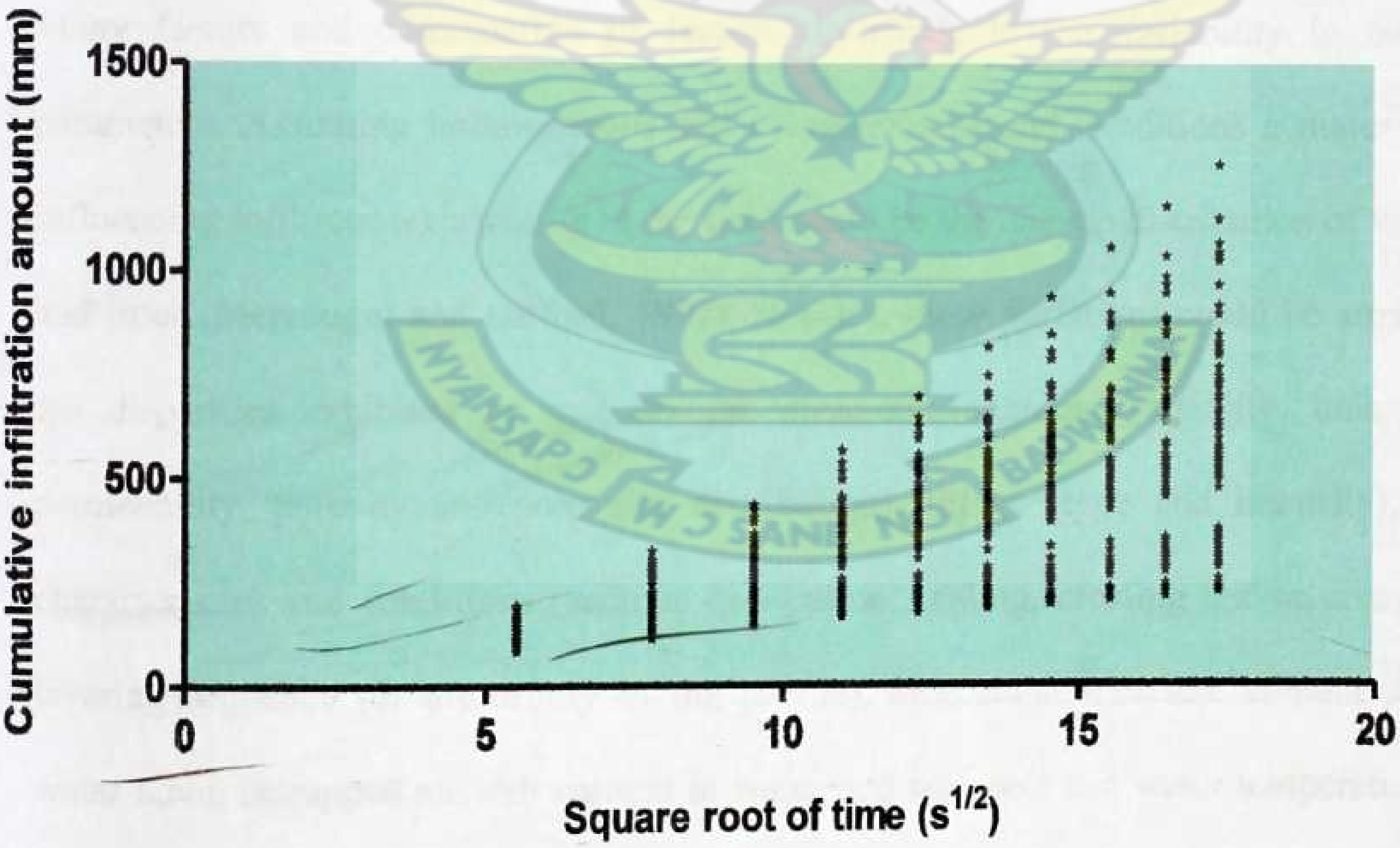

Fig. 3b: Graphical representation of the variations of sorptivity in the field.

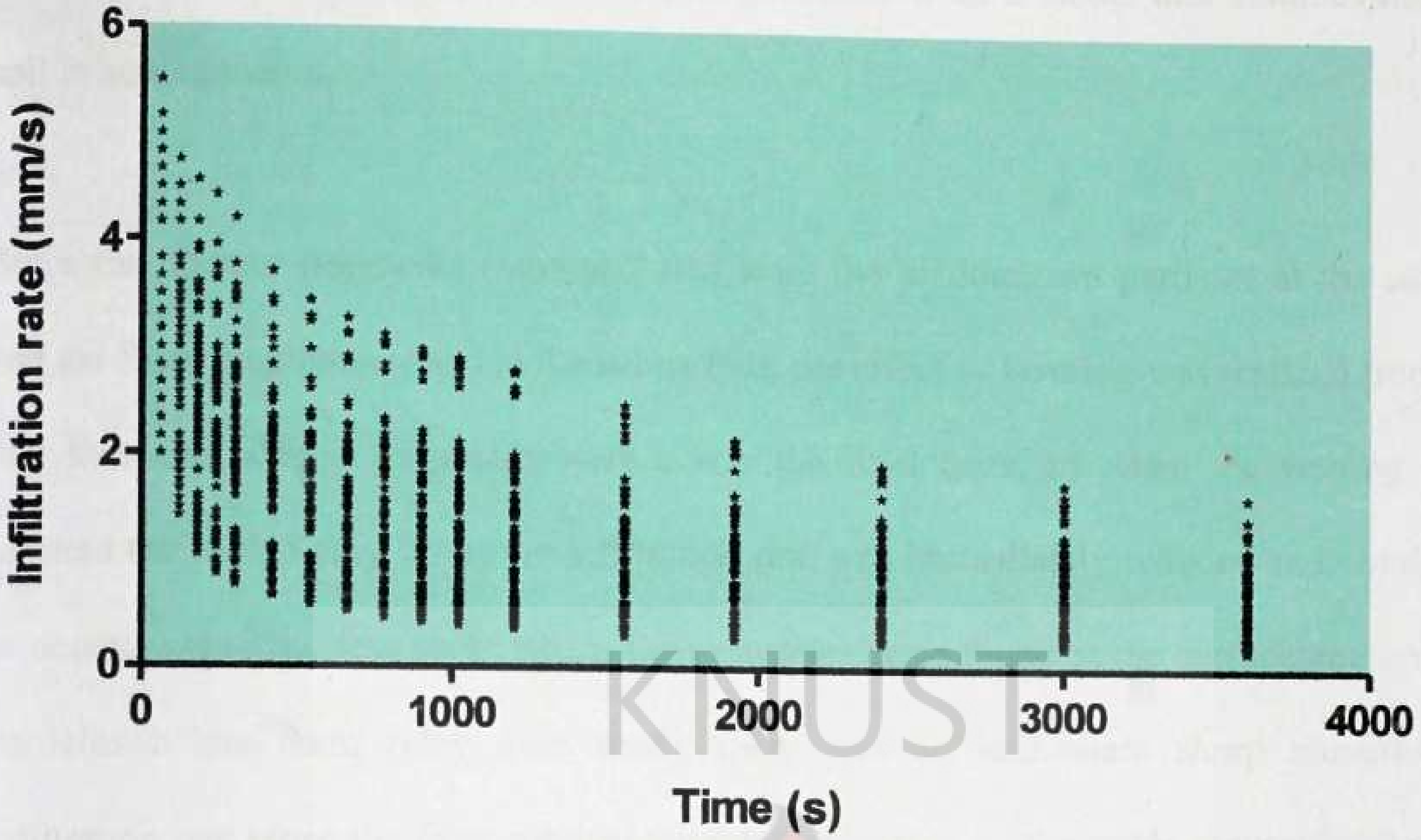

Fig. 3c: Graphical representation of the variations of infiltration rates with time in the field.

Many factors and combination of factors contribute to the variability in infiltration parameters. Assuming homogeneous soil characteristics and conditions a major element influencing infiltration variability in the field could be the uneven distribution of vegetation and litter (Merzougui and Gifford, 1987). Besides, these variations could be attributed to the disparities exhibited by soil texture, structure (aggregate stability, bulk density, permeability, porosity and pore size distribution), tillage (type and intensity), surface characteristics and conditions (such as desiccation, sealing, crusting and/or compaction), layering sequence (or uniformity of the profile), antecedent moisture content, depth of water table, entrapped air, salt content in water and soil, soil and water temperature at the point of sampling. As reported by Jury *et al.* (1991), one reason that field infiltration data express dissimilar features than calculations from theoretical simulations is that field soil profiles are rarely homogeneous with depth, nor is the distribution of water content uniform at the initiation of infiltration. These two effects typically have a tendency to reduce the infiltration rate more rapidly than would be predicted from a model that assumes that the soil is homogeneous.

Since the coarser fragments (sand and silt) were the predominant particles at the surface and the finer fragments (clay) at the subsurface, the effect of layering was realized from the fact that, the coarser fragments were above the finer ones, so when the wetting front reached the buried clay layer, the infiltration rate was immediately reduced and continued to decrease. For the few spots where finer particles were found at the surface and coarser particles below them (clay over sand), there was an immediate sharp reduction in infiltration rate when the front reached the sand. However, as the water accumulated at the interface, the matric potential head at the front increased, allowing the larger pores in the sand layer to fill.

Additionally, report by Jury *et al.* (1991), has shown that differences in texture and permeability between layers influence variations in water entry into the profile through reduction in the infiltration rate irrespective of the surface texture (coarser or finer). Thus, for a finer texture, reduction in infiltration is due directly to its lower permeability, whereas, a subsurface coarse-textured layer generally has a saturated hydraulic conductivity that is greater than the finer textured soil above it. However, the low matric potential at the wetting front prevents the large, highly conducting pores of the coarse-textured region from filling. The unsaturated conductivity of the resulting partially saturated coarse-textured region is actually lower than the wetter finer-textured region above, and the infiltration rate decreases as the front reaches the interface.

Moreover, these variations could be connected to previous land preparation process and intensity, especially tillage, resulting in compaction of the subsoil due to increased bulk density and reduced porosity and permeability. Similarly, studies by Cressie and Horton (1987) showed that the type of tillage applied may result in different types of spatial dependency in the infiltration characteristics. This is due to effects of tillage on soil properties such as increase in bulk density and decrease in porosity at the sub surface through the formation of plough pans. Ersahin (2003) studied the spatial relationship between infiltration rate and some soil properties and reported a strong negative relationship between infiltration rate and bulk density of subsoil (30-60 cm).

4.2 Scaling and Fractal Geometry analyses

The variability of soil hydraulic and hydrologic characteristics in the field were analysed by means of scaling and fractal techniques (Figs. 4a, b and c). The values of the scaling coefficients were obtained by best-fitting the relationships considered as a total group.

4.2.1 Scaling results

The assumptions on which the presented linear scaling theory is based resulted in similar soil hydraulic properties and flow process (infiltration). Thus the heterogeneity of soil hydraulic and hydrologic properties from location-to-location within the study area was approximated by the scaling coefficient for each spot. This is because the linear variability model presents relationships between variability of soil hydraulic properties and parameters that describe the variability of dynamic soil water flow processes - infiltration, redistribution and drainage (Vogel *et al.*, 1991). Table 4.3 presents the statistical summary of scaling parameters of saturated hydraulic conductivity and cumulative infiltration amount.

Table 4.3: Scaling parameters for saturated hydraulic conductivity and infiltration amount

Variable	Depth (cm)	Min.	Max.	Mean	SD
K^* (m s^{-1})	0-10	0.23	2.18	1.024	0.576
	10-20	0.30	2.28	0.980	0.384
*ln K**	0-10	-1.470	0.779	-1.013	0.564
	10-20	-1.204	0.824	0.089	0.384
α_K	0-10	0.226	2.182	1.000	0.517
	10-20	0.304	2.619	1.017	0.477
I^* (mm)	0-10	80.300	3573.000	1269.00	817.80
t^* (min)	0-10	0.380	59.820	16.24	17.54
γ_I	0-10	0.232	2.117	1.001	0.517
γ_t	0-10	0.391	2.656	1.004	0.464

K^* (m s^{-1}) = Scaled K_s; ln K^* = Log transformed K_s; α_K = Scaling factor of K_s; I^* (mm) = Scaled cumulative infiltration amount; t^* = Scaled time; γ_I = Scaling factor of cumulative infiltration amount ; γ_t = Scaling factor of cumulative time.

4.2.1.1 Cumulative infiltration amount

With regard to the field-measured infiltration curves that characterize the infiltration process for the study area, the parameters for the reference infiltration curve I^* (t^*) are represented in Fig. 4a. The level of success of the scaling method can be deduced from the comparison of the degree of scatter in Figures 3a and 4a, respectively. The superposition of all transformed data points yielded a single reference infiltration amount. If the selected analytical expressions are fitted through the transformed data sets, then the resulting fitting parameters would be referred to as the reference cumulative infiltration amount.

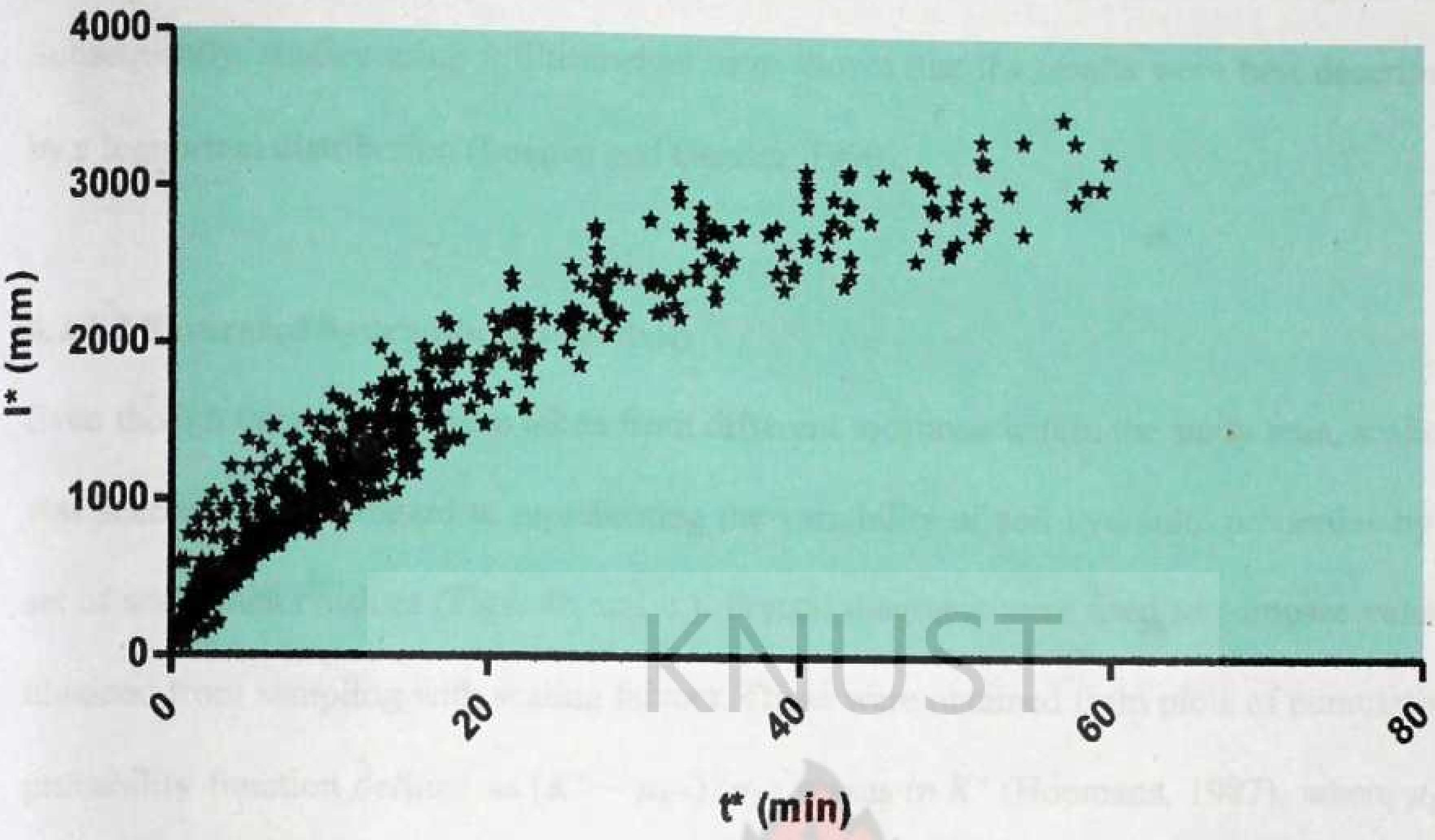

Fig. 4a: Scaled Cumulative infiltration amount for the study area.

At first glance, it can be observed that the use of scaling factors have reduced the extent of scatter of the measured variables, allowing the production of a meaningful average curve, signifying the effectiveness of scaling (Fig. 4a). The higher scattering of data points in Fig. 3a as compared to Fig. 4a denotes the extent of variability of cumulative infiltration amount (I) in the field. This result was expected since the use of scaling factors is known to decompose the overall spot-to-spot variability of measured variables into unison. This is because the scaling factors have ~~caused~~ a linear transformation on each of the involved variables. This variability is inferred as an approximation of the linear component of real soil variability. Accordingly, the variability of cumulative infiltration amount is always linear, hence the unexplained variability after the transformation could be due to the nonlinear component of the total variability. Therefore, the assumption is that the linear component is dominating the nonlinear component (Vogel *et al.*, 1991). No obvious pattern in the distribution of the infiltration parameters has been reported with respect to soil type or position. The frequency distribution, however, has been reported to be lognormal. Subsequently, studies using infiltrometers have shown that the results were best described by a lognormal distribution (Loague and Gander, 1990).

4.2.1.2 Saturated hydraulic conductivity

Even though the samples were taken from different locations within the study area, scaling was successful with regard to representing the variability of soil hydraulic properties by a set of scale factor values (Figs. 4b and c). Fractal diagrams were used to compare values obtained from sampling with scaling factors. These were obtained from plots of cumulative probability function defined as $(K^* - \mu_{K^*})/\sigma_{K^*}$ versus $ln\ K^*$ (Hopmans, 1987), where μ_{K^*} is the mean scaling factor, σ_{K^*} is the standard deviation of K^* and $ln\ K^*$ is the natural logarithmic transformation of K^*.

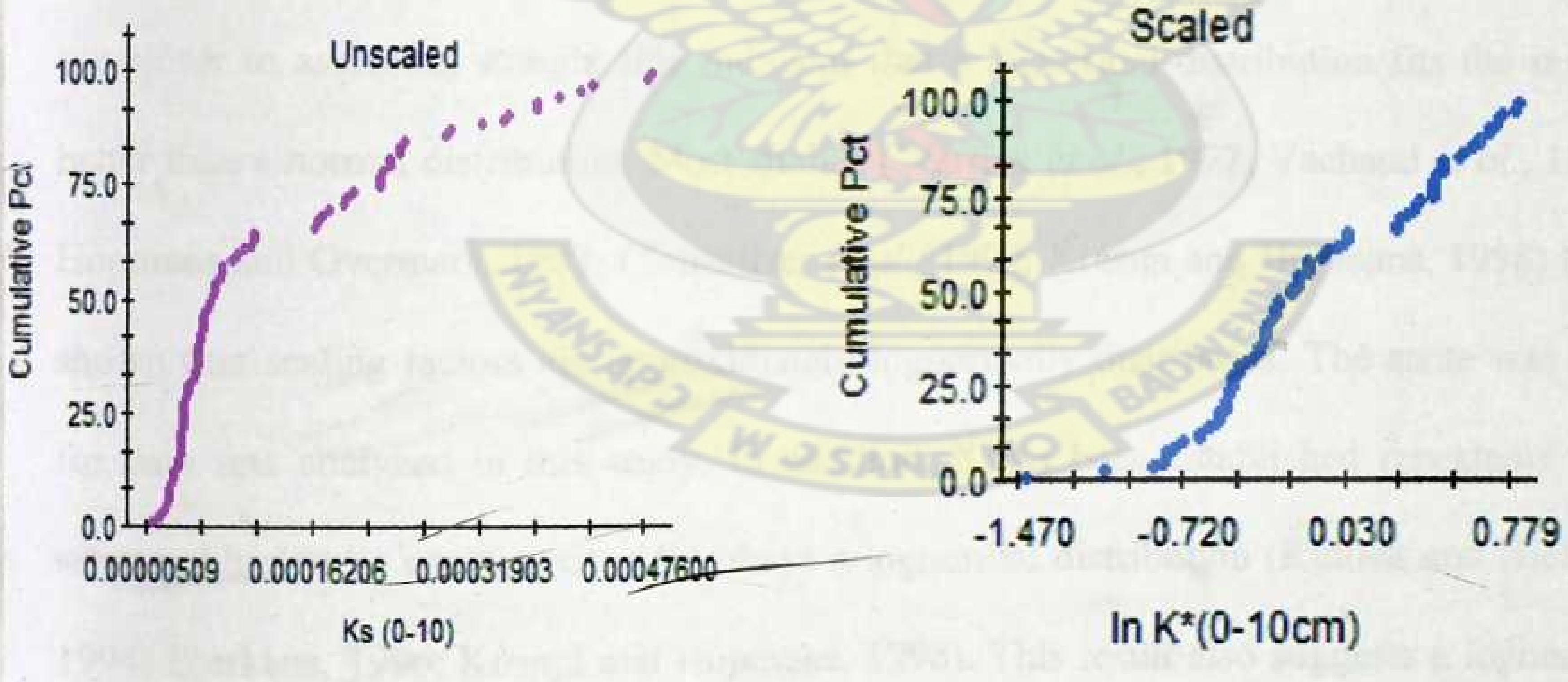

Fig. 4b: Fractal diagrams of unscaled and scaled K_s for the surface layer.

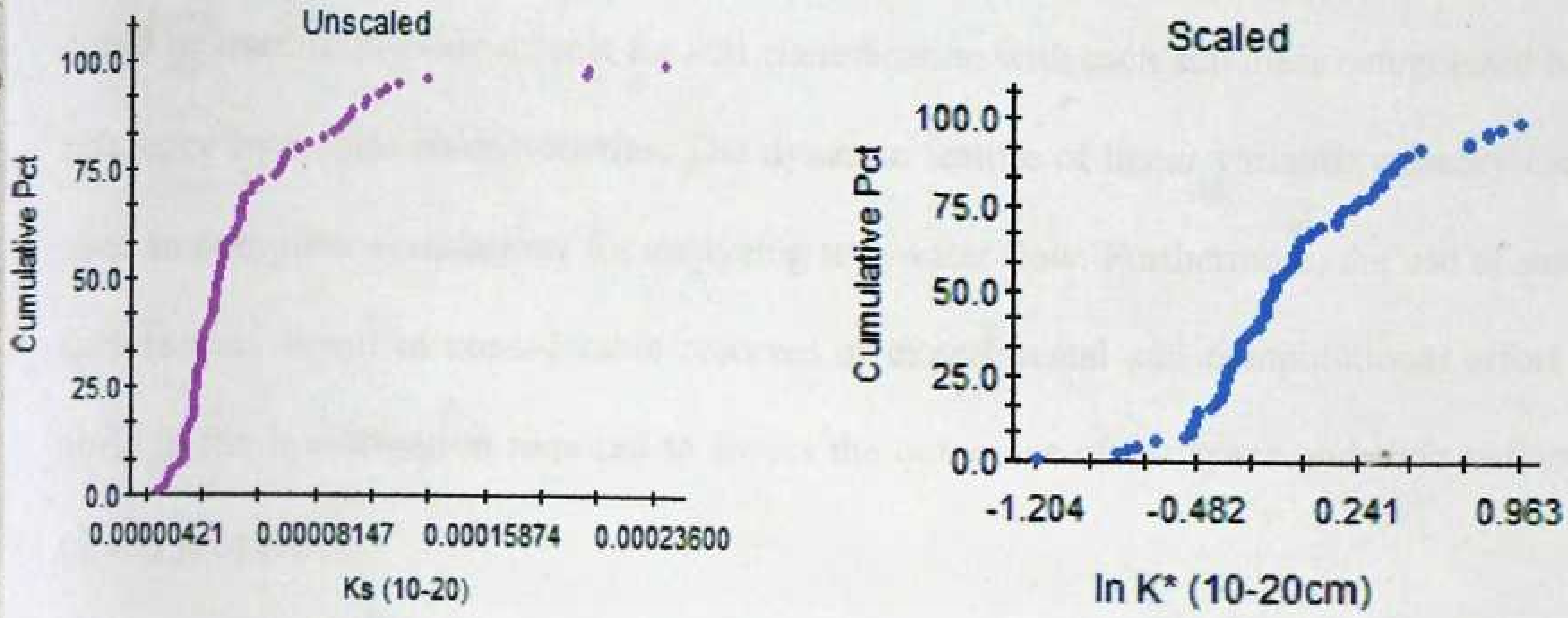

Fig. 4c: Fractal diagrams of unscaled and scaled K_s for the sub-surface layer.

The scaled mean saturated hydraulic conductivity functions for both layers can be viewed as being the representative means of the scaled hydraulic data. From the estimated distribution of scale factor values, a new set of scale factors may be generated to represent the soil hydraulic properties of the area (Hopmans, 1987). The fact that the plots of $ln\ K^*$ are closer to assuming straight line indicates that a lognormal distribution fits the results better than a normal distribution. Most studies (Warrick *et al.*, 1977; Vachaud *et al.*, 1985; Hopmans and Overmars, 1987; Clausnitzer *et al.*, 1992; Kosugi and Hopmans, 1998) have shown that scaling factors are approximately lognormally distributed. The same was true for data sets analyzed in this study. In addition, it has been established repeatedly that saturated hydraulic conductivity (K_s) obeys a lognormal distribution (Kutilek and Nielsen, 1994; Bierkens, 1996; Kosugi and Hopmans, 1998). This result also suggests a lognormal distribution of scaling factors, since the hydraulic conductivity is expected to be proportional to the square of the scaling factor (Jury *et al.*, 1987).

Relationships similar to those given for the infiltration process can be found for other water transport processes, thus a scaling procedure can be applied to the respective dynamic characteristics of these processes. As a consequence, the idea of similar soil properties could be used to provide a basis for soil classification with each soil class categorized by its reference hydraulic characteristics. The dynamic feature of linear variability theory can be used in computer simulations for analysing soil-water flow. Furthermore, the use of scaling factors may result in considerable reserves of experimental and computational effort and abridge the investigation required to assess the outcomes of the space and time variability of soil properties.

The linear variability model, thus serves as a tool to simplify the problem of spatial and temporal variations encountered in the field. This can be achieved through the formulation and interpretation of initial and boundary conditions imposed on a given system of soil profiles (Vogel *et al.*, 1991). This study proposes an interpretation of these empirically derived results. That is, a lognormal scaling factor distribution was derived by assuming that the soil pore radius of the study area was lognormally distributed and that individual soil samples were obtained from random sampling of effective pore volume from the study area.

4.2.2 Fractal Geometry analysis

The fractal geometry provides a statistical tool for characterizing the spatial variability of soil physical and hydraulic properties. From the results, fractal dimensions have provided a single ~~parameter~~ to describe the spatial variability of soil hydraulic and hydrologic properties. To calculate the fractal dimension, a regression analysis was performed between the logarithms of the semivariance [$\gamma(h)$] and the lag (h). The plots of logarithms of omni-directional semivariogram and distance (lag = h) for soil hydraulic and hydrologic properties are shown in Figs. 5a and b, respectively. The least square procedure was used to fit a linear function to the isotropic semivariogram for all soil properties. The semivariance values at distances less than the sampling distance were omitted sequentially to obtain the highest value of the coefficient of regression for isotropic variogram. The fractal dimension (D) was computed using equation (36) from the slope of linear regression given in Table 4.4.

Table 4.4: Fractal indices of soil hydraulic and hydrologic properties in the field

Soil property	Depth (cm)	D	SE	r^2	H
K_s (mms^{-1})	0-10	1.936	0.807	0.307	0.064
	10-20	1.981	3.045	0.032	0.019
I (mm)	0-10	1.819	0.324	0.707	0.181
S (mm s$^{-1/2}$)	0-10	1.817	0.319	0.714	0.183
i (mm s^{-1})	0-10	1.814	0.271	0.775	0.186
K_o (mm s^{-1})	0-10	1.860	0.334	0.704	0.140

K_s (mm s^{-1}) = Saturated hydraulic conductivity; I (mm) = Cumulative infiltration amount; S (mm s$^{-1/2}$) = Sorptivity i (mm s^{-1}) = Infiltration rate; K_o (mm s^{-1}) = Steady state infiltrability; D = Fractal dimension; SE = Standard error; r^2 = Correlation coefficient of the best-fit line, H = Hurst coefficient.

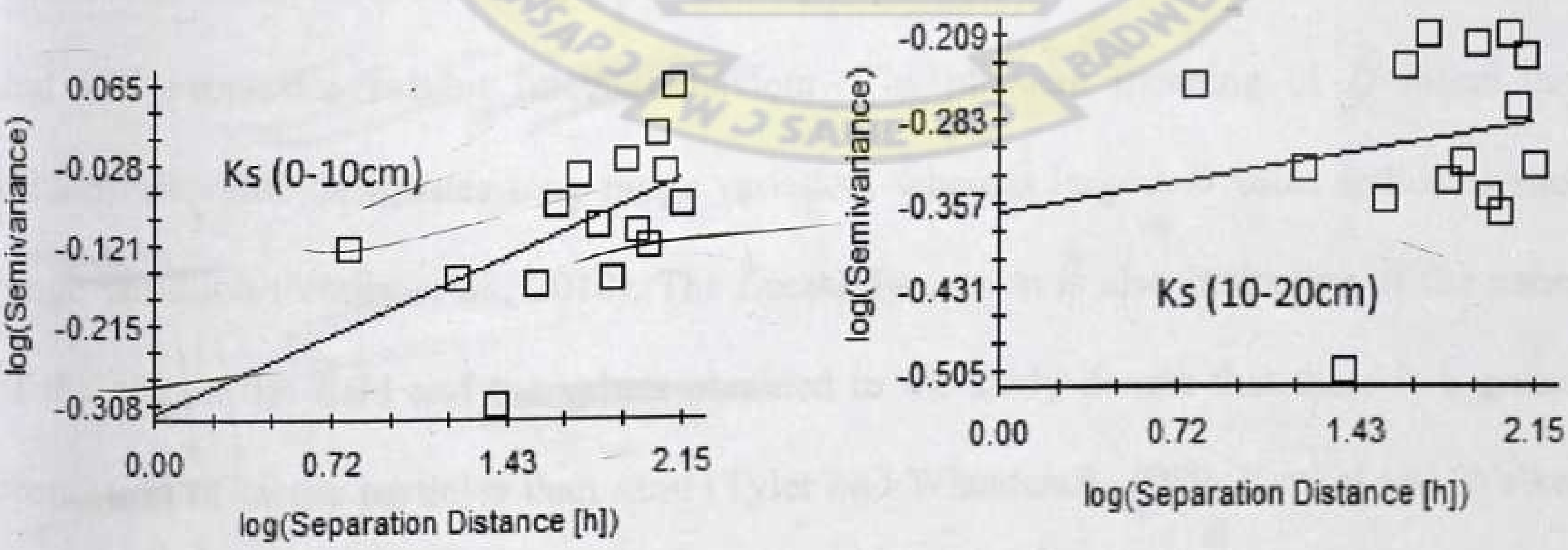

Fig. 5a: Logarithmic plot of empirical variogram for K_s of both layers.

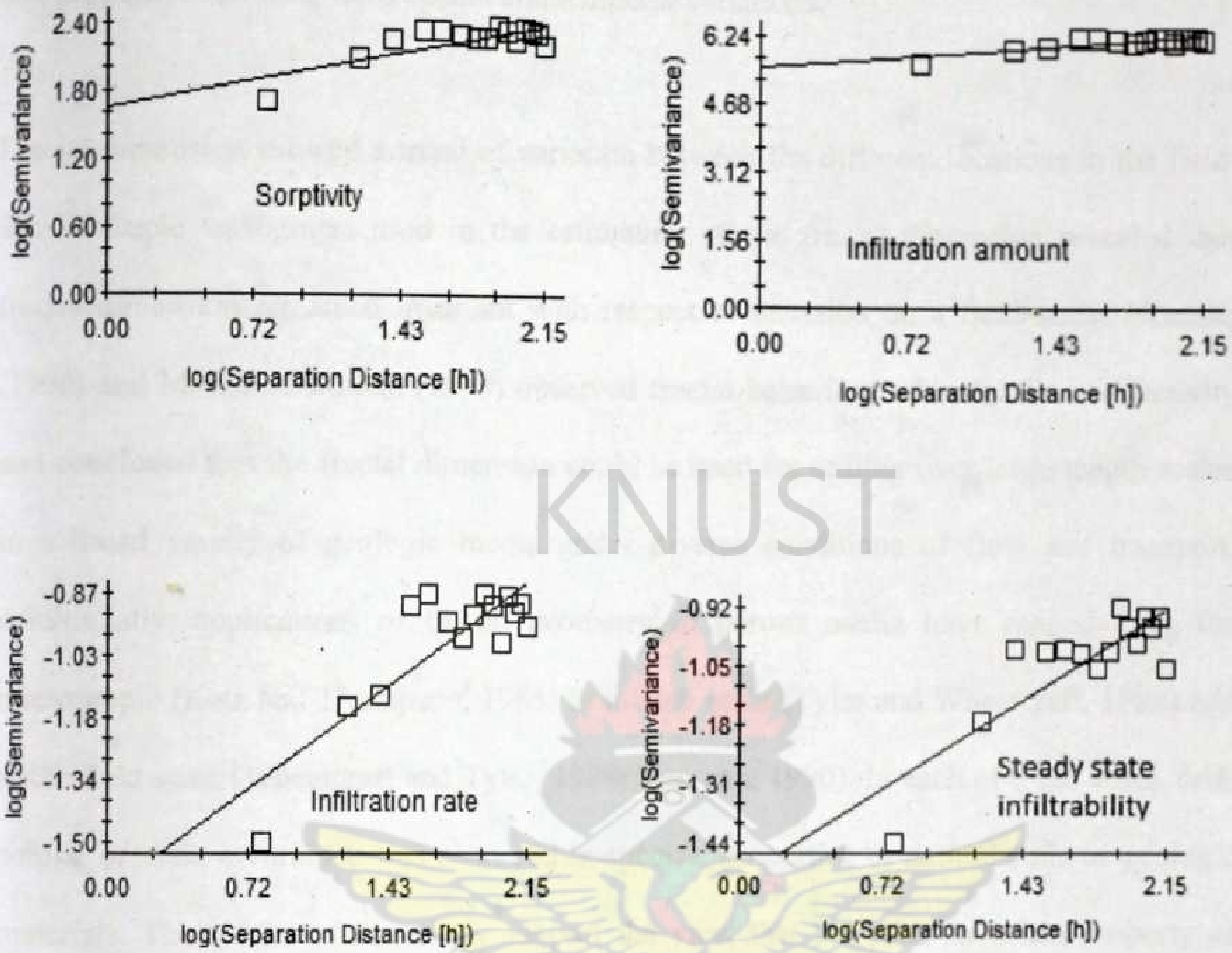

Fig. 5b: Logarithmic plot of empirical variogram for infiltration parameters.

The fractal dimensions for soil properties vary from 1.814 to 1.981. These results indicate that soil properties exhibit fractal behaviour. The physical meaning of *D* infers that, smallest *D* value designates long range variation, whereas largest *D* value indicates short range variation (Vieira *et al*., 2010). The fractal dimension is also indicative of the nature of the ~~soil in~~ the field and the values obtained in the study denote that there is a greater proportion of larger particles than sand (Tyler and Wheatcraft, 1989; Kenkel and Walker, 1993). Additionally, values obtained for the Hurst coefficient range from 0.019 to 0.186, showing an anti-persistent nature (Sugihara and May, 1990) of the soil hydraulic and hydrologic properties. This can be explained by the degree of variability exhibited by the soil properties resulting from spatial and temporal variations.

Fractal dimension showed a trend of variation between the different locations in the field. The isotropic variograms used in the estimation of the fractal dimension revealed that fractal dimension remained invariant with respect to direction on a field scale. Neuman (1990) and Molz and Boman (1993) observed fractal behaviour of hydraulic conductivity and concluded that the fractal dimension could be used for scaling over large length scales in a broad variety of geologic media under diverse conditions of flow and transport. Additionally, applications of fractal geometry in porous media have ranged from the microscopic (Katz and Thompson, 1985) to the lab scale (Tyler and Wheatcraft, 1989) and to the field scale (Wheatcraft and Tyler, 1988; Neuman, 1990). In each of these cases, self-similar or scale invariance was observed in specific properties of natural soils or geologic materials. The results of this study support the view that the scale invariant property of fractals can be applied as a scaling rule to represent spatial variability of soil properties over large areas. This, study therefore, strongly supports the notion that many soils and porous media display fractal scaling in their pore space.

Thus, Fractal behaviour can be used to transfer the information across scales by extrapolating properties observed at one scale to properties at other scale. This is an indicati~~on that~~ soil hydraulic and hydrologic properties show fractal behaviour and cannot capture anisotropic variability of soil properties on a field scale. There is therefore an additional requirement to appreciate the physical interpretation of the fractal dimension and to develop relationships between fractal dimensions and hydraulic and hydrologic characteristics.

4.3 Geostatistical analyses

Semivariograms, which give information about the nature and structure of spatial dependency in the field, were obtained from the field and laboratory data. The directional semivariograms calculated at the angles of 0° (N – S), 45° (NE – SW), 90° (E – W), and 135° (SE – NW) for the measured variables indicated no comprehensible anisotropy. Therefore, omni-directional semivariograms were obtained using the best fitting model by the cross-validation method, and the data were modeled with isotropic functions to determine the spatially dependent variance within the research area. With the data from the sampled areas, the values for soil attributes were predicted for unsampled locations across the field with the maximum reduction of errors. Ordinary Kriging using parameters of the semivariograms were generated. This facilitated detailed representation of the spatial variability within the entire field through the creation of continuous and smoothed attribute maps.

4.3.1 Spatial Structure and Attributes (Semivariogram and Autocorrelation analyses)

Spatial structure analysis (semivariograms and correlograms) indicated spatial variability across field for soil properties studied. Due to the intrinsic and extrinsic soil forming factors, different spatial relationships were determined for the investigated variables. Isotropic models were selected as ideal representation of semivariograms for all soil properties, since the best-fitted models (model with the minimum residual sum of squares) were ~~the same~~ in all directions. Except for silt at the subsurface layer and aggregate stability and porosity at the surface layer which showed pure nugget effect (absence of spatial autocorrelation), all other soil properties within both layers were best-fitted by the transitive variogram models (Gaussian, Exponential and Spherical models), indicating that the spatial correlation structure for these soil properties varied with lag (h).

Class ratios to identify the distinctive classes of spatial dependence (autocorrelation) for the resulting semivariograms indicated the existence of weak to strong spatial dependence for all soil properties studied in the field (Figure 6). At separation distance greater than the range, sampling points will not be subjected to spatial correlation. This has great implication on sampling design, as sampling design should use separation distances that are shorter than the range for a particular depth in order to understand the spatial distribution pattern of the given property. In addition, spacing between sampling points are recommended to be from 0.25 to 0.50 of the range (Mulla and McBratney, 1999; Balasundram *et al.*, 2009). Based on the range values, sampling spacing should be closer for layers with shorter ranges than those with longer ones.

Ideally, the experimental variance should pass through the origin when the distance of sample separation is zero. However, the soil properties had non-zero semivariances as h approached zero. This non-zero variance (the nugget variance (C_o)) represents the unexplained or random variance, which could have resulted from measurement errors or variability of the measured property at a spatial scale smaller than the one of sampling (Journel and Huibregts, 1978). The structural coefficient C_1 as a result represents the component of total variance originating from spatial patterns in the soil. Soil properties displaying a well-defined spatial structure with a characteristic sill and range suggest that the properties vary in a patchy way resulting in areas with small values and other areas with larger ~~ones~~ (Frogbrook *et al.*, 2002). The range of spatial correlation of the variogram provides the average extent of these patches.

Correlograms were also drawn to observe variations in the data. The autocorrelation has a maximum value of '1' at zero lag ($h = 0$), then decreases to zero as lag distance increases.

Detailed descriptions of the autocorrelation for the soil properties across the experimental field for both surface and subsurface layers are shown in Fig. 6 for physical properties, respectively. Assessment of correlograms disclosed intervals of space at which the sequence has a recurring nature; further, it gave information about how far apart variables became independent of each other (similar to h in the semivariogram model). This will aid in selecting the best sampling distance for the analyses of soil properties in the field.

The best-fit models and model parameters, such as nugget variance, sill variance (nugget variance plus the structural variance), and the range of influence, are presented in Table 4.5. Among the different theoretical models tested, exponential model was found as the best fit in most cases. All linear models showed a pure nugget effect, depicting that the variability of soil properties best-fitted by this model was solely contributed by the nugget variance and were spatially independent across the field. When analysing the semivariogram of a particular soil physical property, the occurrence of spatial dependence was ascertained for both sampling depths to determine the distance at which variables are spatially correlated.

In this study, as lag distances increased, correlations dropped either gradually or rapidly to, and then fluctuated about or remained at zero, suggesting that the values being correlated have dependent and/ or no interdependent relationships for the different soil properties. The behaviour of soil properties in space is visually provided in Table 4.5 and Fig. 6 (semivariogram and autocorrelogram).

Table 4.5: Best-fitted semivariogram models and parameters for soil physical properties

Soil property	Depth (cm)	Model	C_o	$C_o + C_1$	A (m)	RSS	‡SD (%)
Sand (%)	0-20	Exponential	1.24E-3	1.005E-2	415.80	7.79E-6	12.34***
	20-40	Gaussian	8.34E-3	1.72E-2	165.76	7.74E-5	48.49**
Clay (%)	0-20	Gaussian	5.88E-2	1.41E-1	188.62	3.52E-3	41.70**
	20-40	Exponential	3.01E-2	1.47E-1	216.90	1.74E-3	20.48***
Silt (%)	0-20	Spherical	1.00E-3	3.16E-1	11.70	6.83E-2	0.32***
	20-40	Linear (NE)	3.96E-1	3.96E-1	----	9.14E-2	100 (pn)
ρ_b (gcm^{-3})	0-20	Spherical	2.74E-4	2.06E-3	6.24	7.56E-7	13.30***
	20-40	Gaussian	7.90E-4	2.10E-3	376.20	3.054E-7	37.62**
f (%)	0-20	Linear (NE)	2.49E-3	2.49E-3	----	1.088E-6	100 (pn)
	20-40	Exponential	1.11E-3	2.93E-3	932.70	7.94E-7	37.88**
ξ_a (%)	0-20	Exponential	7.39E-3	1.60E-2	86.40	5.25E-5	46.19**
	20-40	Exponential	7.60E-3	1.53E-2	637.50	1.58E-5	49.67**
θ_v (%)	0-20	Exponential	9.90E-3	6.20E-2	237.30	2.72E-4	14.52***
	20-40	Spherical	5.47E-3	3.65E-2	0.30	4.27E-4	14.97***
ASt (%)	0-20	Linear (NE)	4.20E-2	4.20E-2	----	1.42E-2	100 (pn)
	20-40	Spherical	1.62E-6	9.94E-6	46.50	1.03E-11	16.30***

*Co = Nugget; Co + C = Sill; A (m) = Range; RSS = Residual sum of squares; ‡SD (%) = Spatial dependence (***, **, pn = Strong and moderate spatial dependence and pure nugget, respectively); NE = Nugget effect.*

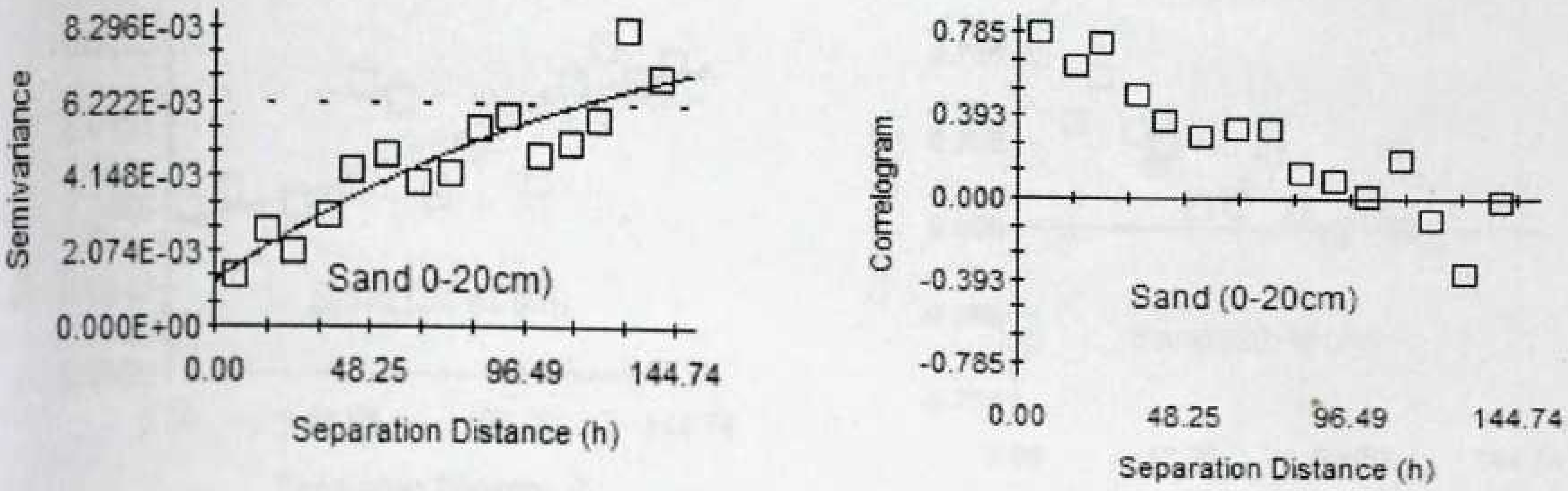

Fig.6a: Best-fitted isotropic semivariogram and autocorrelogram for sand content for the top-layer.

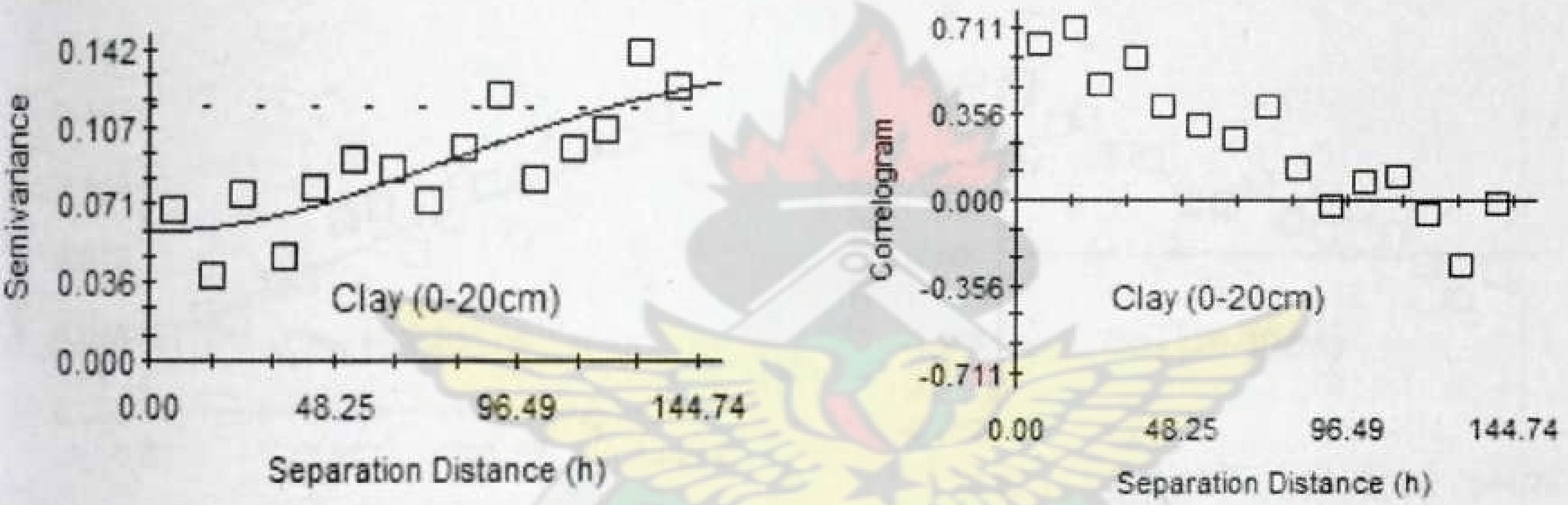

Fig. 6b: Best-fitted isotropic semivariogram and autocorrelogram for clay content for the top layer.

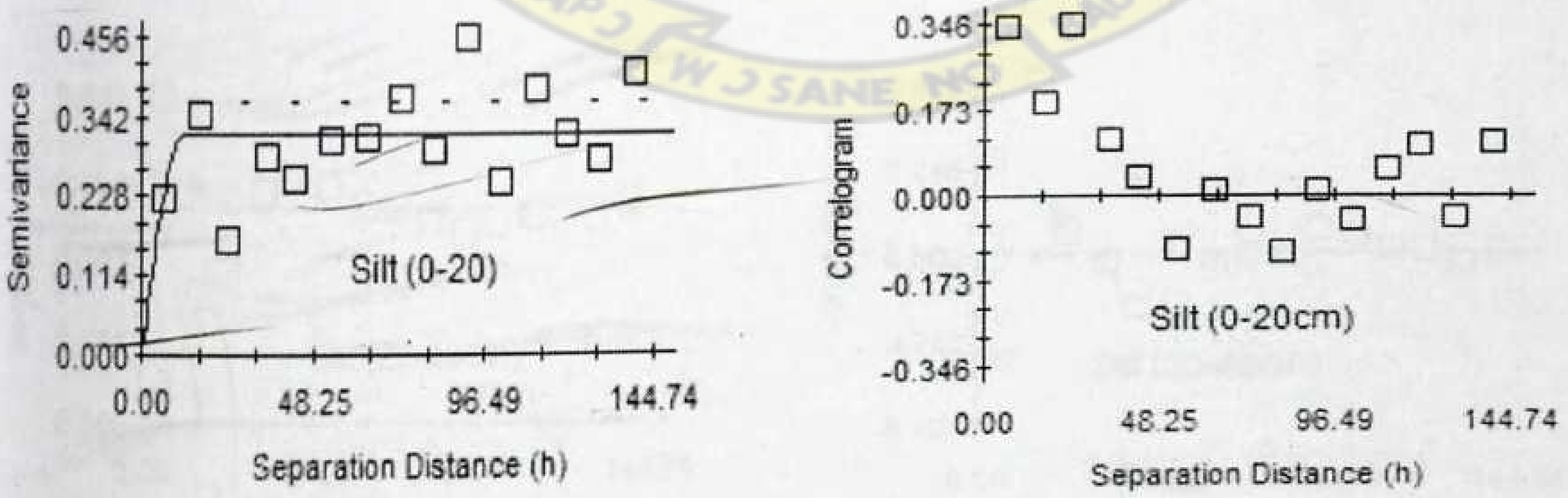

Fig. 6c: Best-fitted isotropic semivariogram and autocorrelogram for silt content for the top-layer.

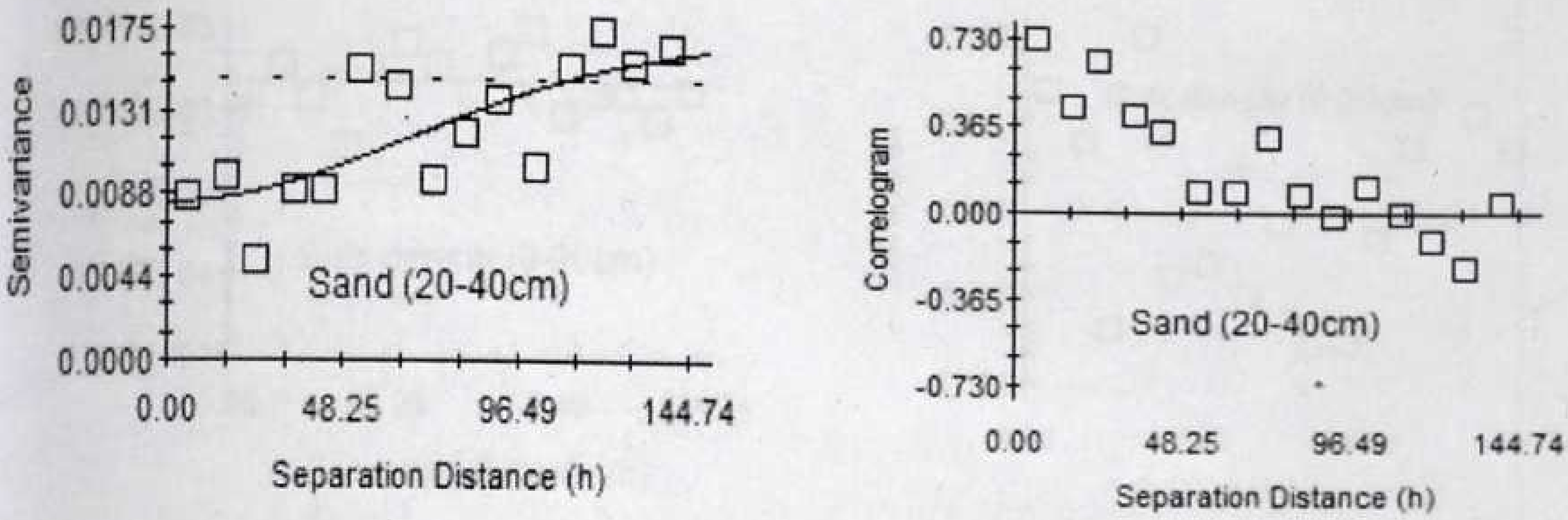

Fig.6d: Best-fitted isotropic semivariogram and autocorrelogram for sand content for the sub-layer.

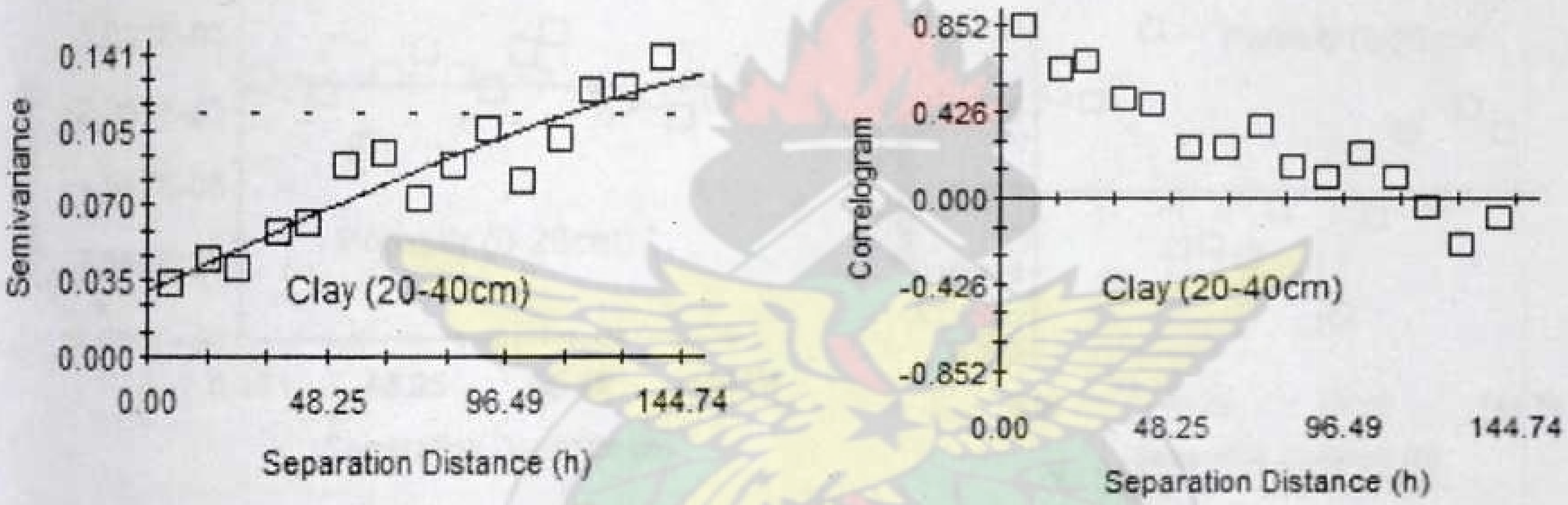

Fig.6e: Best-fitted isotropic semivariogram and autocorrelogram for clay content for the sub-layer.

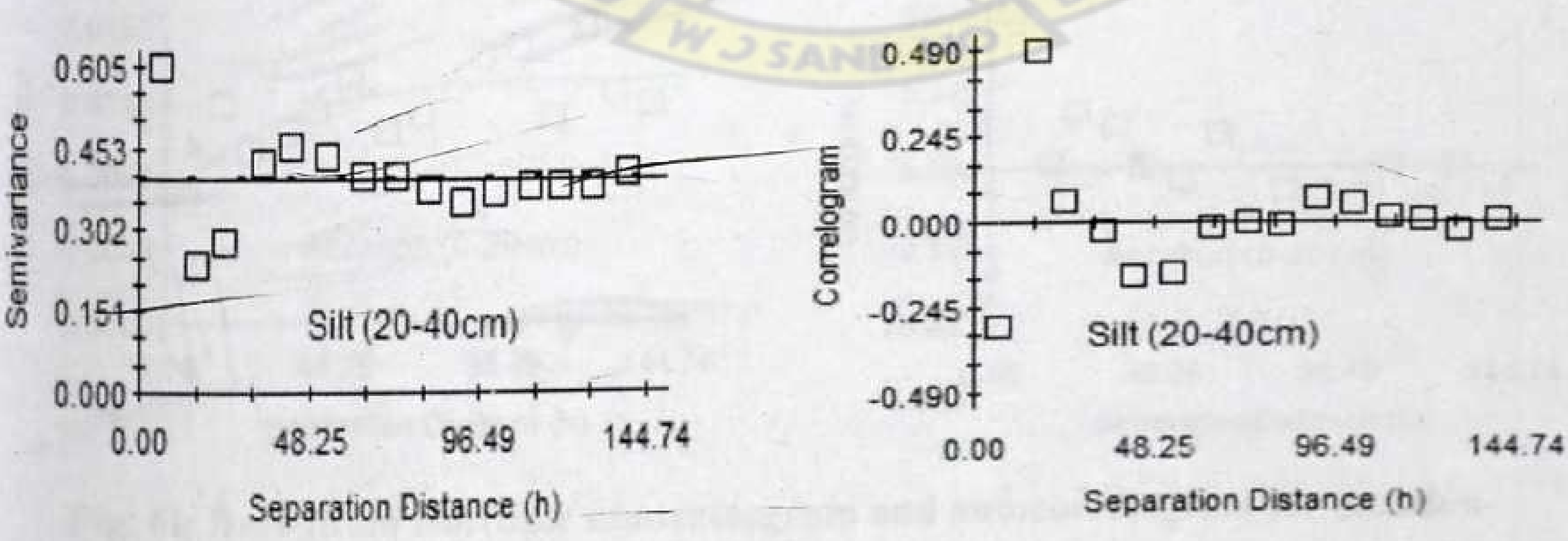

Fig.6f: Best-fitted isotropic semivariogram and autocorrelogram for silt content for the sub-layer.

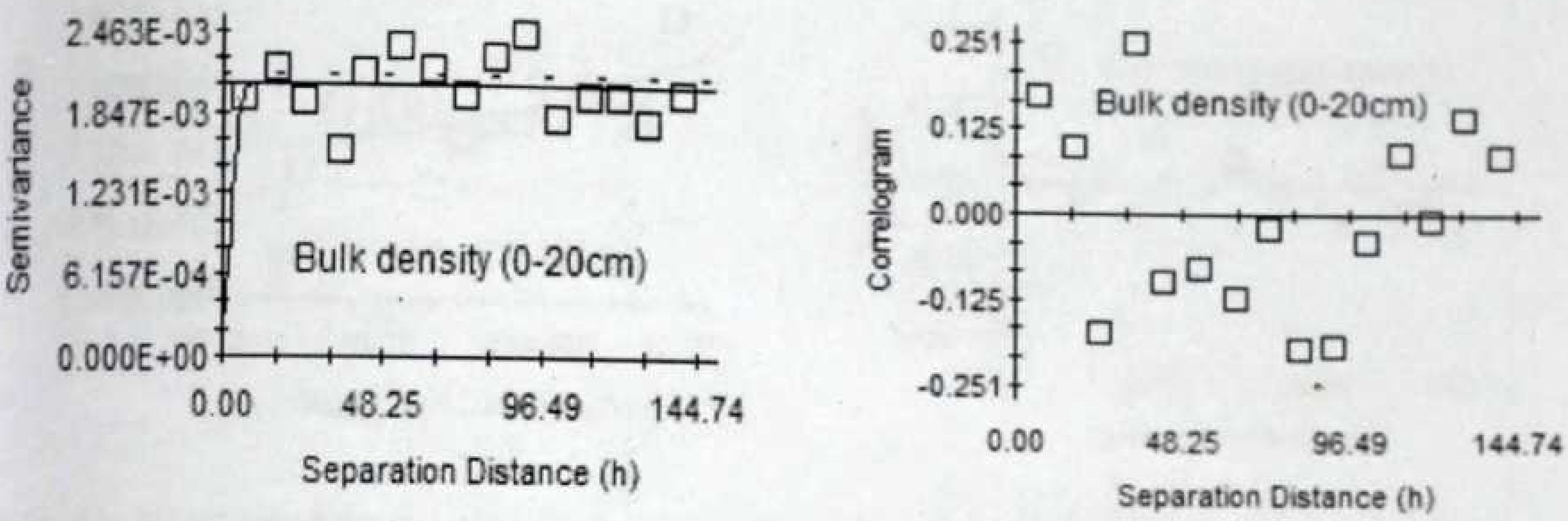

Fig. 6g: Best-fitted isotropic semivariogram and correlogram for bulk density for the surface layer.

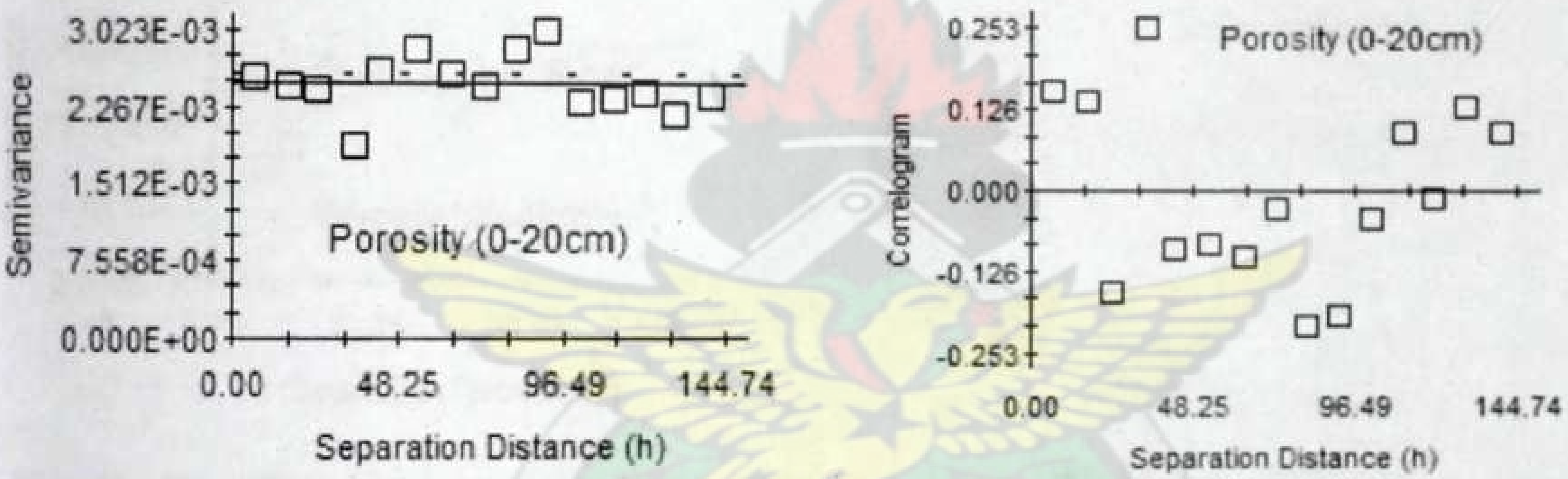

Fig. 6h: Best-fitted isotropic semivariogram and autocorrelogram for total porosity for the surface layer.

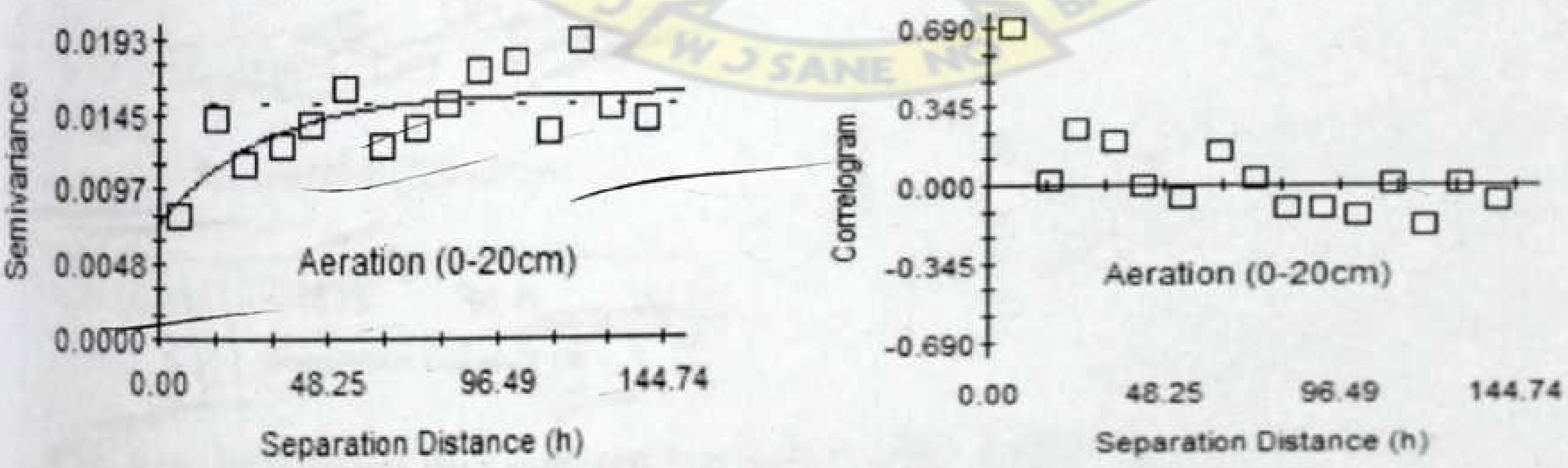

Fig. 6i: Best-fitted isotropic semivariogram and autocorrelogram for aeration-porosity for the surface layer.

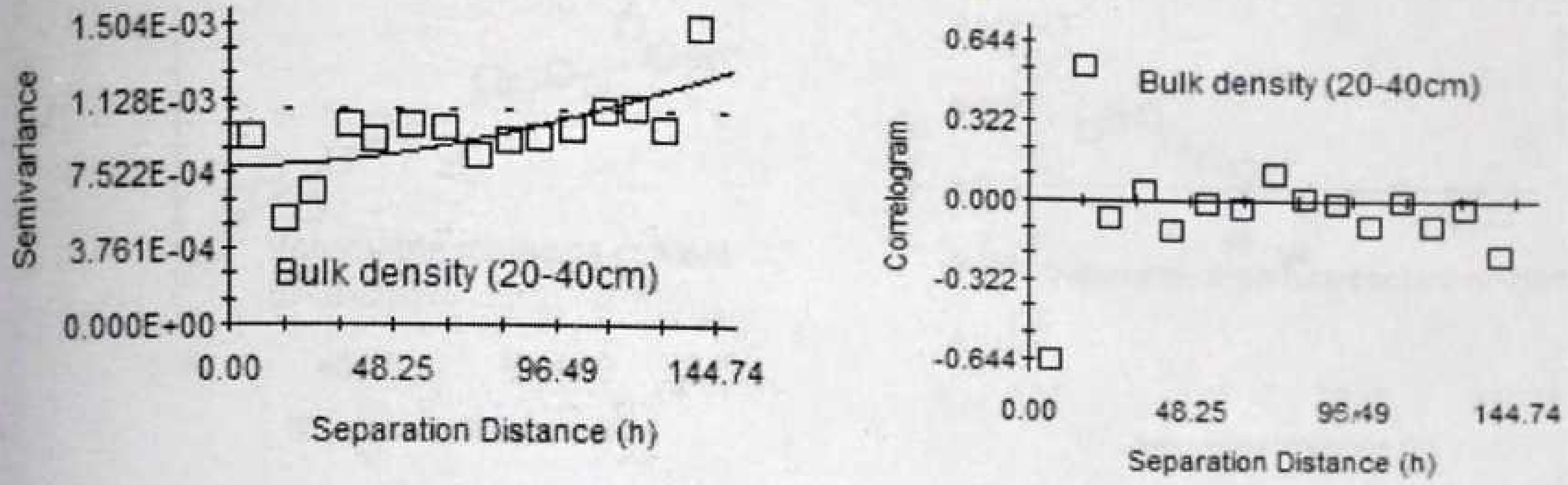

Fig. 6j: Best-fitted isotropic semivariogram and autocorrelogram for bulk density for the sub-surface layer.

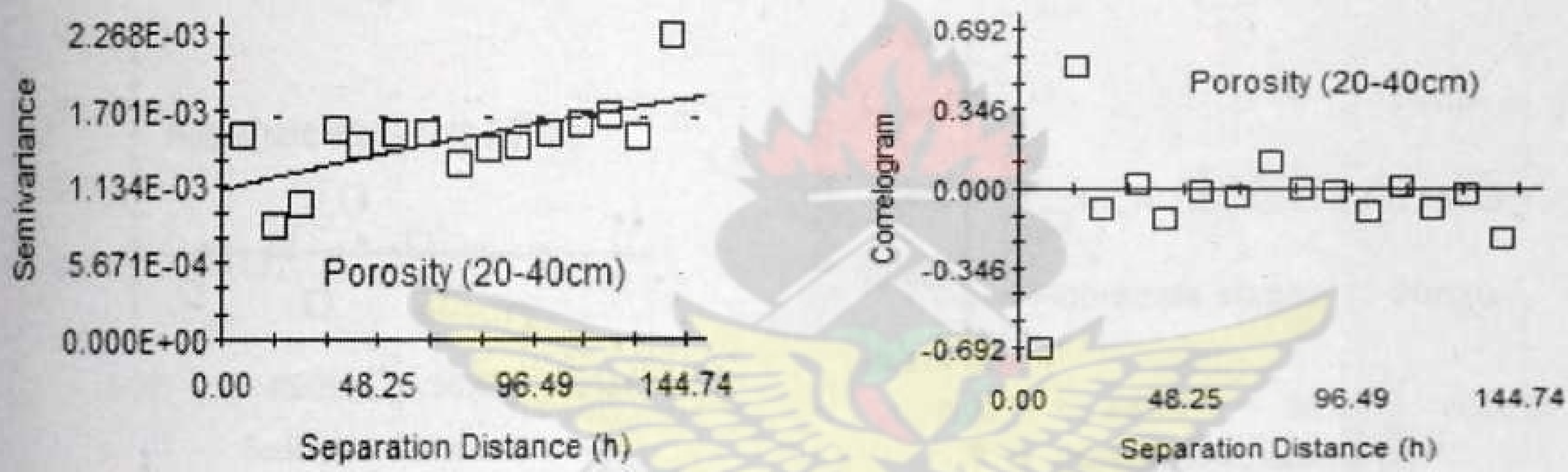

Fig. 6k: Best-fitted isotropic semivariogram and autocorrelogram for total porosity for the sub-surface layer.

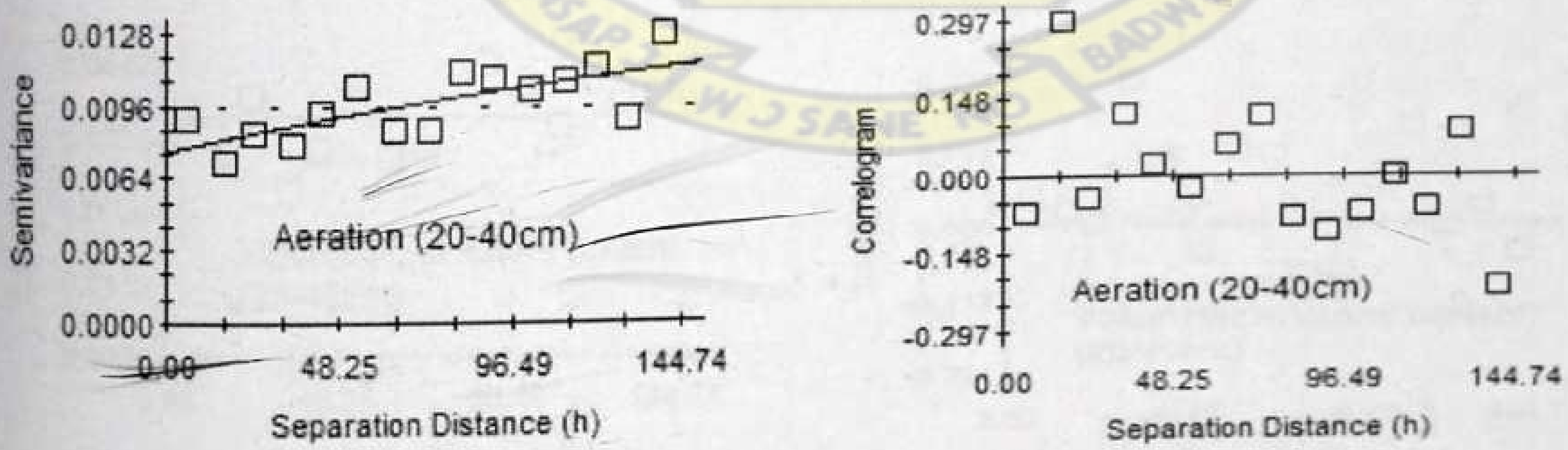

Fig. 6m: Best-fitted isotropic semivariogram and autocorrelogram for aeration-porosity for the sub-surface layer.

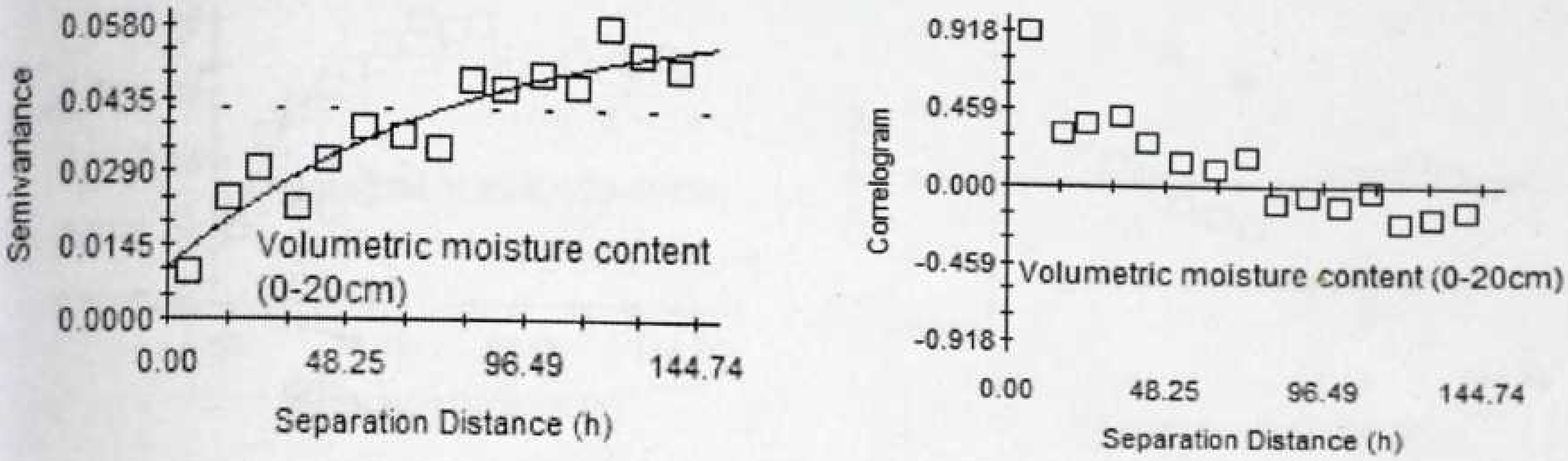

Fig. 6n: Best-fitted isotropic semivariogram and autocorrelogram for volumetric moisture content for the surface layer.

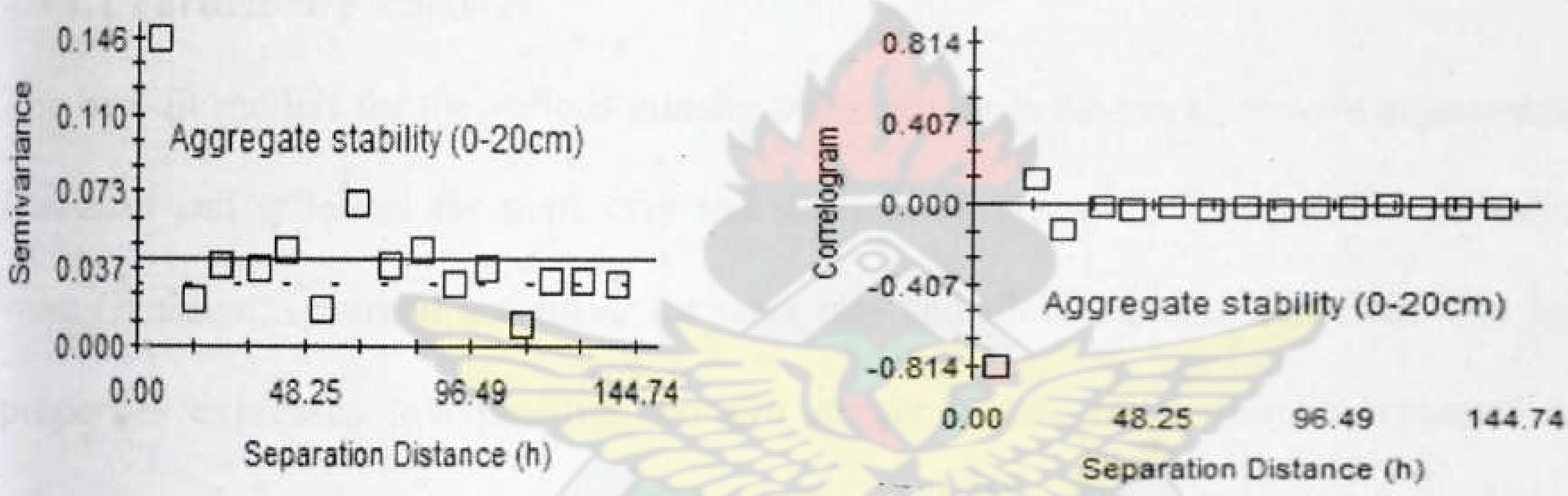

Fig. 6p: Best-fitted isotropic semivariogram and autocorrelogram for aggregate stability for the surface layer.

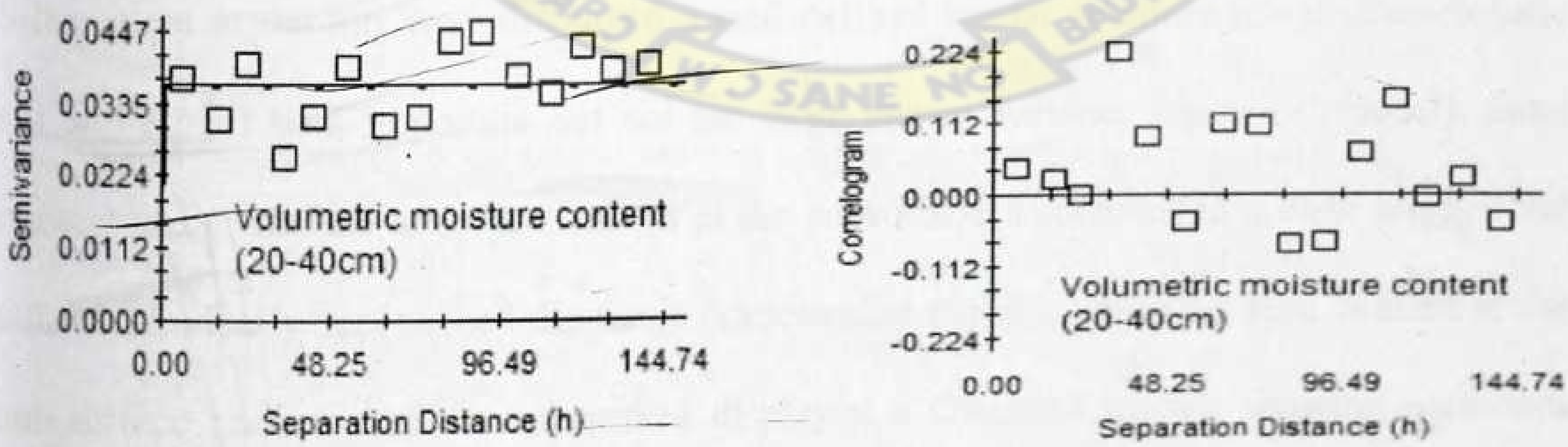

Fig. 6q: Best-fitted isotropic semivariogram and autocorrelogram for volumetric moisture content for the sub-surface layer.

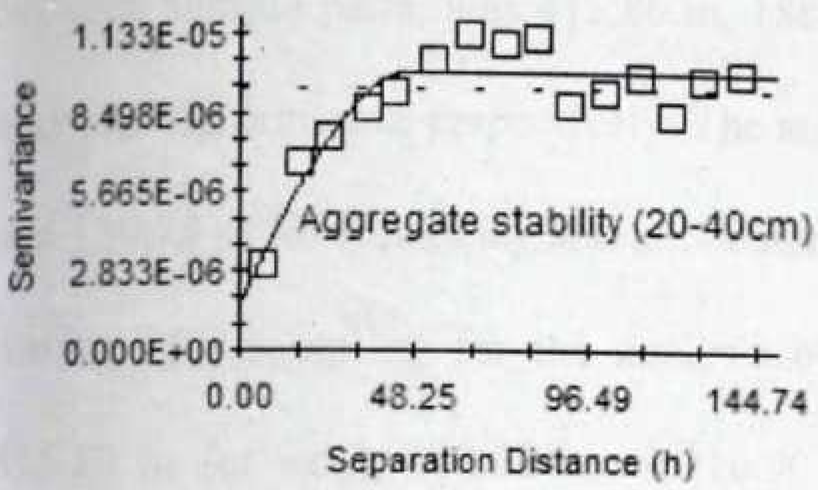

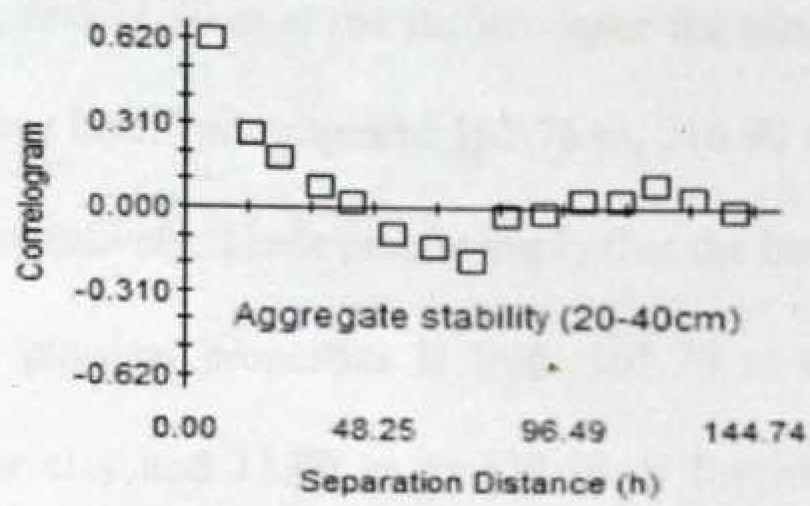

Fig. 6r: Best-fitted isotropic semivariogram and autocorrelogram for aggregate stability for the sub-surface layer.

4.3.1.1 Particle size fractions

The best-fit models for the various primary soil particles in the top layer were exponential, Gaussian and spherical for sand, clay and silt respectively, while those for the sub-layer were Gaussian, spherical and linear for sand, clay and silt contents in that order. The soil properties expressed low positive non-zero nugget values, which can be explained by minimum sampling error, sampling intensity and data recording, short range variability, random and inherent variability.

Silt content at the top layer displayed a well-defined spatial structure (clear characteristic sill and range) with important but ~~not too~~ large nugget variance (spherical model). Sand content at the surface and clay content at the subsurface demonstrated a clear nugget and sill, but gradually approached the range (exponential model), while the sand content at the sub-surface and clay at the subsurface displayed a Gaussian model, showing a smooth variation with small nugget variation as compared to the spatially dependent random variation. Silt content at the sub-layer displayed a linear model (pure nugget) which depicts that this attribute varies at all scales.

The range of influence, which indicates the maximum distance of spatial dependence between sample pairs, was 415.80 m, 188.62 m and 11.70 m at the surface layer for sand, clay and silt contents, respectively. The subsurface layer had ranges of 165.76 m, 216.90 m and 139.78 m for sand, clay and silt contents, respectively. These results imply that the best distance for sampling for the analysis of soil physical properties is from 165.76 m to 415.80 m for sand, 188.62 m to 216.90 m for clay and 11.70 m to 139.78 m for silt. Otherwise, any pair of particle size values with a lag distance greater than 415.80 m for sand content, 216.90 m for clay content and 139.78 m for silt is spatially independent. This suggests that sampling for soil texture analysis should not exceed a maximum distance of 420 m and this will be dependent on the sampling interval as reported by Trangmar *et al.* (1985) and Goovaerts (1997), that sampling intervals influence the semivariogram range. The range values also indicate that the degree of homogeneity for particle size fractions is highest for sand at the surface layer and clay for the subsurface layer and lowest for silt at both depths.

The nugget-to-sill ratio used to classify the spatial dependence of soil properties demonstrated weak to strong spatial dependence for particle size fraction in both surfaces. With the exception of clay content (moderate spatial dependence – SD = 41.70 %), the variables were considered to have a strong spatial dependence at the surface layer based on the ~~values from~~ the ratios (sand = 12.34 %, silt = 0.32 %). With the exception of silt content (SD = 100 %: i.e. pure nugget effect), sand and clay contents at the sub-layer displayed moderate and strong spatial dependencies respectively (sand = 48.49 %, clay = 20.48 %). This result indicated that silt content at the subsurface is spatially independent or spatially uncorrelated (Fig. 6f), which could be probably due to the high variability found in this property (Table 4.1). Though, generally, small nugget values were recorded for the variogram models, moderate spatial dependency displayed by some parameters could be attributed to a relatively higher residual variance (nugget) values.

The differences in the spatial correlation patterns for the primary particles at the different depths could be attributed to intrinsic (soil-forming processes) and extrinsic factors (management and cultivation practices). This inferred that the explainable proportions of the total variation of particles at the surface layer were 87.66 %, 58.30 % and 99.68 % for sand, clay and silt contents respectively, and for the subsurface layer, 51.51 % and 79.52 % for sand and clay contents in that order, while the remaining variation can be attributed to random sources. This signifies that the total variation of silt at the subsurface layer arose from random sources.

4.3.1.2 Bulk density, Porosity, Aeration and Aggregate stability

The soil properties expressed spatial variability across the field with low positive nugget values for some properties indicating small error of the estimation processes. The sources of errors in the estimation processes could be due to many factors such as sampling intensity, positioning, data recording and measurement errors in the determination of soil properties.

In general, the nugget-to-sill ratio used to classify the spatial dependence of soil properties ranged from strong to weak spatial dependence based on the values from the ratios. For example, in this study, the nugget-to-sill ratio showed a strong spatial dependence for bulk density at the surface layer (SD = 13.30 %), while aggregate stability at the surface displayed a pure nugget (very strong spatial independence, SD = 100 %). These spatial relations could be attributed to intrinsic (soil-forming processes) and extrinsic factors (management and cultivation practices). With regard to extrinsic factors (management and cultivation practices). With regard to bulk density, the values for nugget, sill, SD, and range increased from the surface to the deep horizon. This increase indicated higher structured variance, nugget effect/random variability, and range with increase in depth, which may reflect a depositional event or a series of depositional events.

Compared with this study, Tsegaye and Hill (1998) observed lower structural variability in surface bulk density, as judged from a higher nugget (0.003) and lower sill (0.004), that is, percentage nugget attributed 75 % of total variability with a range value of 22 m. The lower range reported by Tsegaye and Hill (1998) could be due to a much smaller sampling interval of 1 m in a relatively small area (45 m x 37 m) located on a level landscape.

4.3.1.3 Moisture content

The semivariogram function for volumetric moisture content (θ_V) was exponential for the two layers. In the surface layer, fairly higher nugget (0.0099), sill (0.062) and higher range (237.30 m) as compared to the subsurface layer, (C_o = 0.00547, $C_o + C_1$ = 0.0365 and A = 0.300 m). This indicates that small estimated errors arose for the subsurface layer as compared to the surface layer. The value for the range at the subsurface layer indicates that θ_V at the subsurface is spatially correlated at a very short distance, signifying that sampling for θ_V should be within a distance of 0.30m. The values of nugget/sill ratios at the surface (14.52 %) and subsurface (14.97 %) exhibited strong spatial dependence, but the surface layer was found to be fairly strongly dependent at a longer distance as compared to the subsurface layer with the shorter distance. This indicates that future sampling for determination of moisture content by volume should be within a maximum distance of

237.30 m. This indicates that future sampling for determination of moisture content by volume should be within a maximum distance of 237.30 m.

4.3.2 Kriging and Cross-validation

The real output of the geostatistical processing is maps illustrating spatial distribution of values measured. The parameters of the best-fitted semivariogram models were used for Kriging to produce the spatial distribution maps of the selected soil properties of the study area (i.e. the parameters of the selected models were used to provide estimates of soil properties at unsampled locations), thus, Kriged estimates provided a visual representation of the arrangement of the population and were used to interpret the spatial variations in the selected soil properties. Regions with white colours always represent higher values of a given parameter. The existence of minor bordered surfaces of different colours in the maps indicated high resolution of maps given by the high measuring density. The contour maps with their associated relative predictive abilities (cross-validation graphs) for physical properties respectively at each depth in the study area have been illustrated in Figures 7.

The spatial maps prepared through ordinary point Kriging procedure were cross-validated by leaving one sample out and predicting for that sample location based on the rest of the samples. Each point on the cross-validation graph represents a location in the input data set for which an actual and estimated value are available. Information about individual points (evaluation indices) resulting from cross-validation of spatial maps of soil properties is given in Tables 4.6 for the physical properties. Figure 7 displays the plots of actual (observed) data against estimated (predicted) data used for the cross-validation process. These maps have greater resolution than the maps presented for mapping units, indicating that when considering land use we can observe the distribution of soil properties in greater detail (Cruz-Rodríguez, 2004).

The model cross validation, thus, shows how well we can predict the soil test value at any sample point from all the other sample points. The results show that, while models can be fit to the data, the model's abilities to predict the soil test values at untested locations within the field are not very good. For example, sample locations for sand at the surface layer must be closer together than 415.8 m (range = 415.8 m) in order to be dependent (to be able to predict something about the soil test value at one location simply by knowing the soil test value at the neighbouring location).

A model that predicts the right value at every single location (ideal model) would have a slope of 1.0, an r^2 of 1.0 and a Y-intercept of 0. Value of Y-intercept greater than 0 and slope less than 1 indicate that the model tends to over predict lower soil test values and under predict higher ones (Brouder *et al.*, 2001). An absolute value of 0.75 for the slope was selected to test the strength of prediction. As a result, a slope of < 0.5 showed a poor prediction, between 0.5 and 0.75 showed a moderate prediction and ≥ 0.75 showed a good prediction,

Spatial maps of basic soil physical properties for 0-20 cm and 20-40 cm soil depth prepared through ordinary Kriging are presented in Fig. 7. Evaluation indices resulting from cross-validation of spatial maps of soil physical properties are given in Table 4.6. Observed values of physical properties for the sampling locations in this study were plotted against their predicted values from the spatial maps (Figs. 7). Among the soil physical properties, scatter plots of observed and predicted values and their spread around the 1:1 line were poor for the surface layer aggregate stability (Fig. 7p) and porosity (Fig. 7h) as well as sub-surface silt content and aggregate stability (Fig. 7f).

Table 4.6: Cross-validation parameters for soil physical parameters for each layer.

Soil property	Depth (cm)	Cross-validation parameter				
		Slope	SE	r^2	Y-intercept	SE-Prediction
Sand (%)	0-20	0.985	0.092	0.595	1.130	0.063
	20-40	0.900	0.119	0.422	7.710	6.192
Clay (%)	0-20	1.111	0.104	0.594	-1.090	3.603
	20-40	1.085	0.107	0.568	-1.170	4.885
Silt (%)	0-20	0.775	0.329	0.066	2.230	3.312
	20-40	-0.117	0.496	0.001	5.210	2.759
Bulk density (gcm^{-3})	0-20	0.587	0.399	0.027	0.584	0.063
	20-40	0.771	0.219	0.137	0.340	0.044
Porosity (%)	0-20	0.244	0.608	0.002	35.380	2.396
	20-40	0.820	0.261	0.112	8.030	1.712
Aeration (%)	0-20	0.695	0.308	0.061	10.930	4.170
	20-40	0.735	0.261	0.093	8.480	2.923
Volumetric water content (%)	0-20	0.849	0.133	0.342	1.800	1.819
	20-40	0.788	0.298	0.082	2.870	2.228
Aggregate stability (%)	0-20	-0.559	1.045	0.004	33.060	8.026
	20-40	0.490	0.173	0.093	10.110	0.058

SE = Standard error of Reg. Coef.; r^2 = coefficient of determination (proportion of variation explained by the best-fit line; Y-intercept = Y-intercept of the best-fit line; SE-Prediction = Standard error of prediction.

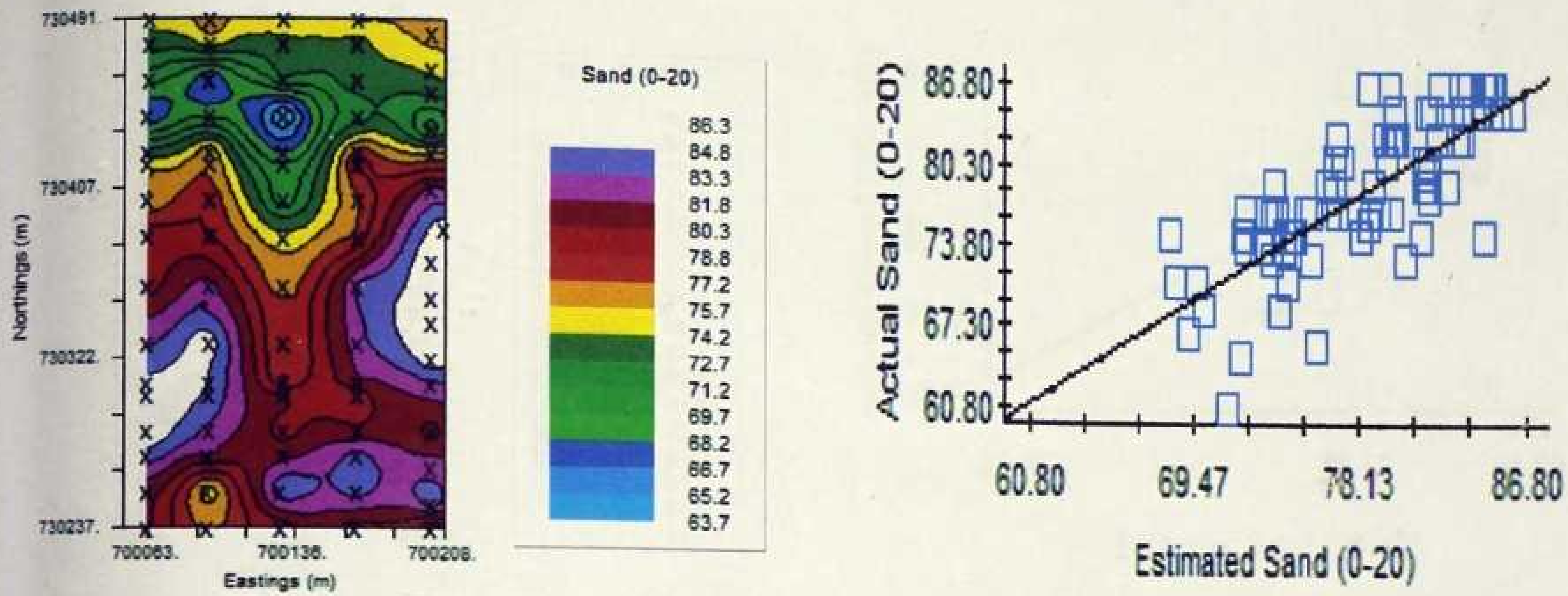

Fig. 7a: Kriged map and Cross-validation graph for sand content in the surface layer.

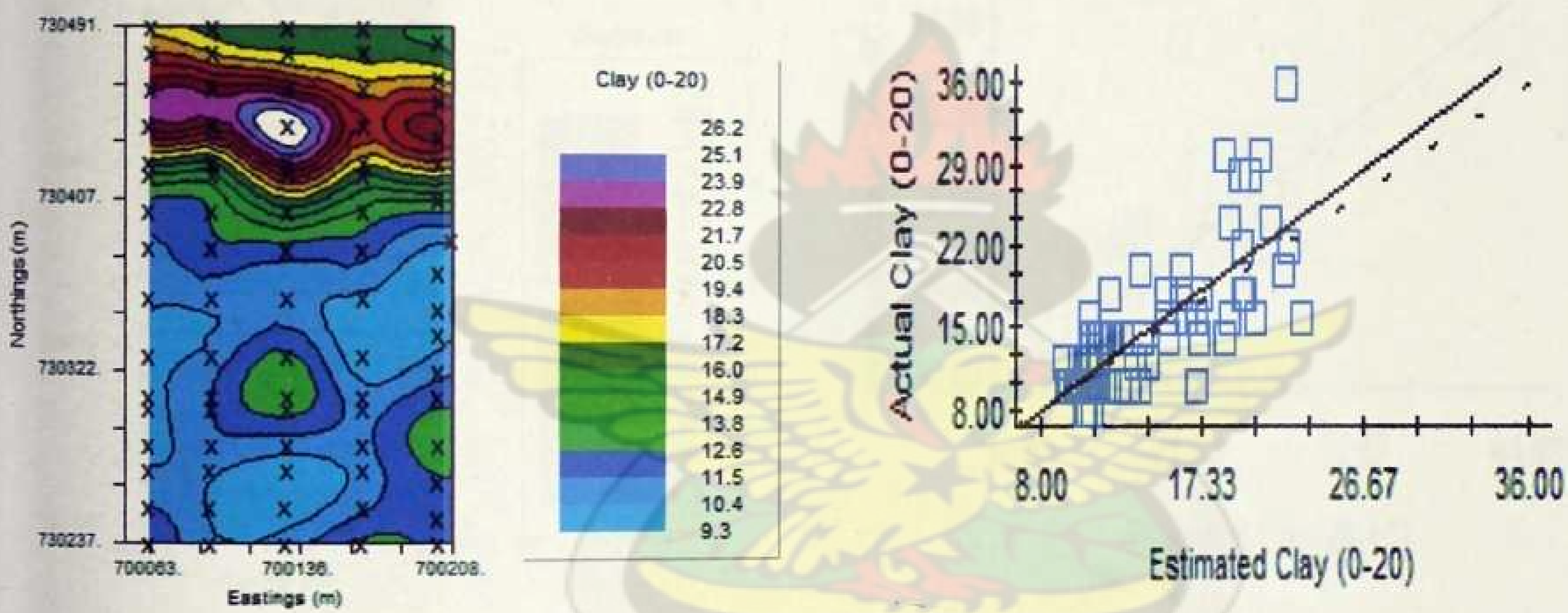

Fig. 7b: Kriged map and Cross-validation graph for clay content in the surface layer.

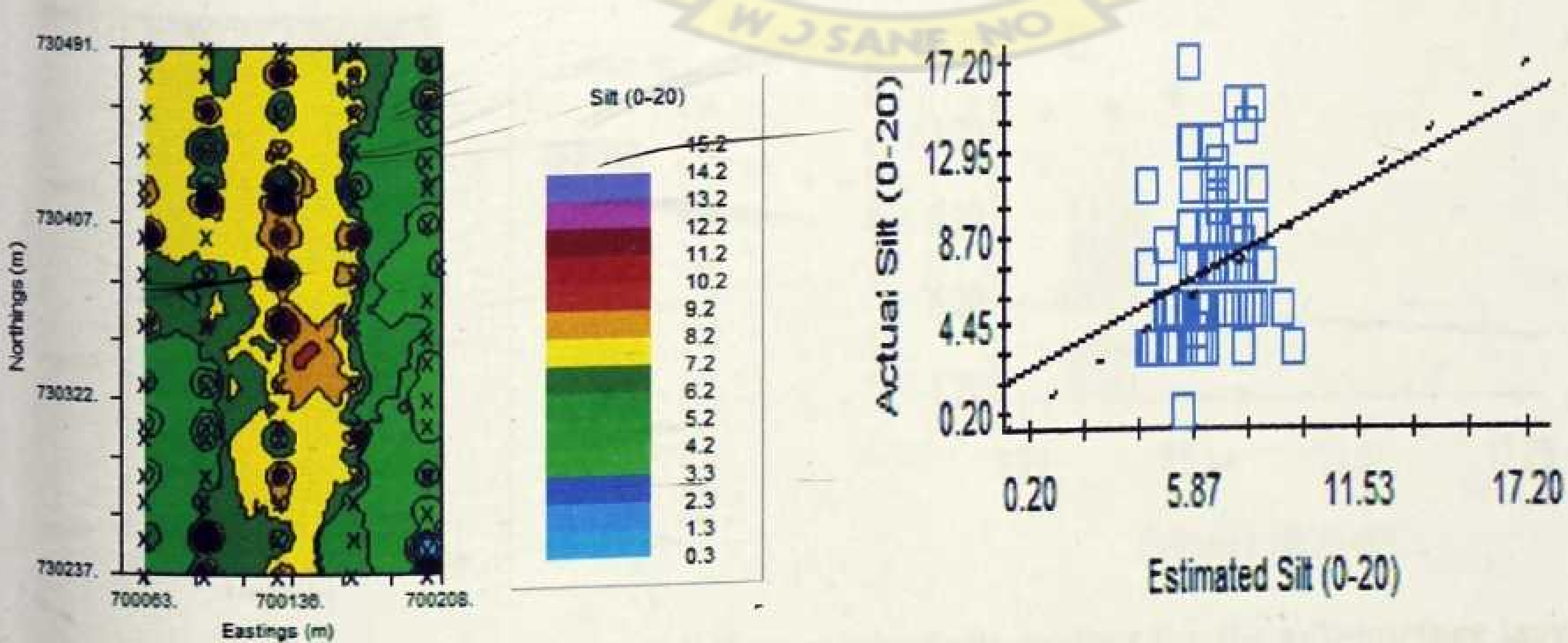

Fig. 7c: Kriged map and Cross-validation graph for silt content in the surface layer.

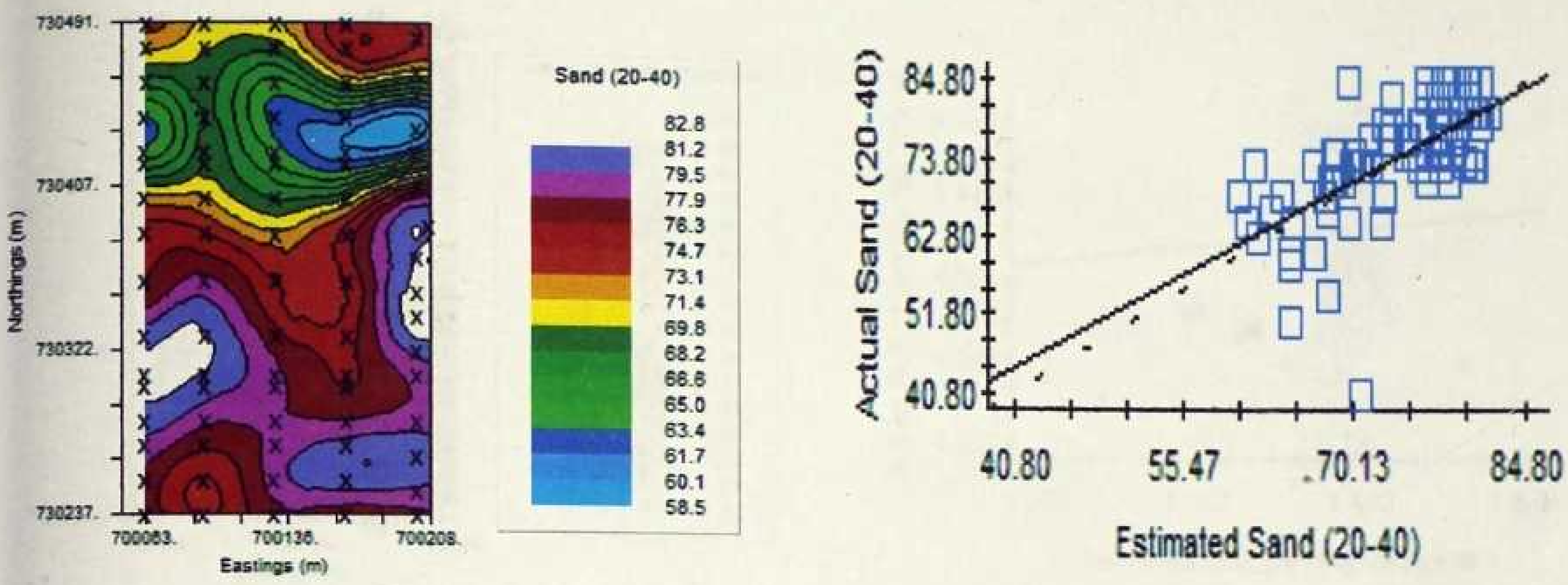

Fig. 7d: Kriged map and Cross-validation graph of sand content in the sub-surface layer.

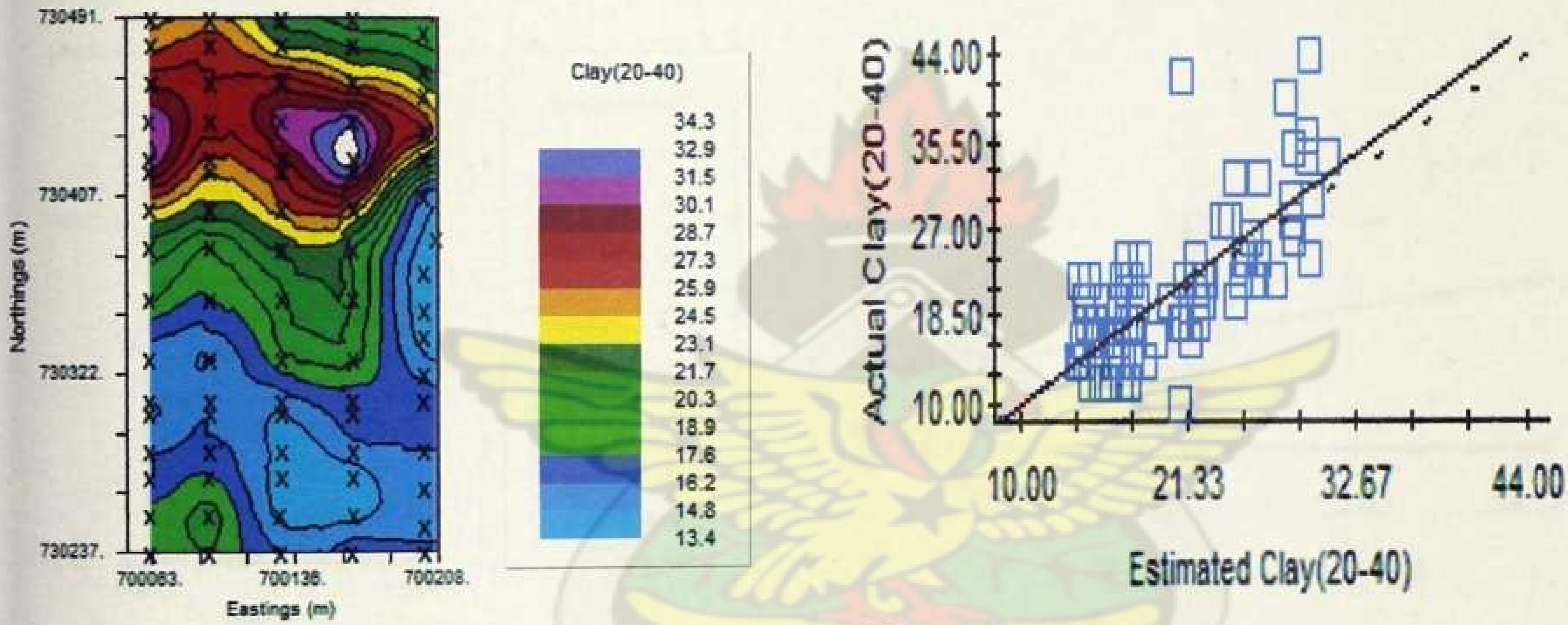

Fig. 7e: Kriged map and Cross-validation graph of clay content in the sub-surface layer.

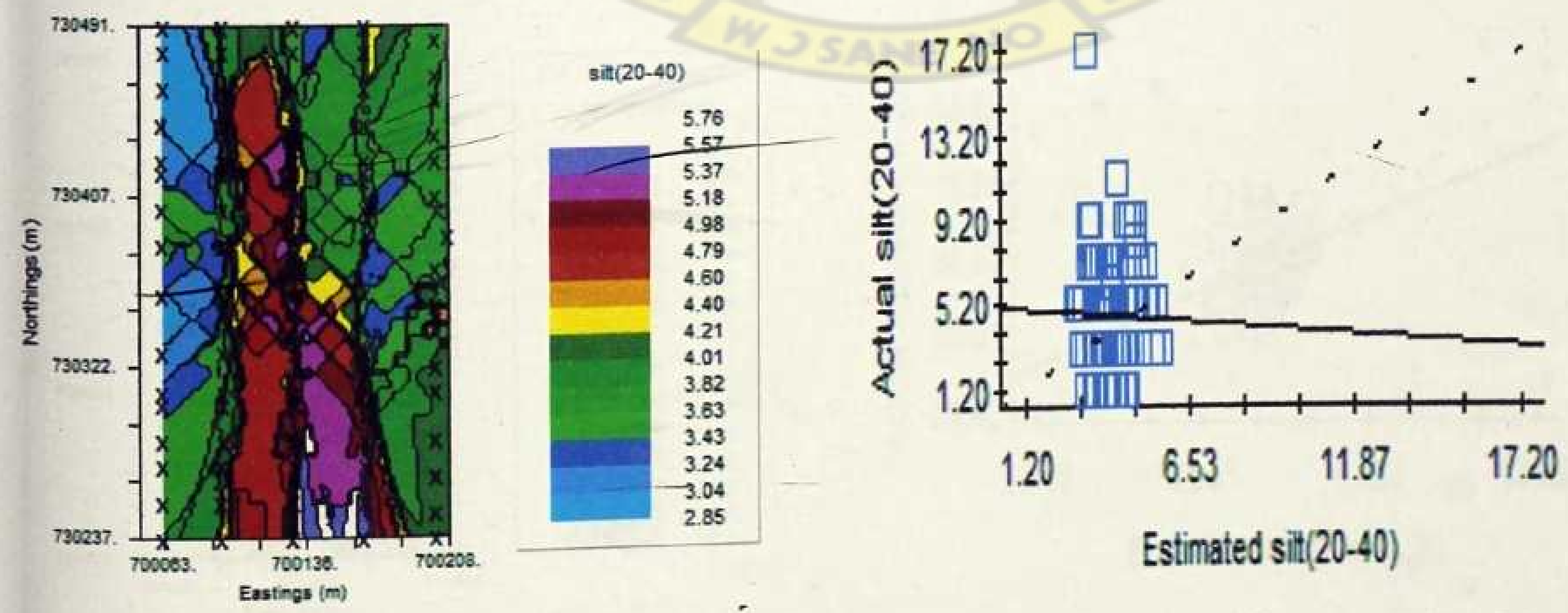

Fig. 7f: Kriged map and Cross-validation graph of silt content for the sub-surface layer.

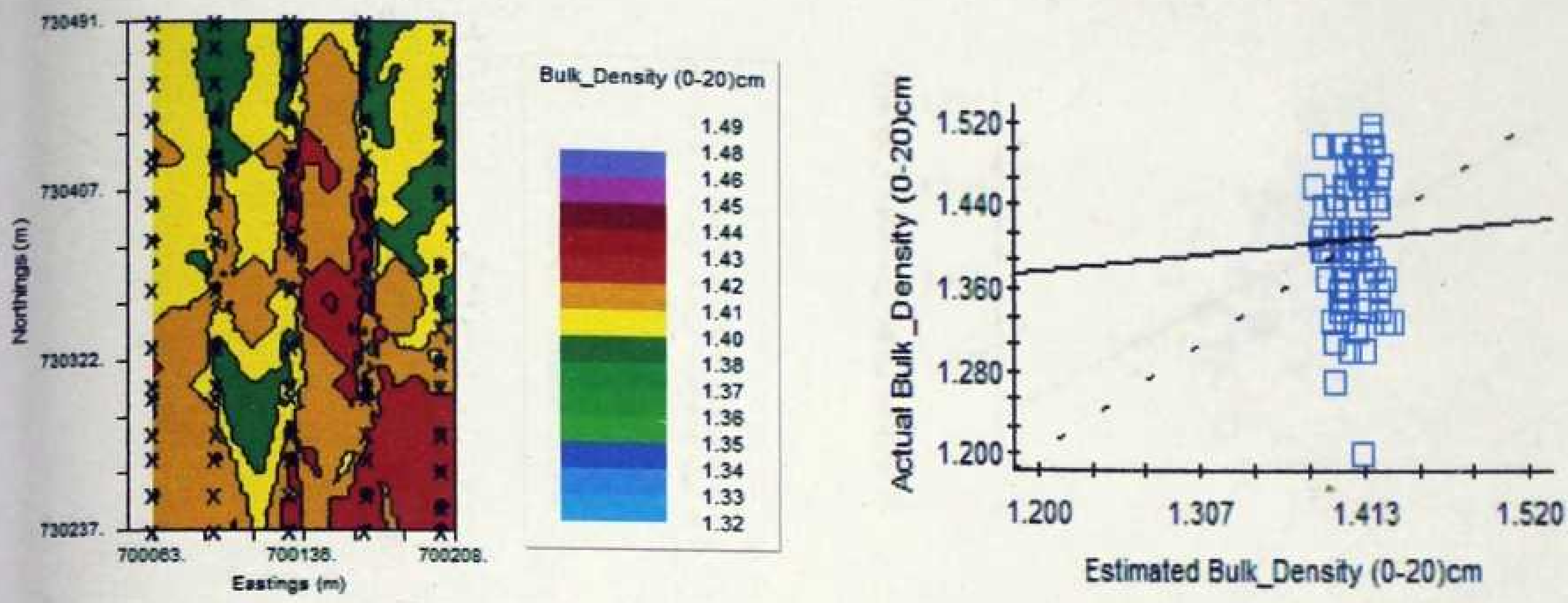

Fig. 7g: Kriged map and Cross-validation graph of bulk density for the surface layer.

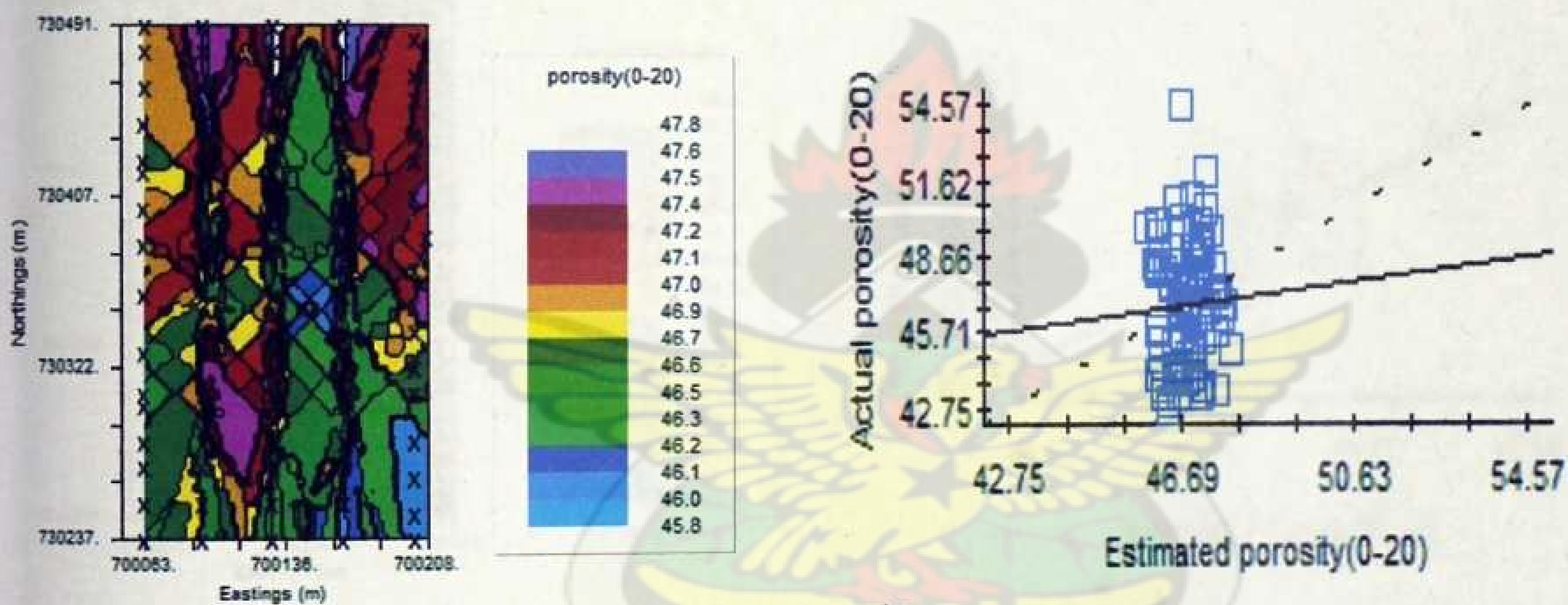

Fig. 7h: Kriged map and Cross-validation graph of total porosity for the surface layer.

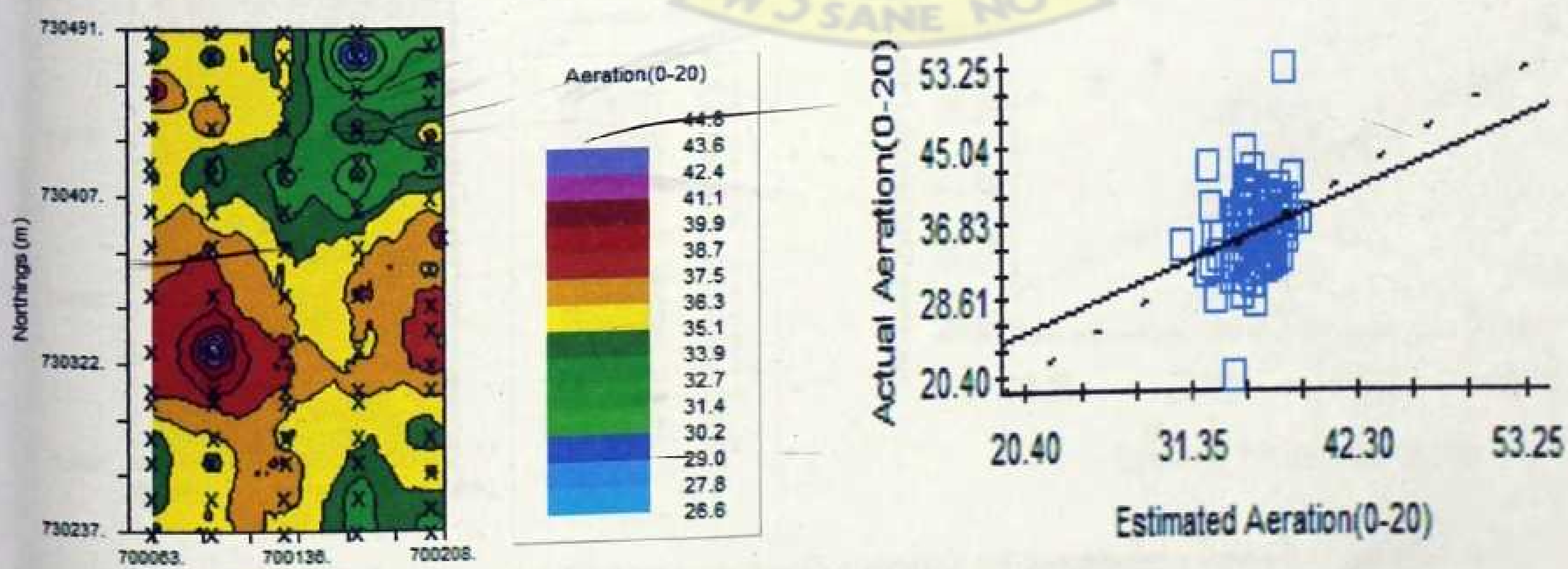

Fig. 7i: Kriged map and Cross-validation graph of aeration-porosity for the surface layer.

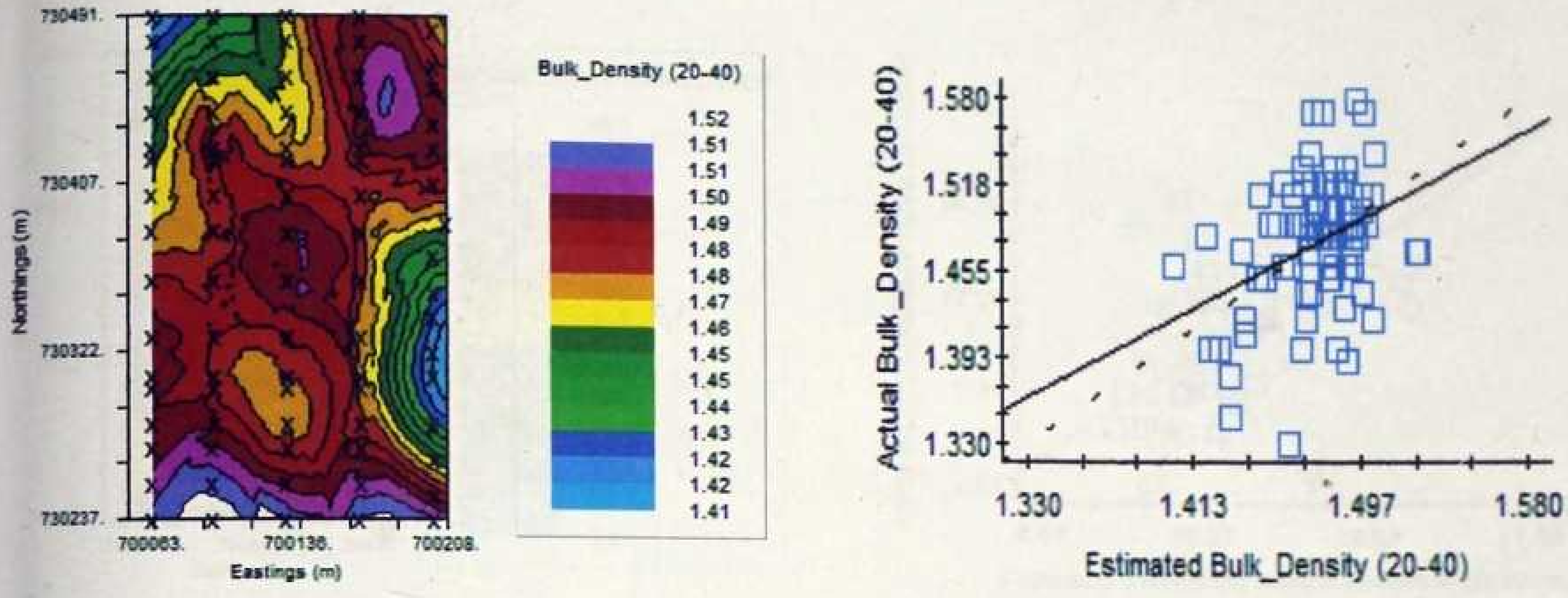

Fig. 7j: Kriged map and Cross-validation graph of bulk density for sub-surface layer.

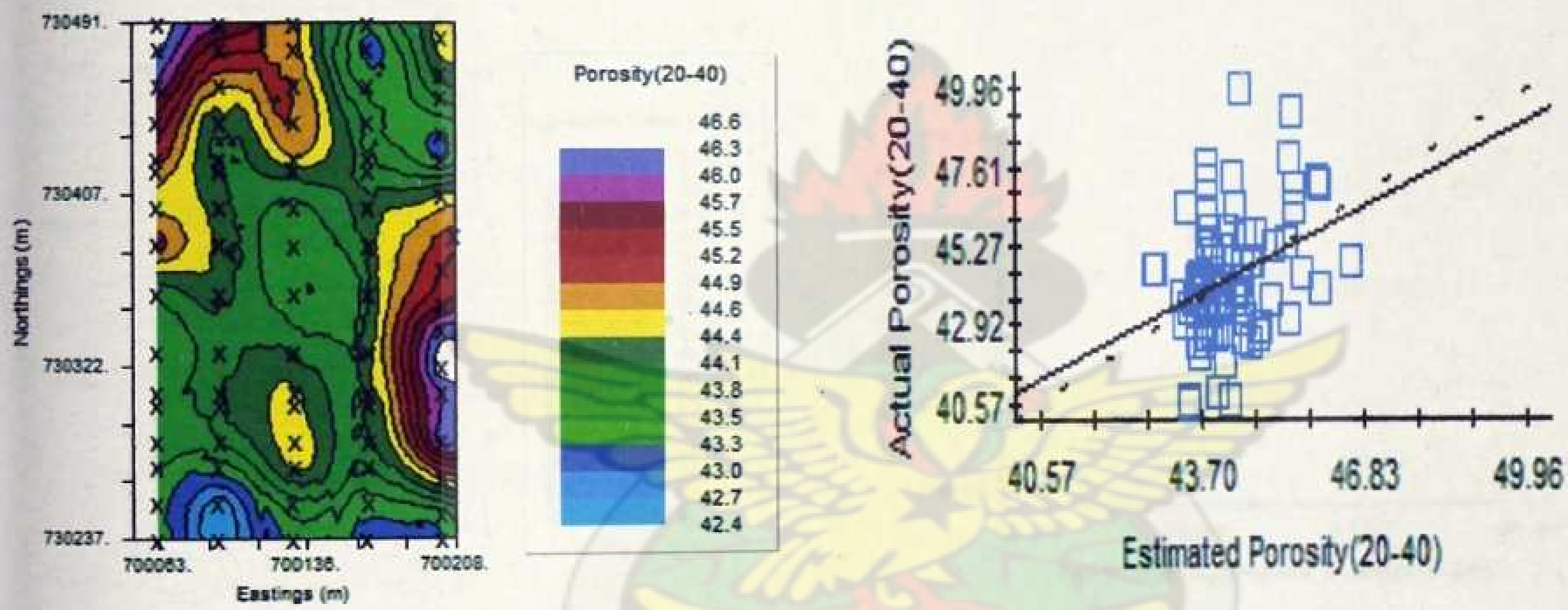

Fig. 7k: Kriged map and Cross-validation graph of total porosity for the sub-surface layer.

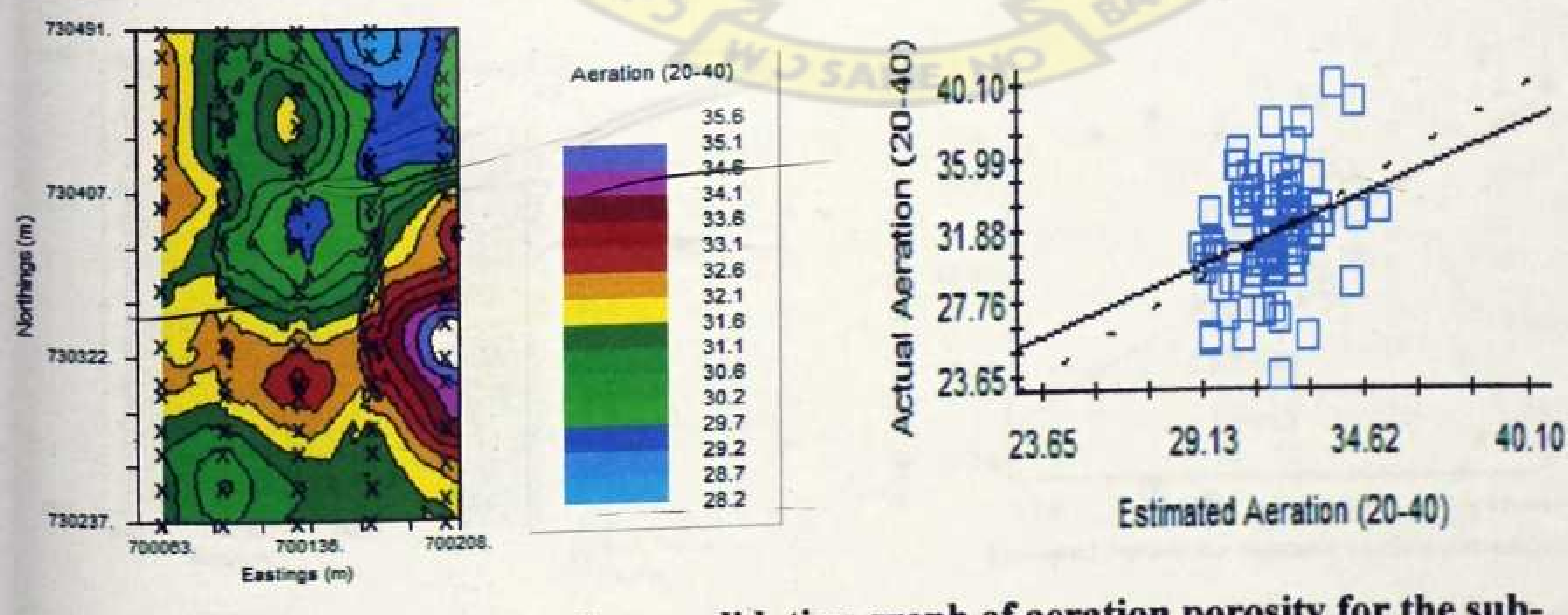

Fig. 7m: Kriged map and Cross-validation graph of aeration porosity for the sub-surface layer.

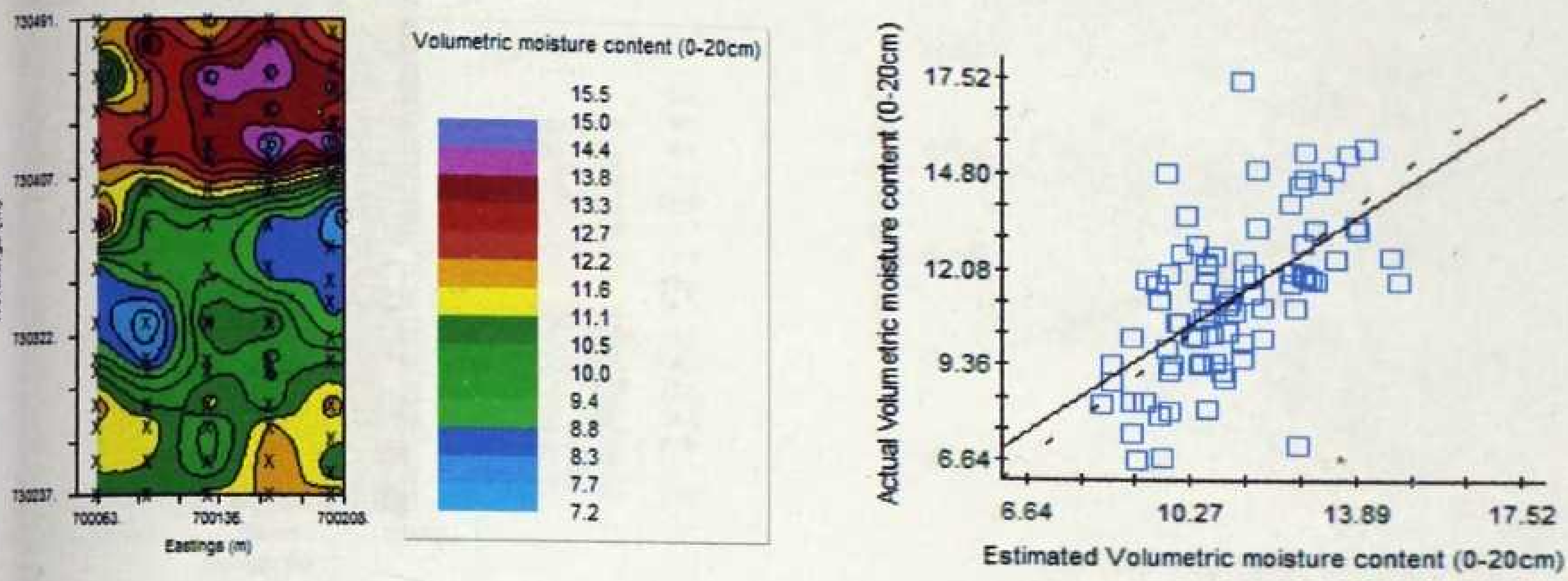

Fig. 7n: Kriged map and Cross-validation graph of volumetric moisture content for the surface layer.

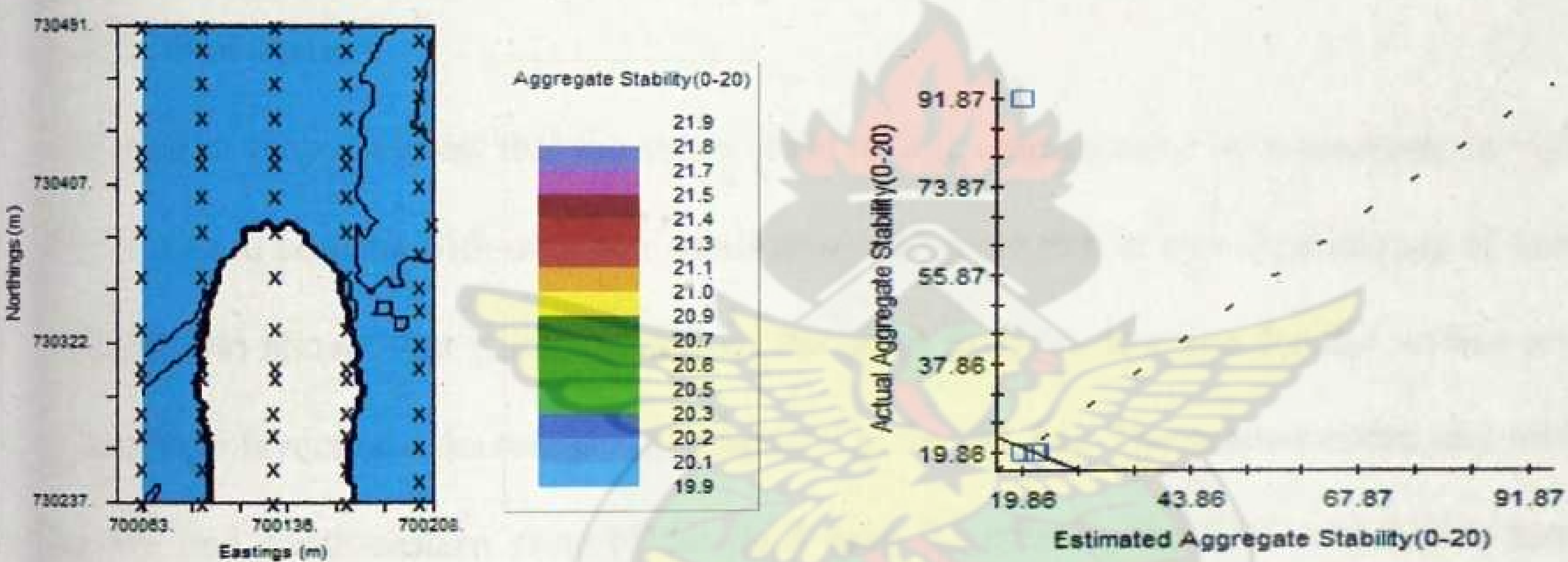

Fig. 7p: Kriged map and Cross-validation graph of aggregate stability for the surface layer.

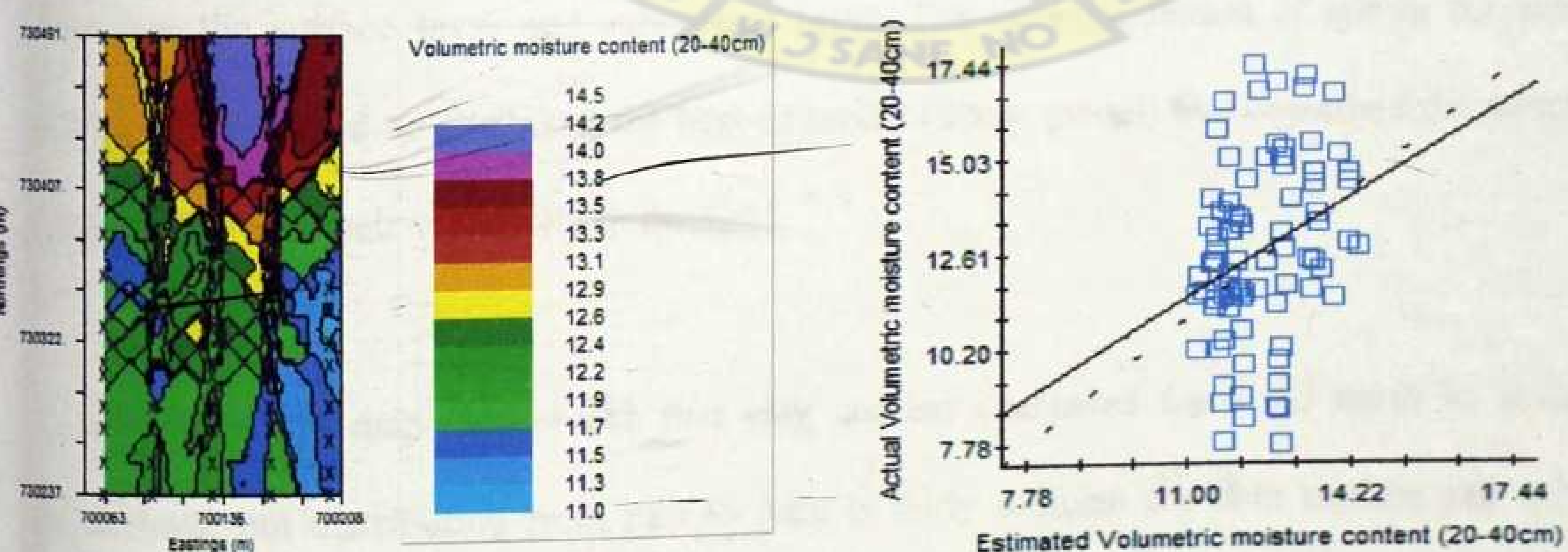

Fig. 7q: Kriged maps and Cross-validation graph of volumetric moisture content for the sub-surface layer.

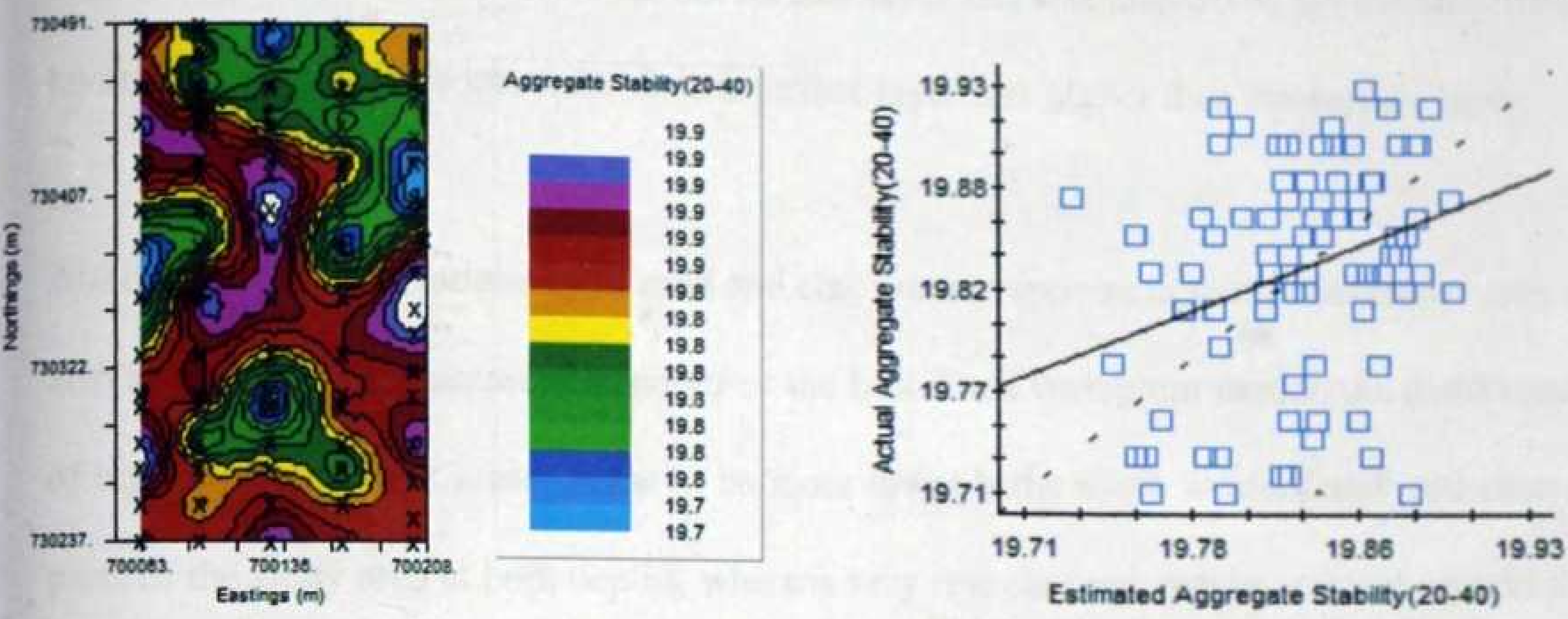

Fig. 7r: Kriged map and cross-validation graph of aggregate stability for the lower depth

4.3.2.1 Soil texture

The spatial maps suggest that the entire study area is characterized by a moderate to high level of sand content with only few small areas which are rich in clay. Spatial map of sand content (%) shows that it increases from the north to south direction for the surface and subsurface layers and decreases with depth (Fig. 7a and 7d). The south-western and mid-eastern and south-eastern parts of the field were the areas in the field with higher sand content for the surface layer and subsurface layer, but slightly higher in the surface than the subsurface. For other parts of the farm, there was no significant difference in silt content between the surface layer and subsurface layer. The poor prediction of silt in the sub-surface layer could be attributed the best-fit model (linear model) that described the nature and structure of their variability in the field.

The distribution map also shows that clay content decreased from the north to south directions, but distribution from east to west is fairly uniform for both surface and sub-surface, except for some few patches. Figures 7b and 7e show that except for a few patches, clay content was less than 22 % for the surface layer and less than 30 % for the subsurface layer. In general, clay content for the subsurface layer was higher than the surface layer.

Although the spatial variability of sand and clay content appears in more continuous way as also suggested by the natural behaviour of the best-fitted variogram model, the distribution of higher sand content areas seems to be more towards the south western and mid-eastern parts of the study area at both depths, whereas very few clay rich patches appear around the mid-western region. Moreover, clay is also found to be well distributed throughout the area but is always with its relatively lower contents. The areas with higher sand are always associated with the lower clay contents. The assumption is that the areas associated with the lower clay contents, (especially on the surface), might be due to the effect of soil erosion or leaching (which removed the easily detachable soil clay leaving behind the coarse grains on the surface).

4.3.2.2 Bulk density, Porosity, Aeration and Aggregate stability

The southern and north-eastern regions of the field have bulk density in the range 1.50 - 1.52 g/cm^3 at the subsurface but lower at the surface (Figs. 7g and j). This shows the presence of compacted subsurface layer in the southern part of the farm, possibly due to tillage practices. The distribution of bulk density at the surface layer ranges from 1.38 - 1.42 g/cm^3 across the field at the surface, with higher values (1.43 g/cm^3) located at the south-eastern part of the field and few patches in the centre. A general trend of increase in bulk density with depth was observed, with higher values (1.42 - 1.52 g/cm^3) at the south-eastern part for the surface layer and southern part and north east for the subsurface.

Patterns of the distribution of total porosity in both sampling layers are represented in Figs. 7h and k. The values range from 45.8 % to 47.8 % in the top-layer and 42.4 % to 46.6 % in the sub-surface layer. The distribution in the surface layer (Fig. 7h) has no distinct trend (patchy), with higher values (47.4 % - 47.8 %) located at the northern, mid-north-eastern and mid-south-western parts, near the centre of the field. The distribution in the subsurface layer (Fig. 7k) has a smooth continuous trend. Except for a patch of 44.4 % to 44.6 % dominant values (43.3 % - 44.4 %), were found to be located in the middle of the field, stretching from north to south. Lower values (42.4 % - 43.3 %) were found to be concentrated in the southern part of the field with a few patches in the north-eastern part, while higher values (45.7 % - 46.6 %) were found in the south-eastern and north-western parts of the field. The poor prediction porosity in the surface layer could be attributed the best-fit model (linear model) that described the nature and structure of their variability in the field.

The distribution of aeration porosity in the field is illustrated by Figs. 7i and m for the top- and sub-layers, respectively. For the surface layer, the range of the distribution is in the order of 26.6 % to 44.8 %, whereas values for the sub-surface layer ranged from 28.2 % to 35.6 %. This suggests that the top layer is highly aerated as compared to the subsurface layer. This could be attributed to the fact that the surface layer has lower bulk density, higher porosity and lower mean moisture content relative to the subsurface layer. The distribution maps for both layers suggest continuous with patchy distributions across the field.

Figures 7p and r display the spatial maps for the distribution of aggregate stability in the field for the surface and sub-surface layers, respectively. The distribution in the surface layer ranged from 19.9 % to 21.9 %, with higher values (21.9 %) in the mid-southern part of the field, stretching northwards to the centre of the field, which forms about 8.2 % of the total area. The remaining 91.8 % of the field is covered by the lower values (19.9 % - 20.1 %). This suggests that the aggregate stability of the surface layer could be classed into two groups (low and high) of three values (19.9 %, 20.1 % and 21.9 %). The distribution in the sub-layer was observed to be very dissimilar to that of the top layer, in that, the values of the property appeared to be distributed in a patchy pattern with a range in the order of 19.7 % to 19.9 %. The poor prediction of aggregate stability in the surface layer could be accredited the best-fit model (linear model) that described the nature and structure of their variability in the field.

4.3.2.3 Soil moisture content (θ_v)

Spatial maps and cross-validation graphs of θ_v prepared through ordinary Kriging for both depths of study are presented in Figs. 7n and 7q. Moisture content in the surface layer ranged from 7.2 % to 15.0 % and for the sub-surface layer, 11.0 % to 14.2 %. Maximum water content for the surface layer was found at the mid north-western part of the farm, where clay content was the highest. Similar form of spatial trend was also observed for the map of the subsurface. Observed values of θ_v for the sampling locations in this study were plotted against their predicted values from the spatial maps (Figs. 7n and q). Scatter plot of observed and predicted values and their spread around the 1:1 line was better for the surface than the sub-surface layer.

The distribution maps suggest that the field could be prone to erosion since the soil has low aggregate stability, high bulk density and subsequently, low porosity. These measurements can help define management zones, which can be combined with less-dense soil samples to provide a more accurate prediction of spatial variability of soil properties.

CHAPTER FIVE

5.0 CONCLUSIONS AND RECOMMENDATIONS

5.1 Conclusions

Conventional statistics, geostatistical methods, scaling as well as fractal techniques can be employed to address and analyse the problem of spatial variability of soil properties in the field. While classical statistical analyses showed variability of some soil properties as reflected in their coefficients of variation, the geostatistical analyses facilitated the recognition of the variability within the area in accordance with the management zone theory.

The study has shown that in spite of the small field size used for the study, soil properties exhibit spatial variability (relatively large and small) as well as non-random spatial patterns, which could be attributed to intrinsic soil properties due to soil forming processes as well as extrinsic factors due to variations in soil management. Once more, it has been revealed that on a small scale, the spatial variability of soil properties is mainly influenced by the variations in moisture content and bulk density which are modified by meteorological conditions, agricultural treatments and crops.

Interpretation of the measured parameters using geostatistics, specifically Kriging, could permit in delineating homogeneous areas in the field that could receive the same level of inputs for agricultural management. Intrinsic variability of locations within the field can be analysed based on the spatial dependence between observations.

In general, the study proved that maps alone do not provide sufficient information to figure out the suitability of soils for sustainable activities, but the assessment of the structure of variability is equally important.

5.2 Recommendations

From the study, the following recommendations have been proposed:

- Spatial variability studies based on localized soil sampling to generate soil property maps should be developed into one of the resources for evaluating and interpreting the mechanical and dynamic properties of agricultural soils.
- Soil sampling, therefore, needs to be effectively and efficiently planned in time as well as space, since important attributes may vary from year- to-year, season-to-season, or even more frequently.
- Knowledge of within-field variability over a number of years and seasons should be made available to farmers and sampling needs to be tailored to the local variability of a site and the farmers' information needs (The objective of sampling should be to provide information helpful to management decisions and to fill knowledge gaps).
- Application maps resulting from the delineation of management zones should be generated for various farm inputs such as tillage intensity, seed rate, fertilizer, pesticides or irrigation application to give specific details of inputs required throughout a field. These maps can be fed to a Variable Rate Technology (VRT) system which can be used to treat those variable fields according to the existing variability.
- Studies on the variation of soil attributes due to temporal (time) together with spatial variation should consequently, be considered in the management plans of individual farmers to optimize input application rates for better yield and economics of crop production.

REFERENCES

Aboulabbes, O. (1984). Infiltration characteristics on a small watershed. MS. Thesis. Utah State University, Logan, Utah.

Addison, P.S. (1997). Fractals and Chaos: An Illustrated Course. Institute of Physics Publishing, Bristol.

Adhikari, K., Carre F., Toth, G. and Montanarella, L. (2009) Site Specific Land Management: General Concepts and Applications. JRC Scientific and Technical Reports, EUR23978 EN – 2009.

Ahuja, L.R., Naney, J.W. and Nielsen, D.R. (1984). Scaling soil water properties and infiltration modeling. Soil Sci. Soc. Am., J. **48**: 970-973.

Aksakal, E.L. and Oztaş, T. (2010). Changes in distribution patterns of soil penetration resistance within a silage-corn field following the use of heavy harvesting equipment. Turk. J. Agric. For. **34**: 173-179.

Arnholt, M., Batte, M.T. and Prochaska, S. (2001). Adoption and Use of Precision Farming Technologies: A Survey of Central Ohio Precision Farmers. OSU AED Economics (AEDE-RP-OO11-O1).

Baker, C.W. (1997). Introduction to Topology. Krieger Publishing Company, Malabar, Florida.

Balasundram, S.K., Ahmed, O.H., Harun, M.H., Husni, M.H.A. and Law, M.C. (2009). Spatial variability of soil organic carbon in palm oil. Int. J. Soil Sci., **4(4)**: 93-103. **ISSN 1816-4978**. Academic Journals Inc.

Berndtsson, R. and Bahri, A. (1996). Soil water, soil chemical and crop variations in a clay soil. Hydrol. Sci. J., **41(2)**: 171-178.

Bierkins, M.F.P. (1996). Modeling hydraulic conductivity of a complex confining layer at various spatial scales. Water Res. Res., **32**: 2369-2382.

Blackmore, S., Godwin, R.J., Taylor, J.C., Cosser, N.D., Wood, G.A., Earl, R. and Knight, S. (1998). Understanding variability in four fields in the United Kingdom. *In*: Robert, P.C., Rust, R.H., Larson, W., (Eds.); Proceedings of the Fourth International Conference on Precision Agriculture. ASA, CSSA, SSSA, Madison, WI, USA, 3-18.

Blumhorst, M.R., Weber, J.B. and Swain, L.R. (1990). Efficacy of selected herbicides as influenced by soil properties. Weed Tech., **4**: 279-283.

Bonsu, M. and Laryea, K.B. (1989). Scaling the saturated hydraulic conductivity of an alfisol. J. Soil Sci. **40**: 731-742.

Bouma, J. and Hole, F.D. (1971). Soil structure and hydraulic conductivity of adjacent virgin and cultivated Pedons at two sites: A typic Argiudoll (silt loam) and a typic Eutrochrept (clay). Soil Sci. Soc. Am. J. **35**: 316-319.

Branson, FA, Gifford, G.F., Renard, K.G. and Hadley, R.F. (1972). Rangeland hydrology. Soc. Range Manag. Range Sci. Series, **1**. Kendall/Hunt Publishing, Co. Dubuque, IA.

Brouder, S., Hofmann, B. and Reetz, H.F.J. (2001). Evaluating Spatial Variability of Soil Parameters for Input Management. Better Crops/Vol. **85(2)**: 8-11.

Burgess, T.M. and Webster, R. (1980). Optimal interpolation and arithmic mapping of soil properties: the semivariogram and punctual Kriging. Soil Sci., **31**: 315-331.

Burrough, P.A, McDonnell, R.A. (1998). Principles of Geographical Information Systems. Oxford University Press Inc., New York.

Burrough, P.A. (1981). Fractal dimensions of landscapes and other environmental data. Nature, **294**: 240-242.

Burrough, P.A. (1983). Multiscale sources of spatial variation in soil: I. The application of fractal concepts to nested levels of soil variation. Eur. J. Soil Sci. **34**: 577-597.

Burrough, P.A. (1986). Principles of Geographical Information Systems for Land Resources Assessment, Oxford University Press, Oxford, UK.

Cambardella, C.A. and Karlen, D.K. (1999). Spatial analysis of soil fertility parameters. Precis. Agric. **1**: 5-14.

Cambardella, C.A., Moorman, T.B., Novak, J.M., Parkin, T.B., Karlen, D.L., Turco, R.F. and Konopka, A.E. (1994). Field-scale variability of soil properties in central Iowa soils. Soil Sci. Soc. Am. J. **58**: 1501-1511.

Cameira, M.R., Fernando, R.M. and Pereira, L.S. (2003). Soil macropore dynamics affected by tillage and irrigation for a silty loam alluvial soil in southern Portugal. Soil Till. Res., **70**: 131-140.

Carter, R.M. (1993). Soil Sampling and Methods of Analysis. Canadian Society of Soil Science, Lewis, Florida, 823.

Cassel, D. K., Wendroth, O. and Nielson, D. R. (2000). Assessing spatial variability in an agricultural experiment station field: Opportunities arising from spatial dependence. Agron. J., **92**: 706–714.

Cassman, K.G. and Plant, R.E. (1992). A model to predict crop response to applied fertilizer nutrients in heterogenous fields. Fertilizer Res. **31(13)**:151-163.

Castriganó, A. and Stelluti, M. (1999). Fractal Geometry and Geostatistics for describing the Field Variability of Soil Aggregation. J. Agric. Engng Res. **73**: 13-18.

Changere, A., and Lal, R. (1997). Slope position and erosional effects on soil properties and corn production on a Miamian soil in Central Ohio. J. Sust. Agric., **11**: 5–21.

Clark, I. (1986). The art of cross validation in geostatistical application. Proceeding of APCOM, 211-220.

Clausnitzer, V., Hopmans, J.W. and Nielsen, D.R. (1992). Simultaneous scaling of soil water retention and hydraulic conductivity curves. Water Res. Res., **28**: 19-31.

Clausnitzer, V., Hopmans, J.W. and Starr, J.L. (1998). Parameter Uncertainty Analysis of Common Infiltration Models. Soil Sci. Soc. Am. J., **62**: 1477-1487.

Crave, A. and Gascuel-Odoux, C. (1997). The influence of topography on time and space distribution of soil surface water content. Hydrol. Processes, **11**: 203– 210.

Cressie, N.A.C. and Horton, R. (1987). A robust-resistant spatial analysis of soil water infiltration. Water Res. Res., **23**: 911–917.

Cruz-Rodríguez, L. (2004). Soil organic carbon and nitrogen distribution in a tropical watershed. MSc. Thesis. University of Puerto Rico, Mayagüez campus.

D'Agostino (1986). Tests for the normal distribution. 367-419. *In*: D'Agostino, R.B. and Stephens, M.A. (Eds.) Goodness-of-fit techniques. New York: Marcel Dekker.

David, M. (1976). The practice of Kriging. Advance Geostatistics in Mining Industry, 31-48.

Davis, B. M. (1987). Uses and abuses of cross-validation in geostatistics. Math. Geol., **19**: 241–248.

Dawson, C. J. (1997). *In*: Stafford, J.V. (Ed.); Precision Agriculture, BIOS Scientific Publishers Ltd. **1**: 45–58.

de Bruin, S. and Stein, A. (1998). Soil-landscape modeling using fuzzy c-means clustering of attribute data derived from a digital elevation model (DEM). Geoderma, **83**: 17–33.

De Lannoy, G.J.M., Verhoest, N.E.C., Houser, P.R., Gish, T.J. and Meirvenne, V.M. (2006). Spatial and Temporal Characteristics of Soil Moisture in an Intensively Monitored Agricultural Field (OPE3). J. Hydrol. , **331**: 719-730.

Deutsch, C.V. and Journel, A.G. (1992). GSLIB. Geostatistical software library and user's guide. Oxford Univ. Press, Oxford.

Diiwu, J.Y., Rudra, R.P., Dickinson, W.T. and Wall, G.J. (1998). Effect of tillage on the spatial variability of soil water properties. Can. Agric. Engng., **40(1)**: 1-7.

Diodato, N. and Ceccarelli, M. (2005). Interpolation processes using multivariate geostatistics for mapping of climatological precipitation mean in the Sannio Mountains (southern Italy), Earth Surface Process, Landforms, **30**: 259–268.

Eliason, M., Heaney, D., Goddard, T., Green, M., McKenzie, C., Peeney, D., Gehue, H., Lachapelle, G. and Cannon, M.E., (1995). Yield measurement and field mapping with an integrated GPS system. 49-56. *In*: Robert, P.C. *et al*. (Ed.); Site-specific management for agricultural systems. Proc. 2nd Int. Conf. on Precision Agric., Minneapolis, MN. 27-30 Mar. 1994. ASA, CSSA and SSSA, Madison, WI.

English B.C., Mahajanashetti, S.B., and Roberts, R.K. (1999). Economics and environmental benefits of variable rate application of Nitrogen to corn fields: Role of variability and weather. A report presented at American Agricultural Economics Association meeting, TN, Aug 8-11.

Entekhabi, D., Asrar, G.R., Betts, A.K., Beven, K.J., Bras, R.L., Duffy, C.J., Dunne, T., Koster, R.D., Lettenmaier, D.P., McLaughlin, D.B., Shuttleworth, W.J., van Genuchten, M.T., Wei, M.Y. and Wood, E.F. (1999). An Agenda for Land Surface Hydrology Research and a Call for the Second International Hydrological Decade. B. Am. Meteorol. Soc., **80**: 2043-2058.

Ersahin, S. (2003). Comparing ordinary Kriging and cokriging to estimate infiltration rate. Soil Sci. Soc. Am. J., **67**: 1848-1855.

Falloon, P.D. and Smith, P. (2000). Modeling refractory soil organic matter. Bio. Fert. Soils, **30**: 388–398.

Famiglietti, J.S., Rudnicki, J.W. and Rodell, M. (1998). Variability in surface moisture content along a hill slope transect: Rattlesnake Hill, Texas, J. Hydrol., **210**: 259–281.

Famiglietti, J.S., Wood, E.F., Sivapalan, M. and Thongs, D.J. (1992). A catchment scale water balance model for FIFE. J. Geophys. Res., **97(D17)**: 18,997–19,007.

FAO/UNESCO (1990). Soil Map of the world. Revised Legend. FAO, Rome, Italy.

Fazeli, M., Shorafa, M. and Khojasteh, D.N. (2010). Comparison of fractal and empirical model for estimation Soil Water Retention Curve. 19th World Congress of Soil Science, Soil Solutions for a Changing World. 1 – 6 August 2010, Brisbane, Australia. 45-48.

Feder, J. (1988). Fractals. New York: Plenum Press.

Federer, C.A. (1982). Subjectivity in separation of organic horizons of the forest floor. Soil Sci. Soc. Am. J., **46**: 1090-1093.

Frangi, J.L. and Lugo, A.E. (1998). A flood plain palm forest in the Luquillo Mountains of Puerto Rico five years after Hurricane Hugo. Biotropica **30**: 339-348.

Franzen, D.W. and Peck, T.R. (2003). Soil sampling for variable rate fertilization. *In*: Hoeft, R.G. (Ed.); Proceeding of Illinois Fertilizer Conference. University of Illinois, Urbana-Champaign, IL, 25–27 January 1993, 81–91.

Freeze, R. A. (1980). A stochastic-conceptual analysis of rainfall and runoff process on a hill slope. Water Res. Res., **16(2)**: 391-407.

Frogbrook Z.L., Oliver M.A., Salahi M. and Ellis R.H. (2002). Exploring the spatial relations between cereal yield and soil chemical properties and the implications for sampling. Soil Use and Manag., **18**: 1-9.

Frogbrook, Z.L. and Oliver, M.A. (2001). Comparing the spatial predictions of soil organic matter determined by two laboratory methods. Soil Use Manag., **17**: 235–244.

Fu, B. and Chen, L. (2000). Agricultural landscape spatial pattern analysis in the semi-arid hill area of the Loess Plateau, China. J. Arid Env., **44**: 291–303.

Fu, B., Chen, L., Ma, K., Zhou, H. And Wang, J. (2000). The relationships between land use and soil conditions in the hilly area of the loess plateau in northern Shaanxi, China. Catena, **39**: 69-78.

Gamma Design Software (2008). GS+ Geostatistics for the Environmental Sciences GS+ Users' Guide, Version 9.0, Plainwell, MI, USA. **ISBN # 0-9707410-0-6**.

Georgakakos, K.P. (1996). Soil moisture theories and observations. J. Hydrol., **184**: 1-152 (special issue).

Geostat workshop (1995). Hampson-Russell Software Services Ltd.

Gessler, P.E., Chadwick, O.A., Chamran, F., Althouse, L. and Holmes, K. (2000). Modeling soil-landscape and ecosystem properties using terrain attributes. *Soil Sci.* Soc. Am. J., **64**: 2046–2056.

Geypens, M., Vanongeval, L., Vogels, N. and Meykens, J. (1999). Spatial variability of agricultural soil fertility parameters in a Gleyic Podzol of Belgium. Precis. Agric., **1**: 319-326.

Gimenez, D., Perfect, E., Rawls, W.J. and Pachepsky, Y. (1997). Fractal models for predicting soil hydraulic properties: A review. Eng. Geol., **48**: 161-183.

Goovaerts, P. (1997). Geostatistics from Natural Resource Evaluation. Oxford University Press, New York.

Goovaerts, P. (1998). Geostatistical tools for characterizing the spatial variability of microbiological and physico-chemical soil properties. Biol. Fert. Soil, **27**: 315–334.

Goovaerts, P. (1999). Geostatistics in soil science: State of the art and perspectives. Geoderma, **89 (12)**: 1-45.

Gülser, C. and Candemir, F. (2008). Prediction of Saturated Hydraulic Conductivity Using Some Moisture Constants and Soil Physical Properties. BALWOIS 2008 - Ohrid, Republic of Macedonia., 1-5.

Gupta, N., Rudra, R.P. and Parkin, G. (2006). Analysis of spatial variability of hydraulic conductivity at field scale. Can. Biosyst. Engng., **48**: 1.55- 1.62.

Gupta, R.K. (1993). Modeling soil water flow process using stochastic approach. Unpublished Ph.D. thesis. Guelph, ON: School of Engineering, University of Guelph.

Haan, C.T. (1977). Statistical Methods in Hydrology, 1st edition. Ames, IA: The Iowa State University Press.

Hald, A. (1952). Statistical theory with engineering applications. John Wiley and sons, New York.

Hawley, M.E., Jackson, T.J. and McCuen, R.H. (1983). Surface soil moisture variation on small agricultural watersheds, J. Hydrol., **62**: 179–200.

Heimlich, R. (1998). Precision Agriculture: Information Technology for Improved Resource Use. Agric. Outlook. (April): 19–23.

Heuvelink, G.B.M. and Webster, R. (2001). Modeling soil variation: Past, present, and future. Geoderma, **100**: 269-301.

Hillel, D. (1982). Introduction to soil physics. Academic Press, Inc. San Diego, California.

Hillel, D. (1998). Environmental Soil Physics. Academic Press, San Diego-London.

Hopmans, J.W. (1987). A comparison of various methods to scale soil hydraulic properties. J. Hydrol. **93**: -256.

Hopmans, J.W. and Overmars, B. (1987). Presentation and application of an analytical model to describe soil hydraulic properties. J. Hydrol. (Amsterdam), **87**: 135-143.

Horn, R. (2004). Time dependence of soil mechanical properties and pore functions for arable soils. Soil Sci. Soc. Am. J., **68(4)**: 1131-1137.

Hu, W., Shao, M.A., Wang, Q.J. and Reichardt, K. (2008). Soil water content temporal-spatial variability of the surface layer of a loess plateau hillside in China. Sci. Agric. (Piracicaba, Braz.), **65 (3)**: 277-289.

Huang, C. and Bradford, J. M. (1992). Applications of a laser scanner to quantify soil micro-topography. Soil Sci. Soc. Am. Proc., **56 (14)**.

Hughes, D.A. and Sami, K. (1992). Transmission losses to alluvium and associated moisture dynamics in a semiarid ephemeral channel system in Southern Africa. Hydrol. Processes, **6**: 45-53.

Iqbal, J., Thomasson, J.A., Jenkins, J.N., Owen, P.R. and Whisler, F.D. (2005). Spatial variability analysis of soil physical properties of alluvial soils. Soil Sci. Soc. Am. J., **69**: 1338–1350.

Isaaks, E. H. and Srivastava, R.M., (1989). An Introduction to Applied Geostatistics. Oxford Univ. Press, New York, Oxford.

Jafarzadeh, A.A., Foroughifar, H., Torabi, H., Aliasgharzad, N. and Toomanian, N. (2010). Spatial Variability Some Physical and Chemical Properties Soil surface In Dasht-e-Tabriz Different Landforms. Geophys. Res. Abst., **12**: EGU2010-336-1.

Jenkins, G.M. and Watts, D.G. (1968). Spectral analysis and its applications. London, UK: Holden-Day Series in Time Series Analysis.

Jirka, S., McDonald, A.J., Johnson, M.S., Feldpausch, T.R., Couto, E.G., and Riha, S.J., (2007). Relationships between soil hydrology and forest structure and composition in the southern Brazilian Amazon. J. Veg. Sci., **18**: 183-194, 2007 IAVS; Opulus Press Uppsala. John Wiley and Sons, UK, **ISBN-13: 9780470209394**.

Johnson, M.S., Lehmann, J., Selva, E.C., Abdo, M., Riha, S.J., and Couto, E.G. (2006). Organic carbon fluxes within and streamwater exports from headwater catchments in the southern Amazon. Hydrol. Process. **20**: 2599-2614.

Jordan, J.P. (1994). Spatial and temporal variability of storm flow generation processes on a Swiss catchment. J. Hydrol., **152**: 357-382.

Journel, A. G. and Huijbregts, C.J. (1978), Mining Geostatistics, London: Academic Press.

Júnior, V.V., Carvalho, M.P., Dafonte, J., Freddi, O.S., Vàzquez, E.V. and Ingaramo, O.E. (2005). Spatial variability of soil water content and mechanical resistance of Brazilian ferralsol. Soil Till. Res. 1-12.

Jury, W.A. (1984). Field scale water and solute transport through unsaturated soils. In: Soil Salinity under Irrigation. Shainberg, I. and Shalhevet, J. (Eds.); Springer Verlag, New York. 115-125.

Jury, W.A. (1985). Spatial variability of soil physical parameters in solute migration: A critical literature review. Electrical Power and Research Institute (EPRI) Report # **EA-4228**, Research Project 2485-6.

Jury, W.A., Gardner, W.R. and Gardner, W.H. (1991). Soil Physics, 5th Ed. Wiley, New York. 268-293.

Jury, W.A., Russo, D. and Sposito, G. (1987). The spatial variability of water and solute transport properties in unsaturated soil: II Scaling models of water transport. Hilgardia, **55(4)**: 33-56.

Kanwar, R.S., Baker, J.L., Horton, R., Jones, L., Handy, R.L. and Lutenegger, L. (1991). Annual progress report of the aquitard/till hydrology project. Department of Agricultural and Biosystems Engineering, Agronomy, and Civil Engineering. Iowa State University, Ames, USA.

Katz, A.J. and Thompson, A.H. (1985). 'Fractal sandstone pores: Implications for conductivity and pore formation'. Physical Review Letters. **54:** 1325–1328.

Kemper, W.D. and Rosenau, R.C. (1986). Aggregate stability and size distribution. *In*: Klute, A. (Ed.); Methods of Soil Analysis, Part 1: Physical Analysis. Soil Sci. Soc. Am., Madison, WI, 425–442.

Kenkel, N.C. and Walker, D.J. (1993). Fractals and ecology. Abstracta Botanica **17(1-2)**: 53-70.

Khakural B.R., Robert, P.C. and Huggins, D.R. (1998). Variability of corn/soybean yield and soil/landscape properties across a southwestern Minnesota landscape: 573-579. *In*: Robert, P.C. *et al.* (Ed.); Proc. 4th Int. Conf. on Precision Agriculture. Am. Soc. Agron., Madison, WI.

Kim, C.P., Stricker, J.N.M. and Feddes, R.A. (1997). Impact of soil heterogeneity on the water budget of the unsaturated zone. Water Res. Res., **33**: 991– 999.

Kitanidis, P.K. (1996). Introduction to geostatistics applications in hydrogeology, California: Cambridge University Press.

Klute, A. (1986). Methods of Soil Analysis. Part 1. Physical and Mineralogical Methods. Second Edition. Am. Soc. Agron., Inc.

Klute, A. and Dirksen, C. (1986). Hydraulic conductivity and diffusivity. Laboratory methods. *In*: Klute, A. (Ed.); Methods of Soil Analysis, Part 1. Physical and Mineralogical Methods, Agronomy Monograph 9. Am. Soc. Agron., Madison, WI. 2nd Edn.

Klute, A. and Wilkinson, G.E. (1958). Some tests of the similar media concept of capillary flow: I. Reduced capillary conductivity and moisture characteristic data. Soil Sci. Soc. Am. Proc. **22**: 278-281.

Kosugi, K. and Hopmans, J.W. (1998). Scaling water retention curves for soils with lognormal pore-size distribution. Soil Sci. Soc. Am., J., **62(6)**: 1496-1505.

Kroulík, M., Mimra, M., Kumhála, F. and Prošek, V. (2006). Mapping spatial variability of soil properties and yield by using geostatic method. Res. Agr. Eng., **52(1)**: 17–24.

Kumar, A., Kanwar, R.S. and Hallberg, G.R. (1994). Modeling spatial variability of saturated hydraulic conductivity using Fourier series analysis. Hydrl. Sci. J., **39(2)**: 143-156.

Kutilek, M. and Nielsen, D.R. (1994). Soil hydrology. Catena Verlag, Cremlingen, Germany.

Lane, L.J., Nichols, M.H. and Paige, G.B. (1995). Modeling erosion on hill slopes: Concepts, theory and data. *In*: Binning, P., Bridgman, R. and Williams, B. (Eds.); Proceedings of the International Congress on Modeling and Simulation (MODSIM '95) November 27-30, 1995, University of Newcastle, Newcastle Australia. Uniprint, Perth.

Lark, R.M., Bolam, H.C., Mayr, T., Bradley, R.I., Burton, R.G.O. and Dampney, P.M.R. (1999). Analysis of yield maps in support of field investigations of soil variation. 151-161. *In*: Stafford, J.V. (Ed.); Proc. 2nd Euro. Conf., Sheffield Academic Press, Sheffield.

Lascano, R.J. and van Bavel, C.H.M. (1982). Spatial variability of soil hydraulic and remotely sensed soil parameters. Soil Sci. Soc. Am., J., **46**: 223-228.

Lavelle, P. and Spain, A.V. (2001). Soil ecology. Kluwer Academic Publishers, Dordrecht, Netherlands.

Leeds-Harrison, P.B., Youngs, E.G., Uddin, B. (1994). A device for determining the sorptivity of soil aggregates. Eur. J. Soil Sci., **45(3)**: 269-272

Legg, B.J. and Stafford, J.V. (1998). Precision Agriculture – new technologies. Proceedings of the Brighton Crop Protection Conference.

Leij, F.J., Romano, N., Palladino, M., Schaap, M.G. and Coppola, A. (2004). Topographical attributes to predict soil hydraulic properties along a hill slope transect. Water Res. Res., **40**: W02407.

Lipiec, J., Kus, J., Slowinska-Jurkiewicz, A. and Nosalewicz, A. (2006). Soil porosity and water infiltration as influenced by tillage methods. Soil Till. Res., **89(2)**: 210–220.

Loague, K.M. and Gander, G.A. (1990). R-5 revisited. 1. Spatial variability of infiltration on a small rangeland catchment. Water Res. Res., **26(5)**: 957-971.

Lodhi, M.A.K. and Johnson, F.L. (1989). Forest understory biomass heterogeneity. Is ''moisture complex'' or associated litter the cause? J. Chem. Ecol., **15(1)**: 429-437.

Logsdon, S.D. and Jaynes, D.B. (1996). Spatial variability of hydraulic conductivity in a cultivated field at different times. Soil Sci. Soc. Am. J., **60**: -709.

Machado, S., Bynum, E.D.J., Archer, T.L., Lascano, R.J., Wilson, L.T., Bordovsky, J., Segarra, E., Bronson, K., Nesmith, D.M., and Xu, W. (2002). Spatial and temporal variability of corn growth and grain yield: Implications for site-specific farming. Crop Sci., **42**: 1564–1576.

Mallants, D., Mohanty, B.P., Vervoort, A. and Feyen, J. (1997). Spatial analysis of saturated hydraulic conductivity in a soil with macropores. Soil Tech., **10**: 115-131.

Mandal, D. and Ghosh, S.K. (2000). Precision farming – The emerging concept of agriculture for today and tomorrow. Current Sci., **79(12)**: 1644-1647.

Mandelbrot B.B., 1989. Fractal geometry: what is it, and what does it do? *In*: Fractals in the Natural Sciences Fleischmann, M. Tildesley, D.J. Ball, and R.C. (Eds.); Royal Society of London/Princeton University Press, New Jersey, USA.

Mandelbrot, B.B. (1982). The Fractal Geometry of Nature. 2nd Edn. Londra: W.H. Freeman.

Mapfumo, E., Chanasyk, D.S. and Chaikowsky, C.L.A. (2006). Stochastic simulation of soil water status on reclaimed land in northern Alberta. J. Spa. Hydrol., **6(1)**.

Mason, D.D., Lutz, J.F. and Petersen, R.G. (1957). Hydraulic conductivity as related to certain soil properties in a number of great soil groups-sampling errors involved. Soil Sci. Soc. Am. Proc., **21**: 554-560.

McBratney, A.B. and Webster, R. (1981). The design of optimal sampling schemes for local estimation and mapping of regionalized variables. Comput. Geosci., **7**: 335-365.

McBratney, A.B. and Webster, R. (1983). Optimal interpolation and isarithmic mapping of soil properties: V. Co-regionalization and multiple sampling strategy, J. Soil Sci., **34**: 137-162.

McConkey, B.G., Ulrich, D.J., and Dyck, F.B. (1997). Slope position and subsoiling effects on soil water and spring wheat yield. Can. J. Soil Sci., **77**: 83–90.

McKenzie, N.J. and Austin, M.P. (1993). A quantitative Australian approach to medium and small scale surveys based on soil stratigraphy and environmental correlation. Geoderma, **57**: 329-355.

Merzougi, M and G. F. Gifford. (1987). Spatial variability of infiltration rates on a semiarid seeded rangeland. Hydrol. Sci. J., **32(2)**: 243-250.

Merzougi, M. (1982). The effect of instrument type in measuring infiltration rates on spatial variability patterns. MS. Thesis. Utah State University, Logan, UT.

Millán H., González-Posada M., Aguilar M., Domínguez J., and Céspedes L. (2003). On the fractal scaling of soil data: particle-size distributions. Geoderma, **117**: 117-128.

Miller, E.E. and Miller, R.D. (1956). Physical theory for capillary flow phenomena. J. Appl. Phys., **27**: 324-332.

Mohanty, B.P., Kanwar, R.S. and Everts, C.J. (1994). Comparison of saturated hydraulic conductivity measurement methods for a glacial-till soil. Soil Sci. Soc. Am. J., **58**: 672-677.

Mohanty, B.P., Shouse, P.J., Miller, D.A. and van Genuchten, M.T. (2002). Soil property database: Southern Great Plains 1997 Hydrology Experiment. Water Res. Res., **38 (5)**: 1-8.

Odeh, I.O.A., McBratney, A.B. and Chittleborough, D.J. (1994). Spatial prediction of soil properties from landform attributes derived from a digital elevation model. Geoderma, **63**: 197–2[illegible]

Oldak, A., Jackson, T.J. and Pachepsky, Y. (2002). Using GIS in passive microwave soil moisture mapping and geostatistical analysis, Int. J. Geogr. Inf. Sci., **16(7)**: 681-698.

Orndorff, K.A. and Lang, G.E. (1981). Leaf litter redistribution in a West Virginia hardwood forest. J. Ecol., **69**: 225-235.

Owe, M., Jones E.B. and Schmugge, T.J. (1982). Soil moisture variation patterns observed in Hand county, South Dakota. Water Res. Bull., **18**: 949-954.

Öztaş, T. (1995). Jeoistatistiğin toprak bilimindeki önemi ve uygulanışı. İ. Akalın Toprakve Çevre Semineri 271-280, Ankara.

Parker, H.M., Journel, A.G. and Dixon, W.C. (1979). The use of conditional lognormal probability distribution for the estimation of open-pit ore reserves in strata-bound uranium deposits-a case study. Proceeding of APCOM, Society of Mining Engineers, 133-148, New York.

Peck, A.J., Luxemoore, R.J. and Stolzy, J.L. (1977). Effects of spatial variability of soil hydraulic properties in water budget modeling. Water Res. Res., **13(2)**: 348-354.

Pélissier, R., Dray, S. and Sabatier, D. (2001). Within-plot relationships between tree species occurrences and hydrological soil constraints: an example in French Guiana investigated through canonical correlation analysis. Plant Ecol., **162**: 143-156.

Perfect, E. and Kay, B.D. (1991). Fractal theory applied to soil aggregation. Soil Sci. Soc. Am. J., **55**: 1555-1558.

Persson, K. and Bangsgaard, J. (1999). Accuracy of fertilizer application for site specific fertilization: 815-824. *In*: Stafford, J.V. (Ed.); Precision agriculture '99, Proc. 2nd Eur. Conf. on Precision agric., Odense, Denmark. 11-15 July 1999. Sheffield Academic Press, Sheffield, UK.

Peterson, C.J. and Campbell, J.E. (1993). Microsite differences and temporal change in plant communities of tree fall pits and mounts in an old-growth forest. Bull. Torrey Bot. Club, **120**: 451-460.

Philip, J.R. (1957). The theory of infiltration, 4, Sorptivity and algebraic infiltration equations, Soil Sci., **84**: 257–264.

Philip, J.R. (1980). Field heterogeneity: Some basic issues. Water Res. Res., **16(2)**: 433-448

Plant, R.E. (2001). Site-Specific Management: The Application of Information Technology to Crop Production. Computers and Electronics in Agriculture, **30**: 9-29.

Qiu, Y., Fu, B., Wang, J. and Chen, L. (2001). Spatial variability of soil moisture content and its relation to environmental indices in a semi-arid gully catchment of the Loess Plateau, China. J. Arid Env., **49**: 723–750.

Rahman, S., Munn, L.C., Zhang R. and Vance, G.F. (1996). Wyoming Rocky Mountain forest soils: Evaluating variability using statistics and geoststistics. Can. J. Soil Sci., **75**: 501-507.

Raich, J.W. and Nadelhoffer, K.J. (1989). Below ground carbon allocation in forest ecosystems: global trends. Ecol., **70(5)**: 1346–1354.

Raine, S.R., Meyer, W.S., Rassam, D.W., Hutson, J.L. and Cook, F.J. (2005). Soil-water and salt movement associated with precision irrigation systems - research investment opportunities, Final report to the national program for sustainable irrigation, Cooperative Research Centre for Irrigation Futures, Toowoomba.

Rao, P. S. C. and Wagenet, R. J. (1985). Spatial variability of pesticides in field soils: Methods for data analysis and consequences: Weed Sci., **33(2)**: 18-24.

Reichardt, K., Timm, L.C. and Bacchi, O.O.S. (2003). Dimensional Analysis, Scaling and Fractals. Lecture given at the College on Soil Physics Trieste, 3-21 March 2003, LNS0418035.

Reynolds, S.G. (1970). The gravimetric method of soil moisture determination, I: A study of equipment and methodological problems. Hydrol., **11**: 258–273.

Rieu M. and Sposito G., (1991a). Fractal fragmentation, soil porosity and soil water properties: I. Theory. Soil Sci. Soc. Am. J., **55**: 1231-1238.

Rieu M. and Sposito G., (1991b). Fractal fragmentation, soil porosity and soil water properties: II. Applications. Soil Sci. Soc. Am. J., 55: 1239-1238.

Roberts, P.C., Rust, R.H. and Larson, W.E. (1995). Site specific management for agricultural systems. Proc. 2nd Int. Conf. on Precision agric., Minneapolis, MN. 27-30 Mar. 1994. ASA, CSSA and SSSA, Madison, WI.

Robock, A., Schlosser, C.A., Vinnikov, K.Y., Speranskaya, N.A. and Entin, J.K. (1998). Evaluation of AMIP soil moisture simulations. Global and Planetary Change, **19**: 181-208.

Rogowski, A. S. (1972). Watershed physics: Soil variability criteria. Water Res. Res., **8(4)**: 1015-1023.

Russo, D. and Bresler, E. (1980). Scaling soil hydraulic properties of a heterogeneous field. Soil Sci. Soc. Am. J., **44**: 681-684.

Santra, P., Chopra, U.K. and Chakraborty, D. (2008). Spatial variability of soil properties and its application in predicting surface map of hydraulic parameters in an agricultural farm. Current sci., **95(7)**: 937-945.

Schepers, A.R., Schepers, J.S., Shanahan, J.F., Liebig, M.A., Johnson, S. and Luchiari, A.J. (2004). Appropriateness of Management Zones for Characterizing Spatial Variability of Soil Properties and Irrigated Corn Yields across Years. Agron. J., **96**: 195-203.

Schimel, D.S. (1995). Terrestrial ecosystems and the carbon cycle. Global Change Biology, **1**: 77-91.

Schlesinger, W.H. (1977). Carbon balance in terrestrial detritus. 1`Annual Review of Ecology and Systematics, **8**: 51–81.

Schlesinger, W.H., Raikes, J.A., Hartley, A.E. and Cross, A.F. (1996). On the spatial patterns of soil nutrients in desert ecosystems. Ecology **77 (2)**: 364–374.

Seyfried, M.S., Wilcox, B.P. (1995). Scale and the nature of spatial variability: Field examples having implications for hydrologic modeling. Water Res. Res., **30(1)**: 173-184.

Shamsi, M. and Mazloumzadeh, S.M. (2009). Studying yield variations using precision farming in a date palm orchard. Int. J. Agric. Tech., **5(1)**: 33-39.

Simmons, C.S., Nielsen, D.R. and Biggar, J.W. (1979). Scaling of field-measured soil-water properties. I. Methodology. II. Hydraulic conductivity and flux. Hilgardia, **47**: 77-174.

Sisson, J.B. and Weirenga P.J. (1981). Spatial variability of steady state infiltration rates as a stochastic process. Soil Sci. Soc. Am. J., 45: 699-704. Southern Amazon. Hydrol. Process, **20**: 2599-2614.

Soil Survey Staff (1998). Keys to Soil Taxonomy. Natural Resources Conservation Service, USDA, 8th Edn. Government Printing Office, Washington, DC. 326.

Sposito, G., and Jury, W.A. (1990). Miller similitude and generalized scaling analysis. *In* Scaling in Soil Physics: Principles and Applications, Hillel, D. and Elrick, D.E. (Eds.); 13-22. Soil Science Society of America, Madison, Wisconsin.

Stafford, J.V. (1997). Precision agriculture. Proc. 1st Eur. Conf. on Precision agric., Warwick, UK.BIOS Scientific Publishers, Oxford, UK.

Stafford, J.V. (2000). Implementing precision agriculture in the 21st century. J. Agric. Engng. Res., **76**: 267-275.

Stave, J., Oba, G., Stenseth, N.C. and Nordal, I. (2005). Environmental gradients in the Turkwel riverine forest, Kenya: Hypotheses on dam-induced vegetation change. For. Ecol. Manag., **212**: 184-198.

Strecker, J. (2004). Fractional Brownian motion simulation: observing fractal statistics in the wild and raising them in captivity. BSc. Thesis: Department of Mathematics and Computer Science, College of Wooster.

Sugihara, G. and May, R.M. (1990). Applications of fractals in ecology. Trends Ecol. Evol. **5**: 79-86.

Svenning, J.C. (2001). On the role of micro-environmental heterogeneity in the ecology and diversification of Neotropical rain-forest palms (Arecaceae). Bot. Rev., **67**: 1-53.

Tanji, K.K. (1996). Agricultural salinity assessment and management. ASCE, New York.

Tarquis, M, Bird, N. R. A., Whitmore, A. P., Cartagena, M. C. and Pachepsky, Y. (2007). Multiscale Entropy-based Analysis of Soil Transect Data. Vadose Zone J., **7**: 563-569.

Teuling, A.J. and Troch, P.A. (2005). Improved understanding of soil moisture variability dynamics, Geophys. Res. Lett., **32**: L05404, doi: 10.1029/2004GL021935, 2005.

Theodossiou, N. and Latinopoulos, P. (2006). Evaluation and optimization of groundwater observation networks using the Kriging methodology. Environmental. Modeling and Software, **21**: 991–1000.

Tillotson, P.M. and Nielsen, D.R. (1984). Scale factors in soil science. Soil Sci. Soc. Am. J., **48**: 953-959.

Timm, L.C., Pires, L.F., Roveratti, R.., Arthur, R.C.J., Reichardt, K., Olivira, J.C.M. and Bacchi, O.O.S. (2006). Field spatial and temporal patterns of soil water content and bulk density changes. Scientia Agricola, **63**: 55-64.

Trangmar, B.B., Yost, R.S. and Uehara, G. (1985). Application of geostatistics to spatial studies of soil properties. Adv. Agric., **38**: 45-94.

Tsegaye, T. and Hill, R.L. (1998). Intensive tillage effects on spatial variability of soil physical properties. Soil Sci., **163**: 143–154.

Tuli, A., Kosugi, K. and Hopmans, J.W. (2001). Simultaneous scaling of soil water retention and unsaturated hydraulic conductivity functions assuming lognormal pore-size distribution. Adv. Water Res., **245**: 677-688.

Turgut, B., Aksakal, E.L. and Öztaş, T. (2008). Assessment of Spatial Distribution Patterns of Soil Properties in the EAARI-Experimental Station (Erzurum). International Meeting on Soil Fertility, Land Management and Agro-climatology. Turkey, 2008. 165-173.

Tyler, W.S. and Wheatcraft, S.W. (1989). Application of fractal mathematics to soil water retention estimation. Soil Sci. Soc. Am. Journal, **53**: 987-996.

Tyler, W.S. and Wheatcraft, S.W. (1992). Fractal scaling of soil particle-size distributions: analysis and limitations. Soil Sci. Soc. Am. J. **56**: 362–369.

USDA-NRCS (2008). Soil Quality Indicators: Available Water Capacity. Soil Quality Information Sheet, June 2008.

Uyan, M. and Cay, T. (2010). Geostatistical methods for mapping groundwater nitrate concentrations. 3rd International Conference on Cartography and GIS (2010), Nessebar, Bulgaria.

Vachaud, G., De Silans, A.P., Balabamnis, P. and Vauclin, M. (1985). Temporal stability of spatially measured soil water probability density function. Soil Sci. Soc. Am. J., **49**: 892-898.

Vartapetian, B.B. and Jackson, M.B. (1997). Plant adaptations to anaerobic stress. Ann. Bot. (Lond.), **79**: 3-20.

Vauclin, M., Vieira, S.R., Benara, R. and Hatfield, J.L. (1982). Spatial variability of surface temperature along two transects of a bare soil. Water Res. Res., **18(6)**: 1677-1686.

Veihmeyer, F.J. and Hendrickson, A.H. (1931). The moisture equivalent as a measure of the field capacity of soils. Soil Sci., **32**: 181-194.

Veneklaas, E.J., Fajardo, A., Obregon, S. and Lozano, J. (2005). Gallery forest types and their environmental correlates in a Colombian savanna landscape. Ecography, **28**: 236-252.

Vieira, S.R., Nielsen, D.R. and Biggar, J.W. (1981). Spatial variability of field measured infiltration rate. Soil Sci. Soc. Am. Proc., **32**: 1040-1048.

Vieira, S.R., Vidal-Vázquez, E., Miranda, J.G.V., Paz-González, A. and Paz-Ferreiro, J. (2010). Fractal analysis and graph theory applied to the spatial and temporal variability of soil water content. EGU 2010-Vienna, Austria.

Viscarra Rossel, R.A., and. McBratney, A.B. (1997). Preliminary experiments towards the evaluation of a suitable soil sensor for continuous 'on-the-go' field pH measurements: 493–502. *In*: Stafford, J.V. (Ed.); Precision agriculture. Proc. 1st Eur. Conf. on Precision Agric., Warwick, UK. BIOS Scientific Publishers, Oxford, UK.

Vogel, T., Cislerova, M. and Hopmans, J.W. (1991). Porous media with linearly variable hydraulic properties. Water Res. Res., **27(10)**: 2735-2741.

Voltz, M. and Webster, R. (1990). A comparison of Kriging, cubic splines and classification for predicting soil properties from sample information. J. Soil Sci., **41**: 473–490.

Vormisto, J., Tuomisto, H. and Oksanen, J. (2004). Palm distribution patterns in Amazonian rainforests: What is the role of topographic variation? J. Veg. Sci., **15**: 485-494.

Voss, R. F. (1985). Random fractal forgeries. *In*: Earnshaw, R.A., (Ed.); Fundamental Algorithms for Computer Graphics, Springer-Verlag, Berlin, 1985.

Warrick A.W. and Gardner W.R. (1983). Crop yield as affected by spatial variations of soil and irrigation. Water Res. Res., **19**: 181–186.

Warrick, A. W., Myers, D. E. and Nielsen, D. R. (1986). Geostatistical methods applied to soil science. *In*: Klute, A. (Ed.); Methods of Soil Analysis, Part 1. Physical and Mineralogical Methods, Agronomy Monograph 9. Am. Soc. Agron., Madison, WI. 2nd Edn. 53–82.

Warrick, A.W. and Nielson D.R. (1980). Spatial variability of soil physical properties in the field. *In*: Hillel, D. (Ed.); Applications of Soil Physics, 319-344. New York, NY: Academic Press, Inc.

Warrick, A.W., Mullen, G.J. and Nielsen, D.R. (1977). Scaling field measured hydraulic properties using a similar media concept. Water Res. Res., **13(2)**: 355-362.

Webster, R. and Oliver, M.A. (2001). Geostatistics for Environmental Scientists. London, UK: John Willey and Sons Ltd.

Webster, R. and Oliver, M.A. (2007). Geostatistics for Environmental Scientists. 2nd Edn.

Weisz, R., Fleischer, S. and Smilowitz, Z. (1995). Map generation in high-value horticultural integrated pest management: Appropriate interpolation methods for site-specific pest management of Colorado Potato Beetle (*Coleoptera*: *Chrysomelidae*). J. Econ. Entomol., **88**: 1650–1657.

Western, A. W. and Grayson, R. B. (1998). The Tarrawarra data set: Soil moisture patterns, soil characteristics, and hydrological flux measurements, Water Res. Res., **10**: 2765–2768.

Western, A.W., Blöschl, G. (1999). On the spatial scaling of soil moisture. J. Hydrol., **217**: 203-224.

Western, A.W., Grayson, R.B., Blöschl, G., Willgoose, G.R. and McMahon, T.A. (1999). Observed spatial organisation of soil moisture and its relation to terrain indices, Water Res. Res., **35**: 797–810.

Western, A.W., Zhou, S., Grayson, R.B., McMahon, T.A., Blöschl, G. and Wilson, D.J. (2004). Spatial correlation of soil moisture in small catchments and its relationship to dominant spatial hydrological processes, J. Hydrol., **286**: 113–134.

Wheatcraft, S.W. and Tyler, S.W. (1988). 'An explanation of scale dependent dispersivity in heterogeneous aquifers using concepts of fractal geometry'. *Water Res. Res.* **24**: 566–578.

Wilding, L.P. (1985). Spatial variability: its documentation, accommodation and implication to soil surveys. *In*: D.R. Nielsen and J. Bouma (Eds.); Soil Spatial Variability. PUDOC, Wageningen. 166-189.

Wilkinson, G.E. and Klute, A. (1959). Some tests of the similar media concept of capillary flow: II. Flow systems data. Soil Sci. Soc. Am. Proc., **23**: 434-437.

Williams, C.J., McNamara, J.P. and Chandler, D.G. (2009). Controls on the temporal and spatial variability of soil moisture in a mountainous landscape: the signature of snow and complex terrain. Hydrol. Earth Syst. Sci., **13**: 1325–1336.

Yang, C., Peterson, C.L., Shropshire, G.J. and Otawa, T. (1998). Spatial Variability of Field Topography and Wheat Yield in the Palouse Region of the Pacific Northwest. Transactions of the ASAE, **41**: 17-27.

Zhang, C. and McGrath, D. (2004). Geostatistical and GIS analyses on soil organic carbon concentration in grassland of southeastern Ireland from two different periods. Geoderma, **119**: 261-275.

Zhang, N., Wang, M. and Wang, N. (2002). 'Precision agriculture - a worldwide overview', Computers and Electronics in Agriculture, **36**: 113–1.

APPENDICES

APPENDIX A

T-test results of Soil physical properties

A-1: Sand content

Table Analyzed	Data 1
Column C	sand 1
vs	vs
Column D	sand 2
Paired t test	
P value	< 0.0001
P value summary	***
Are means signif. different? (P < 0.05)	Yes
One- or two-tailed P value?	Two-tailed
t, df	t=6.625 df=79
Number of pairs	80
How big is the difference?	
Mean of differences	4.150
95% confidence interval	2.901 to 5.399
R square	0.3571
How effective was the pairing?	
Correlation coefficient (r)	0.7256
P Value (one tailed)	< 0.0001
P value summary	***
Was the pairing significantly effective?	Yes

A-2: Clay content

Table Analyzed	Data 1
Column E	clay 1
vs	vs
Column F	clay 2
Paired t test	
P value	< 0.0001
P value summary	***
Are means signif. different? (P < 0.05)	Yes
One- or two-tailed P value?	Two-tailed
t, df	t=10.74 df=79
Number of pairs	80
How big is the difference?	
Mean of differences	-6.563
95% confidence interval	-7.781 to -5.344
R square	0.5935
How effective was the pairing?	
Correlation coefficient (r)	0.6821
P Value (one tailed)	< 0.0001
P value summary	***
Was the pairing significantly effective?	Yes

A-3: Silt content

Table Analyzed	Data 1
Column G	silt 1
vs	vs
Column H	silt 2
Paired t test	
P value	< 0.0001
P value summary	***
Are means signif. different? (P < 0.05)	Yes
One- or two-tailed P value?	Two-tailed
t, df	t=5.652 df=79
Number of pairs	80
How big is the difference?	
Mean of differences	2.488
95% confidence interval	1.610 to 3.365
R square	0.2880
How effective was the pairing?	
Correlation coefficient (r)	0.1858
P Value (one tailed)	0.0495
P value summary	*
Was the pairing significantly effective?	Yes

A-4: Bulk density

Table Analyzed	Data 1
Column A	bulk density 1
vs	vs
Column B	bulk density 2
Paired t test	
P value	< 0.0001
P value summary	***
Are means signif. different? (P < 0.05)	Yes
One- or two-tailed P value?	Two-tailed
t, df	t=8.312 df=79
Number of pairs	80
How big is the difference?	
Mean of differences	-0.06653
95% confidence interval	-0.08248 to -0.05057
R square	0.4665
How effective was the pairing?	
Correlation coefficient (r)	0.2019
P Value (one tailed)	0.0362
P value summary	*
Was the pairing significantly effective?	Yes

A-5: Total porosity

Table Analyzed	Data 1
Column I	porosity 1
vs	vs
Column J	porosity 2
Paired t test	
P value	< 0.0001
P value summary	***
Are means signif. different? (P < 0.05)	Yes
One- or two-tailed P value?	Two-tailed
t, df	t=8.319 df=79
Number of pairs	80
How big is the difference?	
Mean of differences	2.512
95% confidence interval	1.910 to 3.114
R square	0.4670
How effective was the pairing?	
Correlation coefficient (r)	0.2015
P Value (one tailed)	0.0365
P value summary	*
Was the pairing significantly effective?	Yes

A-6: Aeration porosity

Table Analyzed	Data 1
Column K	aeration 1
vs	vs
Column L	aeration 2
Paired t test	
P value	< 0.0001
P value summary	***
Are means signif. different? (P < 0.05)	Yes
One- or two-tailed P value?	Two-tailed
t, df	t=8.547 df=79
Number of pairs	80
How big is the difference?	
Mean of differences	4.006
95% confidence interval	3.071 to 4.940
R square	0.4804
How effective was the pairing?	
Correlation coefficient (r)	0.3924
P Value (one tailed)	0.0002
P value summary	***
Was the pairing significantly effective?	Yes

A-7: Volumetric moisture content

Table Analyzed	Data 1
Column O	vmc 1
vs	Vs
Column P	vmc 2
Paired t test	
P value	< 0.0001
P value summary	***
Are means signif. different? (P < 0.05)	Yes
One- or two-tailed P value?	Two-tailed
t, df	t=4.754 df=79
Number of pairs	80
How big is the difference?	
Mean of differences	-1.357
95% confidence interval	-1.927 to -0.7881
R square	0.2224
How effective was the pairing?	
Correlation coefficient (r)	0.3754
P Value (one tailed)	0.0003
P value summary	***
Was the pairing significantly effective?	Yes

A-8: Aggregate stability

Table Analyzed	Data 1
Column S	A 1
vs	Vs
Column T	A 2
Paired t test	
P value	< 0.0001
P value summary	***
Are means signif. different? (P < 0.05)	Yes
One- or two-tailed P value?	Two-tailed
t, df	t=17.95 df=79
Number of pairs	80
How big is the difference?	
Mean of differences	0.09637
95% confidence interval	0.08567 to 0.1071
R square	0.8030
How effective was the pairing?	
Correlation coefficient (r)	0.6220
P Value (one tailed)	< 0.0001
P value summary	***
Was the pairing significantly effective?	Yes

APPENDIX B

T-test results of saturated hydraulic conductivity

C: Saturated hydraulic conductivity

Table Analyzed	Data 1
Column U	Ks 1
vs	vs
Column V	Ks 2
Paired t test	
P value	< 0.0001
P value summary	***
Are means signif. different? (P < 0.05)	Yes
One- or two-tailed P value?	Two-tailed
t, df	t=6.679 df=79
Number of pairs	80
How big is the difference?	
Mean of differences	7.823e-005
95% confidence interval	5.488e-005 to 0.0001016
R square	0.3609
How effective was the pairing?	
Correlation coefficient (r)	0.6075
P Value (one tailed)	< 0.0001
P value summary	***
Was the pairing significantly effective?	Yes